DESIGN AND SYNTHESIS OF SUPRAMOLECULAR ASSEMBLIES OF ORGANIC AND COORDINATION COMPLEXES

Thesis submitted to

University of Pune

for the degree of

Doctor of Philosophy

in

Chemistry

by

Sunil Varughese

Division of Organic Chemistry
National Chemical Laboratory
Dr. Homi Bhabha Road
Pune 411 008

December 2006

Dedicated to my
Beloved Parents

National Chemical Laboratory

Division of Organic Chemistry
Dr. Homi Bhabha Road
Pune – 411 008. India
Fax: +91 20 25902624
E-mail: vr.pedireddi@ncl.res.in

CERTIFICATE

This is to certify that the work presented in the thesis entitled "**DESIGN AND SYNTHESIS OF SUPRAMOLECULAR ASSEMBLIES OF ORGANIC AND COORDINATION COMPLEXES**" submitted by **Sunil Varughese**, was carried out by the candidate at National Chemical Laboratory, Pune, under my supervision. Such materials as obtained from other sources have been duly acknowledged in the thesis.

December 2006
Pune

Dr. V. R. Pedireddi, FRSC
(Research Guide)

DECLARATION

I hereby declare that the matter embodied in this thesis entitled "**Design and Synthesis of Supramolecular Assemblies of Organic and Coordination Complexes**" is the result of investigations carried out by me in the Division of Organic Chemistry, National Chemical Laboratory, Pune under the supervision of **Dr. V. R. Pedireddi**.

In keeping with the general practice of reporting scientific observations, due acknowledgements have been made wherever the work described is based on the findings of other investigators.

Pune **Sunil Varughese**
December 2006

ACKNOWLEDGEMENTS

It is a great pleasure to express my thanks and appreciations towards the people who have in many ways assisted me to reach this stage. It gives me an immense pleasure to express my deep sense of gratitude and profound thanks to my research guide Dr. V. R. Pedireddi for all the advice, guidance, support and encouragement during every stage of this work. Although this eulogy is insufficient, I preserve an everlasting gratitude for him.

My heartfelt thanks go to Prof. K. N. Ganesh, former head of the division, for his relentless support and encouragement throughout my research period.

I am very much grateful to Prof. R. N. Mukherjee, IIT Kanpur, for introducing me into the fascinating field of research and teaching me the initial lessons of research career. I take this opportunity to thank my teachers, Prof. M. Padmanabhan, Dr. Suresh Mathew, Prof. P. K. Radhakrishanan and my other teachers of School of Chemical Sciences, Mahatma Gandhi University, for their encouragement and motivation.

My special thanks to Dr. Joy, Dr.Sathyanarayana and Dr. Joshi for their help, encouragement and fruitful discussions during the course of this work. I am indebted to express my gratitude to Dr. Mohan Bhadbhade, Mr. Rajesh Gonnade and Dr. Vedavati Puranik for their help in x-ray analysis.

I would like to place on record my thanks to Prof. Gururow, IISc, Bangalore; Prof. Judith Howard and Mike Turner, University of Durham, UK; Prof. Kristof Wozniak, University of Warsaw, Poland; Prof. Roland Boese, University of Essen, Germany; Dr. U. P. Singh, IIT Roorki and Dr. E. Suresh, CSMCRI, Bhavnagar, for their invaluable contribution by collecting the single crystal x-ray datasets discussed in the thesis.

I sincerely thank my colleagues for their help in various capacities, co-operation and maintaining cheerful atmosphere in the lab. Thank you Seetha, Manish, Kapil, Marivel, Sathya, Prakash, Amit, Deepika, Parul and Sreeja. I am thankful to my friends Jhumpa didi,, Vaibhave, Reji, Vinod, Deepa, Josi, Josia, Manoj, Pranchal, Amol and all my childhood friends for their immense support and encouragement.

I take this opportunity to thank Dr. Srinivas Hotha and Dr. Ramana for their help and encouragement throughout my stay over here.

It gives me great pleasure to thank my beloved parents, for their love, tremendous patience, trust and encouragement during many years of studies. They have been my constant source of strength and have brought a great deal of happiness to my life.

Special thank my brother, Sushil, my grand parents and all my family members; for their expectations and hope, that kept me awake all along.

I thank director NCL and Dr. Gurjar, head of the division, for allowing me to work in this premier institute, providing the infrastructure and his great sense of appreciation and recognition is highly inspirational.

It is my sincere thanks to CSIR, New Delhi, for the financial support.

I take this opportunity to thank each and every person who have helped and supported me throughout my education period and apologize to all those who have helped me but are not acknowledged.

At last but not the least, I thank whole heartedly, the omnipotent God, the illimitable superior spirit, who reveals himself in the slight details I am able to perceive with my frail and feeble mind.

Sunil Varughese

TABLE OF CONTENTS

Chapter-3

Hydrogen bond Mediated Metal-Organic Open-frame Networks

Chapter-4

Molecular Recognition Studies of 3,5-Dihydroxy and 4-Bromo-3,5-dihydroxybenzoic acids

ABSTRACT

The research work reported in this thesis entitled **"DESIGN AND SYNTHESIS OF SUPRAMOLECULAR ASSEMBLIES OF ORGANIC AND COORDINATION COMPLEXES"** was carried out to evaluate the collective influence of different intermolecular interactions on the structure and properties of coordination assemblies as well as the organic molecular complexes formed by the process of self-assembly and their utilization for targeted synthesis of novel and exotic supramolecular assemblies. Design and synthesis of supramolecular assemblies by the legitimate choice of the building blocks and the reaction conditions, have gained a lot of attention, not only due to the aesthetically appealing architectures but also for the promising properties exhibited by these materials. Thus, the observations, made during the course of the PhD program, have been compiled into four chapters as described below. While Chapter-1 gives an introduction to the contemporary research in the areas of supramolecular chemistry, with an emphasis on the coordination polymers and the metal-organic frameworks as well as organic assemblies, Chapter-2 and Chapter-3 illustrate the effect of hydrogen bonds on the supramolecular coordination assemblies of transition and lanthanide ions. Chapter-4 is an account of a detailed analysis of the utilization of various dihydroxybenzoic acids in supramolecular synthesis for the creation of molecular adducts, by the cocrystallization technique.

Chapter-1: The synthesis of supramolecular assemblies by the utilization of the knowledge of intermolecular interactions and self-assembly – *supramolecular synthesis* – have gained popular attention in the recent times, due to their potential utility in the synthesis of complex and topologically directed materials with tailor-made properties. Studies of both organic and coordination polymers and the utility of their unique functional properties in the nanoporous coordination environment for various applications such as enantiomeric catalysis, gas storage, selective separation, drug delivery etc. are some of the representative examples. This is made possible by the concerted effort in exploiting the directionality of the coordination bond and hydrogen bonds to design the frameworks with desired architectures and properties, as evident from the intense research towards the generation of fascinating arrays of host materials with advanced structure-property relationships in the nanoporous framework hosts, with the precise controlling and tuning of the pore shape, size and the periodicity of the units. Elaborate discussion of the contemporary research work in these areas is presented in Chapter-1.

Chapter-2: The studies on metal-organic assemblies have been largely focused on synthesizing the frameworks making use of the coordinate bonds, formed between the metal center and the organic ligand. But only limited examples are known in the literature about the effect of intermolecular interactions on the coordination mode of the ligand as well as the architecture of the resulting supramolecular assembly. For this purpose, to explore the impact of intermolecular interactions in coordination polymers, reactions with the ligands that are prone to form hydrogen

bonds, in addition to the coordinate bonds with the metal sites have been chosen as prime substrates. In this regard, 3,5-dinitrobenzoic acid and its derivatives were studied along with Co(II) and Mn(II) metal salts, such that, while, the carboxylate functional group can involve in the formation of coordinate bonds, $–NO_2$ groups and the substituents ($–CH_3$, –Cl, –OH etc.) can take part in the intermolecular hydrogen bonding. Salient features of these assemblies are discussed in Chapter-2, dividing it into two sections, depending upon the nature of the assemblies obtained.

Part-A: The influence of solvent of crystallization on the self-assembly of coordination polymers

In general, supramolecular architectures of the resultant coordination assemblies, that are purely governed by coordinate bonds are rigid, but structures that are being stabilized by hydrogen bonds could be flexible as the nature of the interactions are often governed by various external factors like, solvent of crystallization, pH, temperature, the presence of counter ions etc. But systematic analysis of these factors and their influence on the coordination geometry are limited in literature.

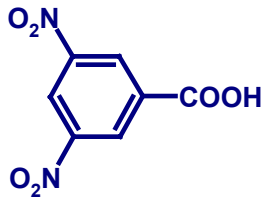

3,5-Dinitrobenzoic acid

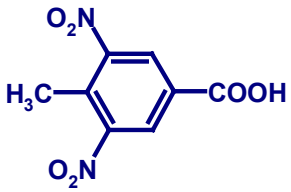

3,5-Dinitro-4-methyl-benzoic acid

In this direction, to demonstrate the effect of solvent of crystallization on the coordination assemblies, studies were carried out by preparing coordination polymers

of 3,5-dinitrobenzoic acid and its methyl derivative (3,5-dinitro-4-methyl-benzoic acid) with Co(II) and 4,4'-bipyridine (***bpy***) in the presence of various solvents and the solvent mixtures such as methanol, methanol-acetone, methanol-DMSO, etc. The structural variations and the coordination modes of the carboxylate towards the metal ions, as shown schematically in Figure-1, are discussed in this section in detail.

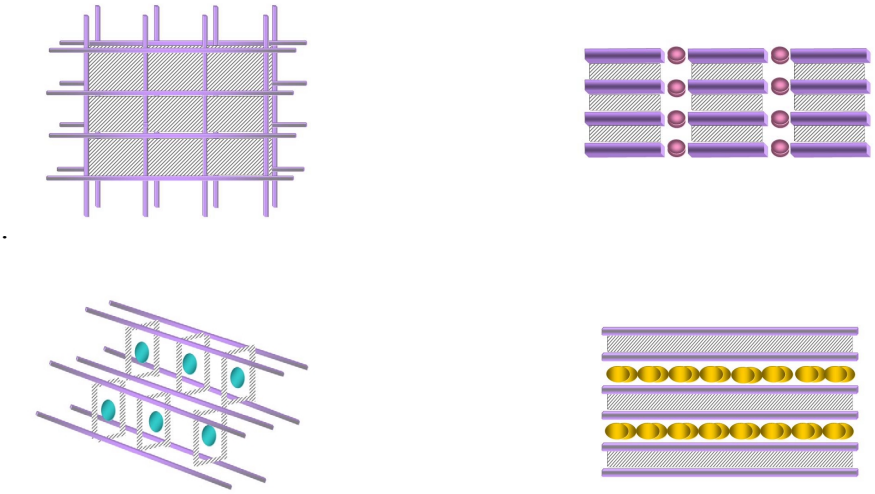

Figure-1: Schematic representation of the coordination assemblies, with the variation in the solvent of crystallization.

Part-B: The influence of different aza-donor compounds on the self-assembly of coordination polymers

The effect of N-donor ligands on the coordination mode of the carboxylate towards the metal ions and the resultant architectures were analyzed with the reaction of 3,5-dinitrobenzoic acid and Mn(II) in the presence of various aza-donor ligands with varying dimensions and coordination modes. For this purpose, different types of

fluxional molecules like, 4,4'-bipyridine, 1,2-bis(4-pyridyl)ethene, 1,2-bis(4-pyridyl)ethane, 1,3-bis(4-pyridyl)propane, 2,2'-bipyridine and 1,10-phenanthroline.

4,4'-bipyridine

(***bpy***)

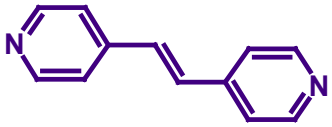

1,2-bis(4-pyridyl)ethene

(***bpyee***)

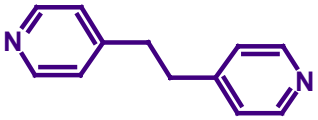

1,2-bis(4-pyridyl)ethane

(***bpyea***)

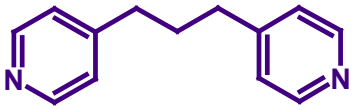

1,3-bis(4-pyridyl)propane

(***bpypa***)

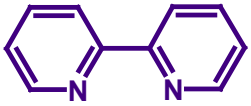

2,2'-bipyridine

(***22bpy***)

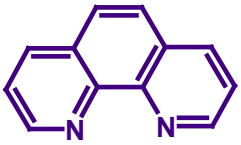

1,10-phenanthroline

(***110phe***)

The resultant architecture varies from the zero-dimensional bimetallic units to infinite one-dimensional coordination polymers, as represented schematically in Figure-2, held together by intermolecular interactions like C-H···O hydrogen bonds. The salient features of the complexes are described in this section.

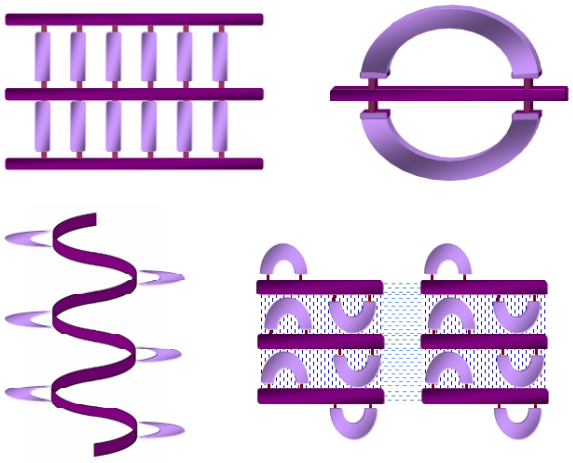

Figure-2: A schematic representation of the coordination assemblies formed by various spacer ligands in conjunction with 3,5-dinitrobenzoic acid and Mn(II)

Chapter-3: The generation of porous solids has attracted the attention, because of the interest in the creation of nanometer-sized cavities/channels. Though the transition metals are well studied in the preparation of coordination frameworks, the utility of lanthanide ions in the preparation of coordination assemblies are not well explored. Thus, metal-organic frameworks of Pr(III) ions with 3,5-dinitrobenzoic acid and its derivatives (3,5-dinitro-4-methylbenzoic acid and 4-amino-3,5-dinitrobenzoic acid) as the primary ligands in the presence of various N-donor ligands, such 4,4'-bipyridine, 1,2-bis(4-pyridyl)ethane and 1,2-bis(4-pyridyl)ethene as the spacer ligands, were prepared. The complexes were found to form host-guest architectures, with the dimension of the host framework varying with the incoming ligands. A snapshot of the assemblies is shown in Figure 3 and a detailed discussion of these assemblies is given in this chapter.

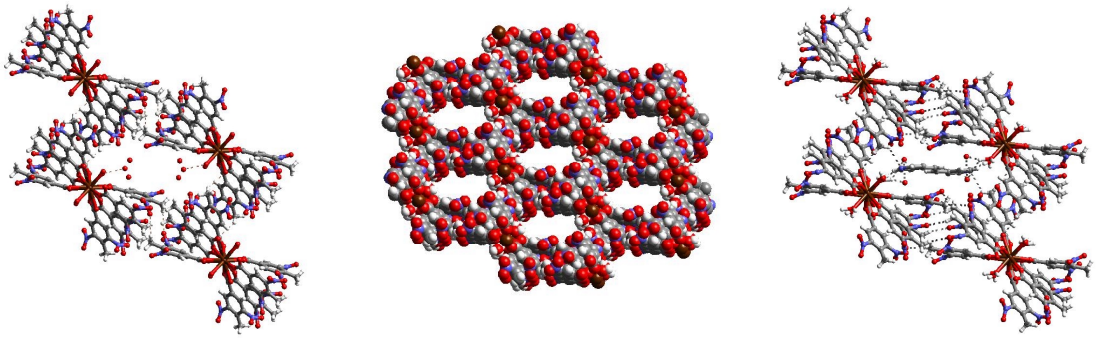

Figure 3: Shows a representative example of the porous framework formed, along with the host-guest assemblies formed with water and 1,2-bis(4-pyridyl)ethane.

Chapter-4: Materials research today increasingly relies on the molecular building blocks that are self-assembled into the organized structures with desired architectures, properties and functions, which are brought about by the utilization of various non-bonded interactions, resulting from the recognition between the complimentary functional groups existing in the molecules involved in the process. Among the potential functional groups like –COOH, -OH, -$CONH_2$ etc. which yield directional intermolecular interactions (for example, hydrogen bonds), -COOH group has been well utilized in the supramolecular synthesis. In this process, knowing the potentiality of –OH groups to form hydrogen bonds, 3,5-dihydroxybenzoic acid and its –Br derivative were chosen to explore their ability to yield a variety of supramolecular architectures to demonstrate the competitive nature of functional groups, particularly between –OH and –COOH in the molecular recognition studies, as compiled in this chapter.

In this section, an account of the competitive nature of the recognition processes involving the –COOH as well as –OH groups towards various N-donor ligands such as 4,4'-bipyridine, 1,2-bis(4-pyridyl)ethane and 1,2-bis(4-pyridyl)ethene were studied by co-crystallizing with 3,5-dihydroxybenzoic acid and 4-bromo-3,5-dihydroxybenzoic acid. The three dimensional architectures were analyzed and rationalized in terms of ladder and interpenetrated structures, as shown in Figure 4. A detailed discussion of these assembles would be presented in this section.

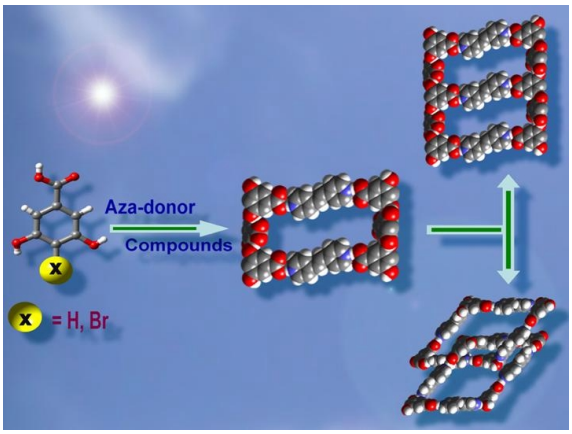

Figure 4: A schematic representation of the formation of ladder as well as interpenetrated assemblies, depending on the dimension of the cyclic network formed by the self assembly process.

Sunil Varughese **Dr. V. R. Pedireddi, FRSC**

(Research Student) (Research Guide)

Chapter-1

An Overview of Supramolecular Chemistry and Molecular Recognition

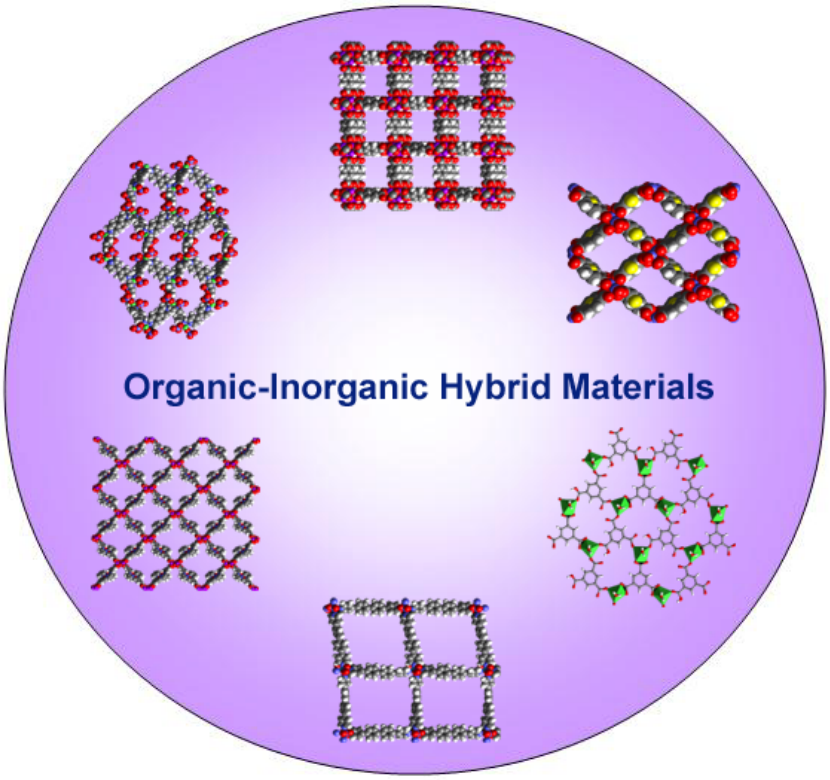

"The important thing in Science is not so much to obtain new facts as to discover new ways of thinking about them"

-W. L. Bragg-

1.1 Introduction

During the last two centuries, chemists have developed a remarkable degree of control over molecular architecture, with the ability to introduce a wide range of substituents in predictable positions on increasingly complex molecular scaffolds and controlling the stereochemistry at particular chiral centres, leading to the preparation of numerous compounds which have been serving the demands of human requirements.[1] However, in the last few decades, the quest for the synthesis of nanoscale composites and assemblies, employing the noncovalent bonds, has led to the birth of a highly interdisciplinary field of chemical research – *supramolecular chemistry*.[2] This branch of contemporary science is concerned with advancing the structural complexity beyond the molecules towards ordered oligo- and poly-molecular entities which are held together by noncovalent bonds. Thus, supramolecular chemistry is the chemistry beyond the molecule.[3] According to Lehn, *"supermolecules are to molecules and the intermolecular bond what molecules are to atoms and the covalent bond"*.[4] The understanding of intermolecular interactions is, therefore, as vital to supramolecular chemistry as the understanding of the covalent bond to molecular chemistry.

1.2 Noncovalent interactions

While a wide range of synthetic methodologies and covalent bonds are utilized in the preparation or the transformation of molecular entities, in the studies of supramolecular chemistry, the utilization of noncovalent bonds, such as hydrogen

bonds, halogen bonds etc. play a pivotal role for the creation of supramolecular assemblies. In this process, the geometric and energetic factors of the intermolecular interactions are important parameters that control the construction of the supermolecules with desired structural and chemical properties.[5]

The concept of hydrogen bonding is becoming increasingly important for the understanding of, how molecules align themselves in the formation of molecular clusters. This dates back to the Pauling's observation that the boiling point of acetyl chloride (51 ^{o}C) is substantially higher than that of triflouroacetyl chloride (< 0 ^{o}C), which, he attributed to the hydrogen bonding, existing in the case of acetyl chloride. In his own words, hydrogen bond is defined as *"an atom of hydrogen, under certain conditions, is attracted by rather strong forces to two atoms, instead of only one, so that it may be considered to be acting as a bond between them."* [6]

In 1920, Latimer and Rodebush[7] suggested that *"a free pair of electrons on one water molecule might be able to exert sufficient force on the hydrogen held by a pair of electrons on another water molecule to bind the two molecules together."* This scientific speculation initiated new dimensions of research on hydrogen bonds as evident from the seminal report on hydrogen bonds by Pimental and McClellan in 1960, listing over 2000 references dealing specifically with the hydrogen bonding.[8] Further, the noted work on the crystallographic evidence of the existence of several interactions like C-H$^{\cdots}$O, C-H$^{\cdots}$N and C-H$^{\cdots}$Cl hydrogen bonds by Taylor and Kennard, opened a new era in the studies of hydrogen bonds as design elements in the synthesis of supermolecules.[9]

The seminal contributions of several researchers, to name a few, Etter, Leiserowitz, Schmidt, Desiraju, Steiner, Jeffrey and Saenger have conducted extensive studies in the organic compounds for the evaluation of the patterns, directionality and strength of hydrogen bonds and have observed that certain interactions in organic molecular solids are associated with only certain geometrical motifs.[10-15] Etter and co-workers encoded these hydrogen bond patterns, by analyzing the interactions in organic solids in a systematic and consistent fashion, establishing the pattern-preference displayed by many functional groups – *graph set analysis of hydrogen bonds*- and thus introducing a nomenclature for the hydrogen bond patterns in the solid-state chemistry.[16] Making use of these repeating geometric motifs as design elements, attempts were made to prepare novel assemblies with tailor-made properties as well as to understand various biological processes like enzyme recognition, drug activity etc. Thus, the utility of hydrogen bonds are widespread in chemistry and biology and have so many structural and mechanistic consequences.

1.3 Self-assembly

According to Lehn,[17] molecules undergo self-assembly when they:

(i) *Selectively bind via molecular recognition*

(ii) *Grow through sequential binding of the components in the proper orientation*

(iii) *Terminate the assembly once the process has reached the completion.*

This concept was further supported by Hamilton and co-workers by considering self-assembly as the process by which, the non-covalent interaction between two or more molecular subunits form an aggregate, whose novel structures and properties are determined by the strength of the binding forces and the nature and positioning of the components.[18] Whitesides recognizes cooperativity as an important characteristic in self-assembling system.[19] During the process of the self-assembly, there is a large decrease in entropy while bringing many molecules together to form an aggregate. The enthalpy of the non-covalent interactions must be large enough to offset this unfavorable decrease in entropy. Though, individually each non-covalent interaction may not be large enough to overcome this unfavorable entropy change, but collectively, they are able to promote the aggregations. It is well known that, the molecular components of an aggregate often undergo conformational change to promote aggregations. Thus the cooperativity, meant by Whitesides, involves both conformational changes and multiple non-covalent interactions, offsetting the destabilizing decrease in entropy.

Nature provides a very large ensemble of complex assemblies formed by the self assembly of very simple molecular building blocks and the examples vary from the simple water cluster to the complex biological molecules like DNA, RNA and proteins.[20-21] Much of the work in mimicking the natural systems has been in designing helical structures which resemble DNA and RNA. Thus numerous supramolecular helices which are held together by hydrogen bonds and metal-ligand coordinate bonds were reported by different research groups.[22-23]

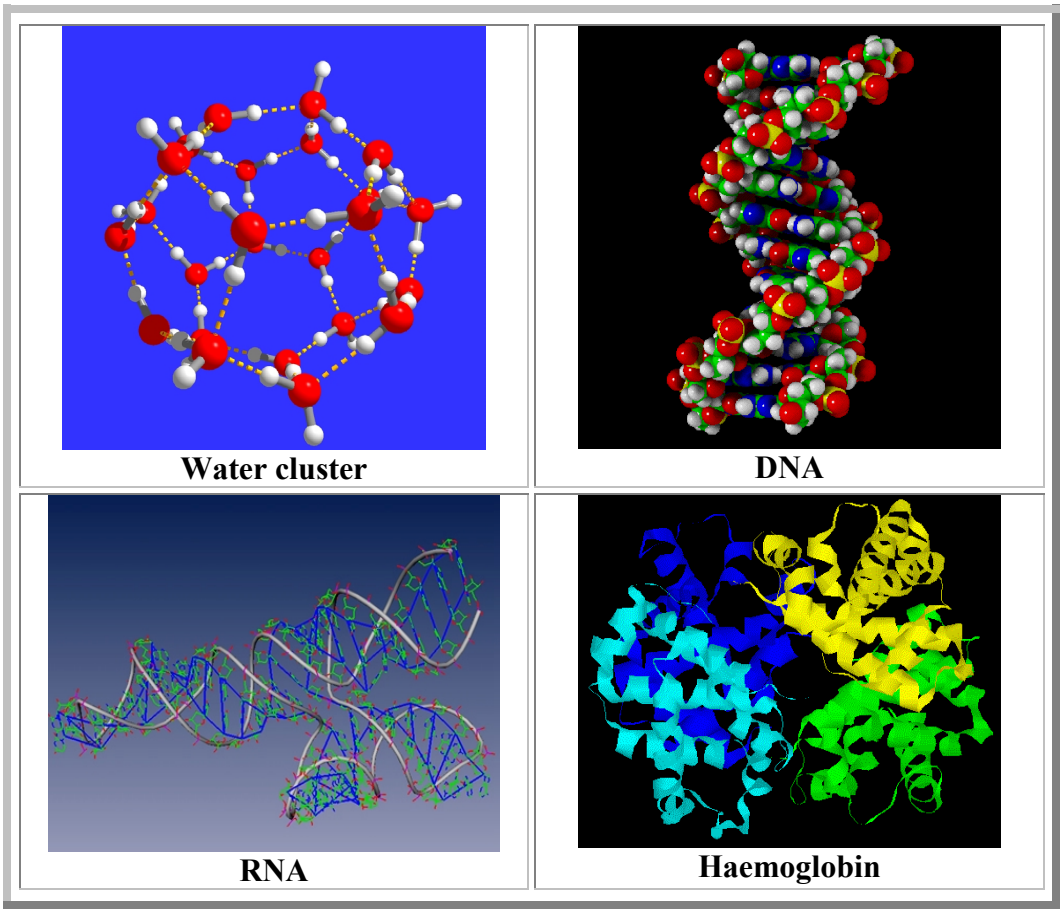

Further, much progress has been made in the design of molecular building sets which are often termed as "Tinker toys"[24] and "Molecular Meccano"[25] in the literature. Towards this, various hydrogen bonding interactions and metal-ligand coordination phenomena has been utilized in various supramolecular architectures. The most economical approach to design a self-assembling aggregate is to use only one self-complimentary molecule, as illustrated by Wuest and Ducharme in their work with the systems based on 2-pyridinone motif (see the Scheme 1). Crystalline 2-pyridinones are known to exist typically as hydrogen bonded dimers. This type of

associations was also found to occur, even in solutions as confirmed by ^{1}HNMR and ^{13}CNMR studies.[26]

Scheme 1

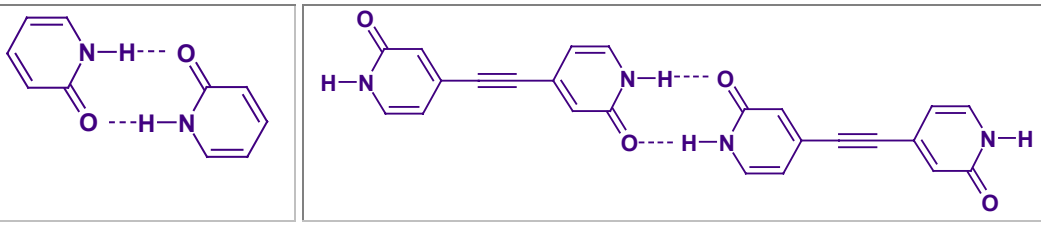

(a) (b)

Scheme 2

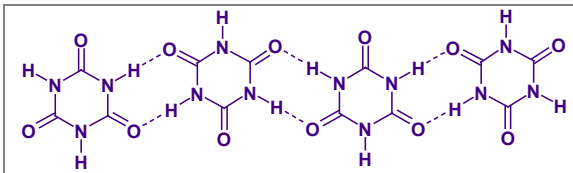

(a)

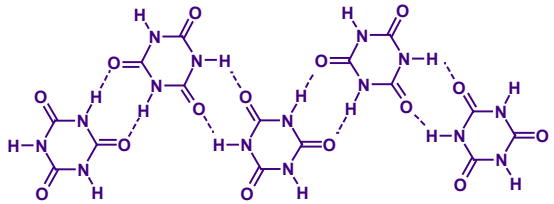

(b)

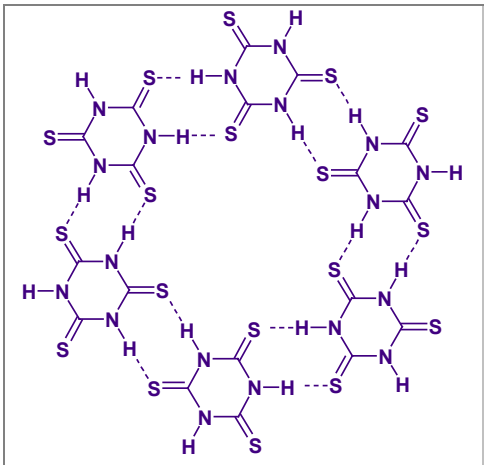

(c)

The utilization of the self-complimentary molecules was well elucidated through cyanuric acid and its thio-derivative for the synthesis of supramolecular assemblies, as shown in Scheme 2. Cyanuric acid (Scheme 2a and 2b) and trithiocyanuric acid undergo (Scheme 2c) self-assembly, by making use of N-H···O

and N-H···S hydrogen bond respectively in a predictable manner, to form the supramolecular assemblies that vary from tapes to cyclic architectures.[27]

Further, Whitesides and co-workers as well as Pedireddi and Rao have utilized the hydrogen bonding pattern of melamine and cyanuric acid to design a number of novel solid state structures and solution phase aggregates as shown in Scheme 3.[28-29] In these classes of supramolecular assemblies, the core is rigid and is therefore not dependent on the conformations of a flexible linker as in other systems. Wuest and co-workers termed those molecular building blocks that are independent of the conformational flexibility and the reaction conditions, yielding highly predictable molecular assemblies as *molecular tectons*.[30]

Scheme 3

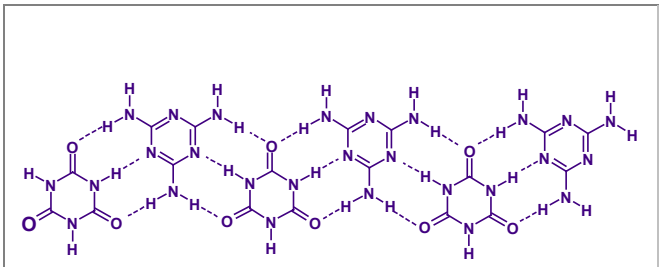

(a)

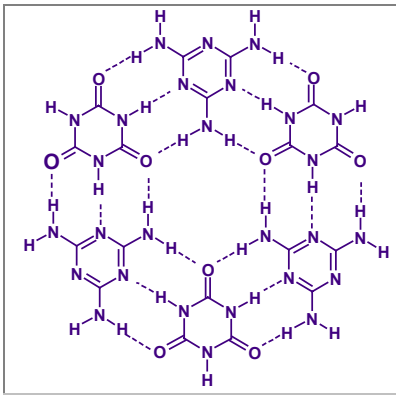

(b)

Thus the self-assembly is an attractive and viable alternative to covalent synthesis for the construction of large multicomponent architectures. The self-assembled complexes are in dynamic equilibrium with their monomeric components and alternative aggregates or complexes and the structure of the assembly is critically

dependent on solvent, concentration and other external influences like temperature pressure etc.[31] This understanding of the structure directing factors such as thermodynamics and the kinetics of the self-assembly and the creation of multi-component supramolecular architectures utilizing non-covalent bonding interactions and cooperativity, led to a new paradigm in the area of synthesis – *supramolecular synthesis.*[32]

1.4 Supramolecular Synthesis

Supramolecular chemistry is the chemistry of the intermolecular interactions, based on the underlying theme of mutual recognition.[33] Molecules recognize each other through a combination of geometrical and chemical factors and the complimentary relationship between interacting molecules is the characteristics of the recognition process. According to Dunitz, crystal is *"a supermolecule par excellence"*, an assembly of literally millions of molecules self-crafted by mutual recognition at an "amazing level of precision".[34] Thus, the crystal of a compound can be considered as the ultimate supermolecule and its assembly governed by various chemical and geometrical factors of individual molecules is the perfect example of solid-state molecular recognition, in other words, *crystal engineering*.

The need for rational approaches towards solid-state structures of fundamental and practical importance is the basis of crystal engineering, which seeks to understand intermolecular interactions and recognition phenomena in the context of crystal packing.[35] It has been developed by the structural chemists and crystallographers and

their quest to better understand various non-covalent interactions involved in the solid-state and to the design of novel materials and solid-state reaction strategies.[36] The motivation behind this broad interest is both scientific and utilitarian. While the studies of intermolecular bonds have great relevance for the fundamental sciences, they are also promising in terms of practical applications. This involves an intelligent control of the recognition and assembly processes that lead from components to superstructures via tailoring of intermolecular interactions resulting in materials with desired collective chemical and physical properties.[37]

The studies of the molecular assemblies in the context to supramolecular chemistry can be well-classified into

(i) The molecular recognition studies involving organic building blocks.

(ii) The studies of the metal-organic assemblies or coordination polymers.

Since the utilization of the solid state chemistry for the efficient photodimerization of *trans*-cinnamic acids, by Schmidt in the early 1960s, the molecular recognition studies of organic molecules emerged as a frontier area of research.[38] In these studies, the structural control in molecular materials is often frustrated by the delicate, noncovalent nature of the intermolecular interactions that govern solid-state assembly. This problem is readily apparent from numerous investigations wherein the desirable crystalline architectures are thwarted by an inability to maintain structural control when making even the slightest changes in the

structures of the molecular components. It becomes even more challenging when synthesizing materials consisting of two or more molecular components – *co-crystals*.[39] Though the hybrid nature of such materials can expand the range of achievable properties, multiple components add complexity with respect to the number of possible compositions and structural permutations. Design strategies therefore require predictable assembly, preferably through the use of molecular or supramolecular "modules" that organize through specific intermolecular interactions.[40] Further, new insights derived from modern supramolecular chemistry are paving way for the molecular level control of solid state structures with the arrangement of functional molecular components into defined solid architectures. The area of supramolecular chemistry of organic assemblies is well studied and documented in the literature as monographs, reviews and articles.[41-44]

1.5 Supramolecular chemistry of coordination assemblies

Coordination polymers are materials in which, the coordinate bonds formed between the organic molecules and the metal ions are utilized to generate a solid network and this approach offers great structural rigidity because the coordinate bonds are strong with explicit geometries.[45] Considering the design elements involved, the coordination polymers consist mainly of two central components – connectors and linkers.[46] In addition, there are other auxiliary components such as blocking ligands, counter ions and nonbonding guests or template molecules. Transition metal ions are often utilized as versatile connectors in the construction of coordination polymers.[47]

Depending on the metal ion, their oxidation states and coordination numbers, they can give rise to various geometries, which can be linear, T or Y–shaped, tetrahedral, square-planar, square-pyramidal, trigonal-bipyramidal, octahedral, trigonal-prismatic, pentagonal-bipyramidal and the corresponding distorted forms. Further the variation in the coordination numbers and the geometries can be realized by changing the reaction conditions such as solvents, counter ions and ligands.[48] Even though not well studied, lanthanide complexes with new and unusual network topologies and properties, are gaining interest in the recent time, due to their large coordination numbers and unprecedented properties.[49] In addition, the ability of numerous organic ligands with required functional groups that can facilitate the formation of dative bonds, added a great significance for the development of supramolecular chemistry of coordination assemblies. For example, the neutral linkers like, pyrazine, 4,4'-bipyridine, 1,2-bis(4-pyridyl)ethane and 1,2-bis(4-pyridyl)ethene, as well as various anionic linkers such as di-, tri-, tetra- and hexa-carboxylate molecules, have been extensively utilized in the preparation and analysis of the coordination assemblies.[50-52]

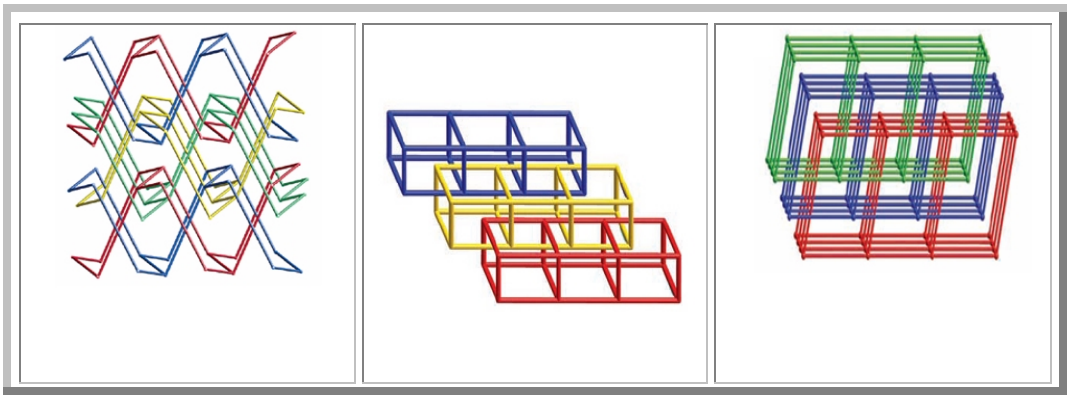

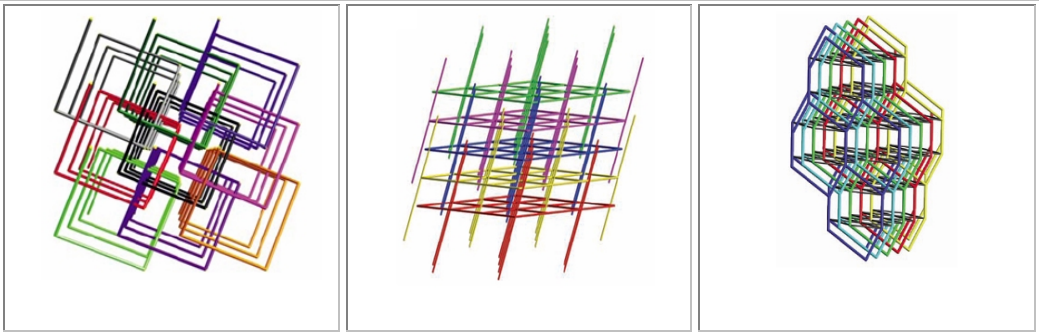

Figure 1: Schematic representation of various coordination assemblies reported in the recent literature.

Since the early 1990s, there has been an exponential growth in the research of the materials with polymeric structures based coordination complexes. Early papers by Robson, Moore, Yaghi, and Zaworotko highlighted the possibilities of the exotic architectures like porous networks, zeolite analogues, nanoballs, one-dimensional coordination polymers etc., as shown in Figure 1.[53-54] The novel properties offered by these coordination polymers, led to the advanced understandings of structure–property relationships in nanoporous framework hosts. In principle, through the wide choice of metal ions and the infinite variety of ligands, a broad range of structural, magnetic, electrical, optical, and catalytic properties might be rationally incorporated into such materials.[55-57]

One of the main advantages of the coordination assemblies over other porous materials is the easy and efficient synthetic methodologies and crystallization techniques available for their synthesis. These include slow evaporation of the reaction mixture, solvent diffusion vapor diffusion etc. by which the reaction mixtures are slowly allowed to form a homogeneous mixture.[58] Further, hydrothermal and

solvothermal techniques, which are essentially non-ambient synthetic strategies, are found to be popular to carry out reactions in which, the individual reactants are having solubility problem at the ambient conditions.[59]

Recently novel methodology like ionothermal synthesis, making use of the non-conventional organic solvents like, ionic liquids as the reaction media, has been shown to be a highly promising alternative synthetic route for the synthesis of a wide variety of zeotype network assemblies.[60] Development of faster and economical routes for the synthesis of MOFs and inorganic–organic hybrid solids is an integral aspect of materials science and often it is a challenging task in the supramolecular synthesis of coordination assemblies. In recent times, microwave-assisted synthesis has been effectively utilized to reduce the reaction time and this simple and energy-efficient heating process has become a rapidly developing synthetic method in the preparation metal-organic assemblies.[61] Further, green chemistry approaches like solvent-free grinding and solvent-drop grinding, as demonstrated by Jones and co-workers for the synthesis of organic assemblies, which was extended by Braga and co-workers for coordination assemblies, have emerged as an efficient route to generate MOFs in an environmental friendly manner.[62-63]

During the course of progress in the studies involving metal-organic assemblies, efforts have been made to extend the design, synthesis and characterization of coordination frameworks to incorporate specific functionalities into the nanoporous hosts, which was well discussed in a recent review by Kitagawa.[64] The pore walls of microporous coordination polymers generally consist of organic bridging

ligands, and therefore the properties of pore surface can be easily functionalized by the modifications using organic ligands, as shown in Figure 2. Such functionalized pore walls can be utilized for various chemical functions, like enantioselective separation, catalysis etc.[65-66] Lin *et. al.* utilized this approach for building a chiral framework, which was utilized for the catalysis of $ZnEt_2$ additions to aromatic aldehydes with efficiency and enantioselectivity.[67]

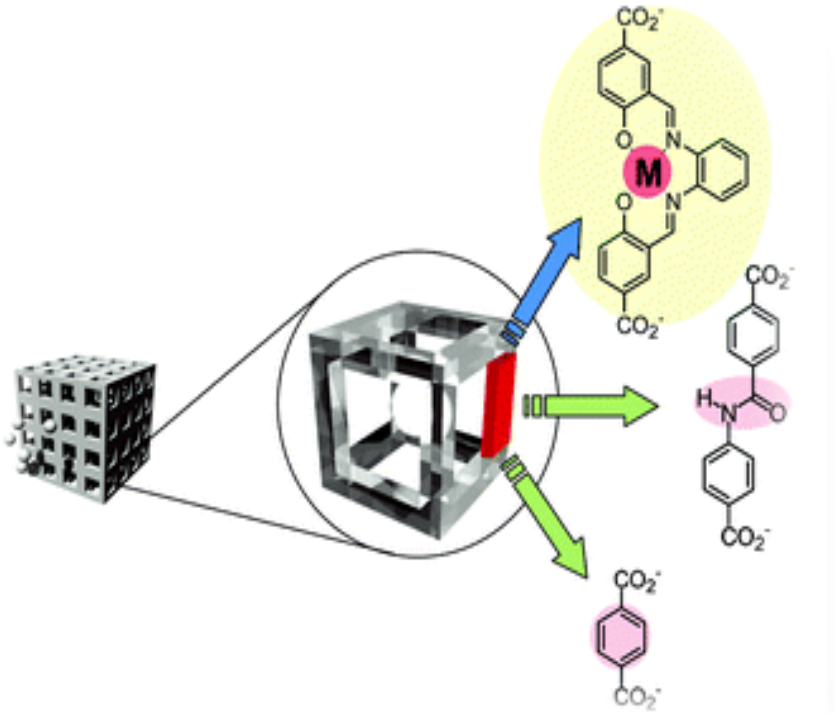

Figure 2: Schematic representation of surface engineering by dicarboxylate-type ligands in microporous coordination polymers

Another strategy is to incorporate metal sites capable of forming coordinatively unsaturated metal centers (UMCs), for example, by the removal of the coordinated water.[68] Since UMCs can interact with Lewis-base guests through coordination bonds, as schematically represented in Figure 3, they can show highly selective incorporation for guests as well as hydrogen bonding sites. While, this strategy was well utilized by Yaghi and co-workers for the hydrogen sorption studies,[69] Fujita and Kitagawa utilized the open metal sites as the catalyzing centers for cyanosilylation of imines and polymerization reactions respectively.[70-71]

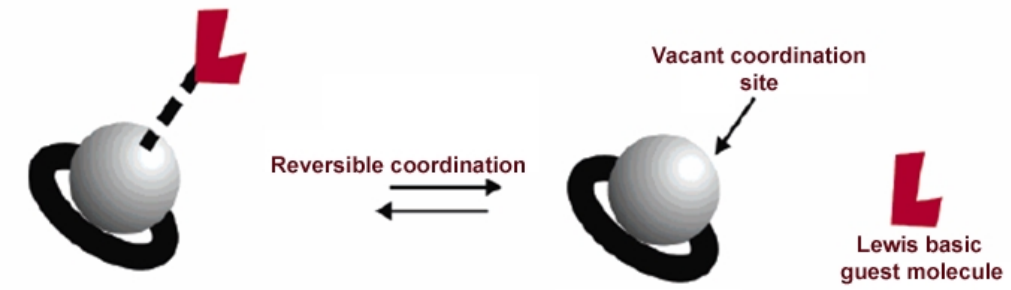

Figure 3: Principle of a coordinatively unsaturated metal complex as binding site for the reversible coordination of a lewis basic guest molecule

The stable metal-organic frameworks, formed by making use of coordinate bonds, are known to be highly versatile and further, it was exploited in the pursuit of unique properties, exhibited by these materials in the nanoporous environment, such as:

(i) Gas adsorption properties

(ii) Chemical functional properties

(iii) Electronic and magnetic properties

(iv) Optical properties

(v) Structural dynamic properties

These properties of metal-organic frameworks will be discussed in the following sections with the representative examples reported in the recent literature.

1.5.1 Gas Adsorption Properties

The quest to explore environmental friendly, renewable energy resources, led towards, exploring the opportunities for hydrogen fuel and its utility as an alternative energy resources. But, the conventional storage of large amounts of hydrogen in its molecular form is difficult and expensive because it requires employing either extremely high pressures (as a gas) or very low temperatures (as a liquid). However, metal-organic frameworks (MOFs), with their extraordinary low density (1.00 to 0.20 g/cm3) and high surface area (500 to 6000 m^2/g) make them ideal candidates for the storage and separation of gases such as H_2, N_2, Ar, CO_2 and CH_4. [72]

In 1999, Yaghi and co-workers reported the metal-organic framework (MOF-5) of composition Zn_4O(1,4-benzenedicarboxylate)$_3$ with three-dimensional porous structure, which adsorbed hydrogen up to 4.5 weight percent (17.2 hydrogen molecules per formula unit) at 78 K as shown in Figure 4b and 1.0 weight percent at room temperature and pressure of 20 bar.[73]

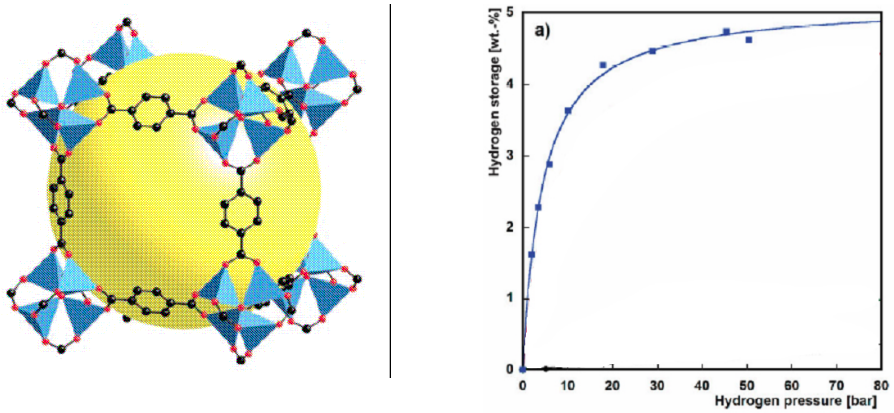

(a) **(b)**

Figure 4: (a) Solid-state structures of MOF-5 (b) Hydrogen gas sorption isotherm for MOF-5 at 77 K.

Further, various gas adsorption sites in several metal-organic frameworks, were examined and evaluated in detail to study the adsorption of Ar and N_2 on the internal surface of a large-pore open-framework material.[74] For example, in the case of MOF-5, five different primary adsorption sites on the $Zn_4O(CO_2)_6$ and the edgewise $C_6H_4\cdots Ar$ and $C_6H_4\cdots N_2$ interactions (as shown in Figure 5) previously unknown in gas-phase studies of aromatic van der Waals complexes, were identified.

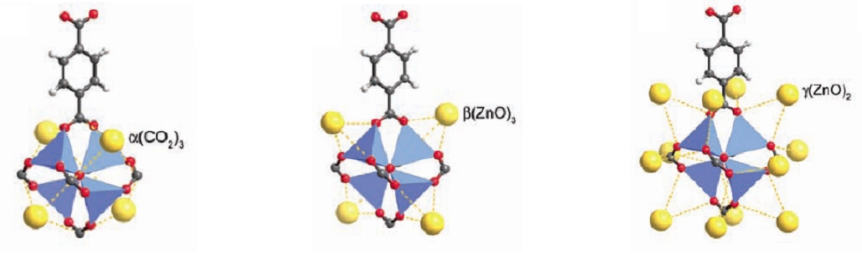

(a) **(b)** **(c)**

(d) **(e)**

Figure 5: Schematic representation of the symmetry-independent sites, partially occupied by Ar atoms, at 30 K (shown as yellow spheres) in the pores of MOF-5.

G. Férey *et al.* combined the targeted chemistry and computational design to create the crystal structure of porous chromium terephthalate, MIL-101, with very large pore sizes and surface area, as shown in figure 6. Its zeotype cubic structure has a giant cell volume (~702,000 $Å^3$), a hierarchy of extra-large pore sizes (~30 to 34 Å), and a Langmuir surface area for N_2 of ~5900 ± 300 m^2/gm. Hydrogen storage measurement revealed that the porous material has taken about 4.5 weight percent at 77 K and at 3 MPa, which seems to be the highest for MOFs.[75]

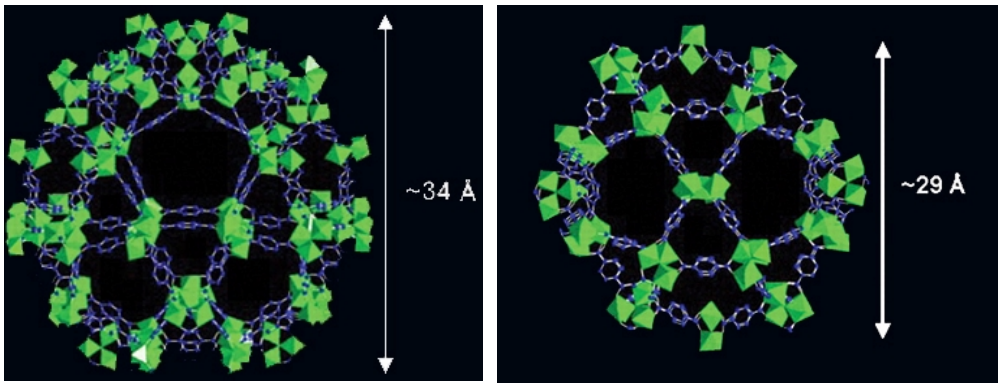

Figure 6: Ball-and-stick view of the two types of cages present in the

complex MIL-101.

In addition to hydrogen, the adsorption studies of various other gases as well as different hydrocarbons were also studied extensively.[76] In this regard, the dinitrogen isotherm measurement studies for MOF-177 at 77 K exhibits the highest uptake of N_2 (as shown in Figure 7b), for any material to date, and gives rise to a monolayer-equivalent surface area of 4500 m^2/g, with micropore volume calculated to be 0.69 cm^3 and the framework has cavities of 10.9–11.8 Å diameter connected in all directions by channels as revealed by single-crystal X-ray diffraction studies.[77]

Based on the knowledge gained from the numerous studies, several new postulates have been forwarded for the preparation of novel frameworks with better efficiency and utility. In this regard, it has been observed that, a material with high gravimetric and volumetric hydrogen capacity at practical conditions should have a high surface area with pores of appropriate dimension for hydrogen and a large heat of adsorption. [78] Thus, the creation of metal-organic frameworks focus for new materials with high surface area and appropriate void dimension that can evolve as potential candidates for the gas storage materials, is an upcoming new dimension in the studies of coordination assemblies.

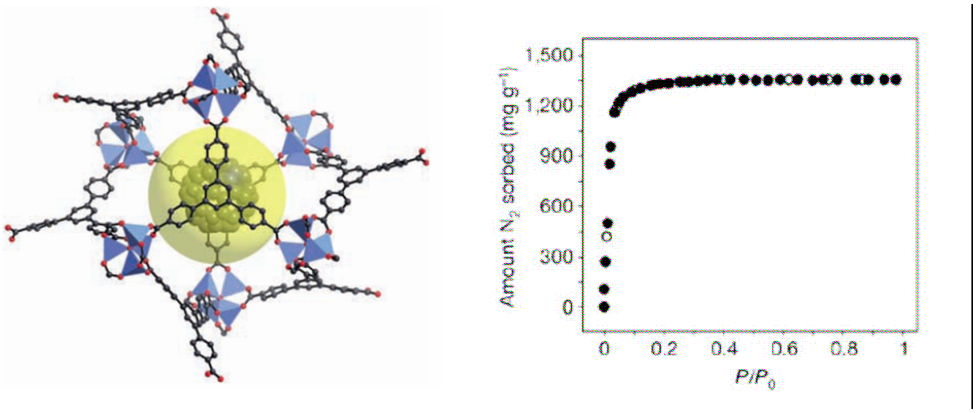

(a) **(b)**

Figure 7: Solid-state structures of (a) MOF-177 and (b) Nitrogen gas sorption isotherm at 78 K for MOF-177.

1.5.2 Chemical functional properties

The coordination polymers, with channels in their three-dimensional structures, provide reactive sites within the nanoporous environment. Among a number of chemical properties sought in the nanoporous environment of the chiral coordination assemblies, size, shape and enantioselective separation and catalytic properties have proven to be the most challenging and exciting.[79]

Lin and co-workers, recently illustrated the importance of homochiral assembly for the enantioselective catalytic activity. Towards this, they synthesized a chiral nanoporous assembly, $[Cd_3Cl_6$((R)-6,6'-dichloro-2,2'-dihydroxy-1,1'-binaphthyl-4,4'-bipyridine$)_3]$.x(guest) and did chemisorption of titanium isopropoxide sites onto the hydroxyl units of the chiral bridging ligands of the apohost, as shown in Figure 8, thus creating a chirally functionalized metal-organic framework. The resulting

functionalized solid was found to catalyze $ZnEt_2$ additions to aromatic aldehydes with efficiency and enantioselectivity comparable to those for the free $Ti(O^iPr)_2$-functionalised ligand.[80]

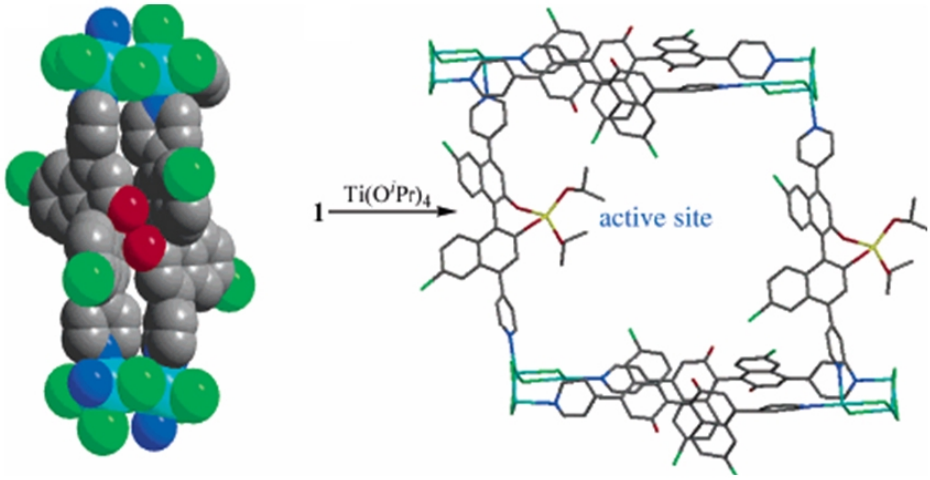

Figure 8: Representation of the post-synthetic modification of the chiral nanoporous framework [Cd_3Cl_6((R)-6,6'-dichloro-2,2'-dihydroxy-1,1'-binaphthyl-4,4'-bipyridine)$_3$] with titanium isopropoxide to form an enantioselective heterogeneous catalyst with active titanium sites.

Further, the utility of the one-dimensional nanochannels of crystalline porous compounds in the polymerization reactions were demonstrated successfully by Kitagawa and coworkers. In this case, the host components provide a specific molecular-level flask for the reaction of the monomeric guest molecules and allow low-dimensional restrained polymerization, which is different from the bulk and solution polymerization in conventional flasks. Towards this, the pillared-layer complex [{Cu_2(pyrazine-2,3-dicarboxylate)$_2$(4,4'-bipyridine)}$_n$] was utilized in

catalyzing the spontaneous polymerization of substituted acetylenes in the nanochannels.

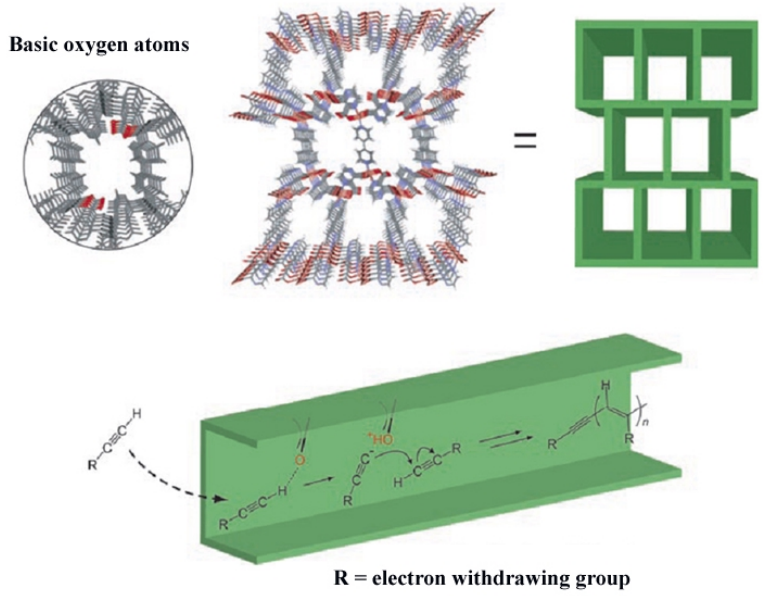

Figure 9: Spontaneous catalytic polymerization of substituted acetylenes in [{Cu_2 $(pzdc)_2(L)\}_n$] (L = 4,4'-bipyridine).

In the case of acidic mono-substituted acetylenes, the basic oxygen atoms from the carboxylate ligands in [{Cu_2(pyrazine-2,3-dicarboxylate)$_2$(4,4'-bipyridine)$\}_n$] produce the reactive acetylide species that subsequently initiate anionic polymerization in the nanochannel. The schematic representation of the polymerization reaction in the nanochannel is shown in Figure 9. The porous metal-organic framework leads to the drastic acceleration of the polymerization, yielding one dimensional molecular wires, formed in the restrained channels of the coordination complex.[81]

Further, the nanochannels of metal-organic frameworks can be utilized for the selective separation, as demonstrated for the separation of specific hydrocarbon from their other homologues. This was illustrated in a recent report, in which, the microporous metal-organic framework of [Cu(4,4'-(hexafluoroisopropylidene) bis(benzoate)(4,4'-(hexafluoroiso-propylidene)bis-(benzoic acid)$_{0.5}$], based on a bimetallic paddle wheels and one dimensional microchannels with hydrophobic internal surfaces was utilized to selectively adsorb C_2, C_3, and *n*-C_4 olefins and alkanes, as shown in Figure 10a.[82]

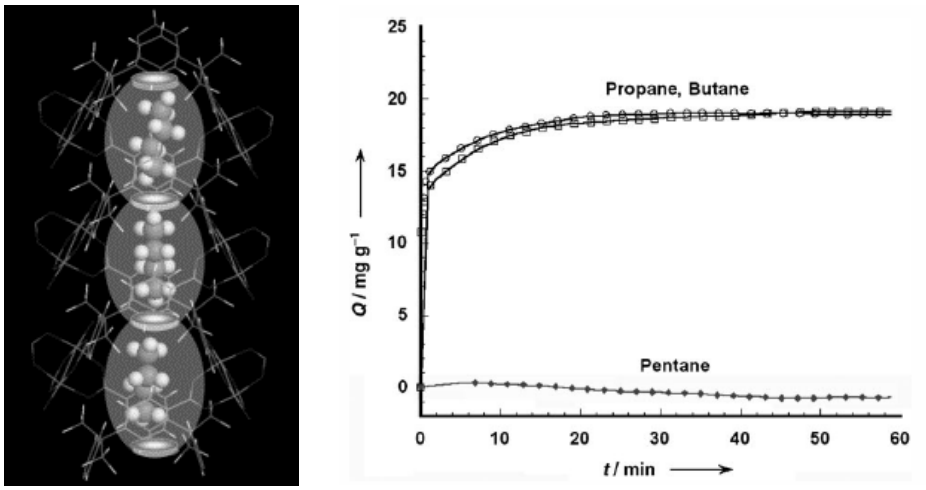

(a) **(b)**

Figure 10: (a) Arrangement of butane molecules in the microchannel of the metal organic porous assembly, [Cu(4,4'-(hexafluoroisopropylidene)bis (benzoate)(4,4'-hexafluoro-iso-propylidene)bis-(benzoic acid)$_{0.5}$], with one molecule per cage. (b) Adsorption of propane, butane, and pentane at 90^{o}C and 650 torr as a function of time and Q (the weight of hydrocarbon molecules adsorbed in the adsorbent).

Other than adsorption and separation, metal-organic frameworks can also be utilized to create host networks for several functional materials like, drug molecules, dyes, nonoparticles etc. While Yaghi and co-workers reported the quantitative inclusion of C_{60} and large polycyclic dye molecules (e.g. Astrazon Orange R) into the cavities of metal-organic framework, Fischer *et. al.* utilized the host network of MOF-5 to efficiently and selectively absorb palladium precursor, $[(\eta^5\text{-}C_5H_5)Pd(\eta^3\text{-}C_3H_5)]$ (see Figure 11) and the pentacarbonyl iron, $[Fe(CO)_5]$ by typical metal organic chemical vapor deposition (CVD) technique, to yield, a metal-organic assembly, with four $[(\eta^5\text{-}C_5H_5)Pd(\eta^3\text{-}C_3H_5)]$ precursors in the cavity.

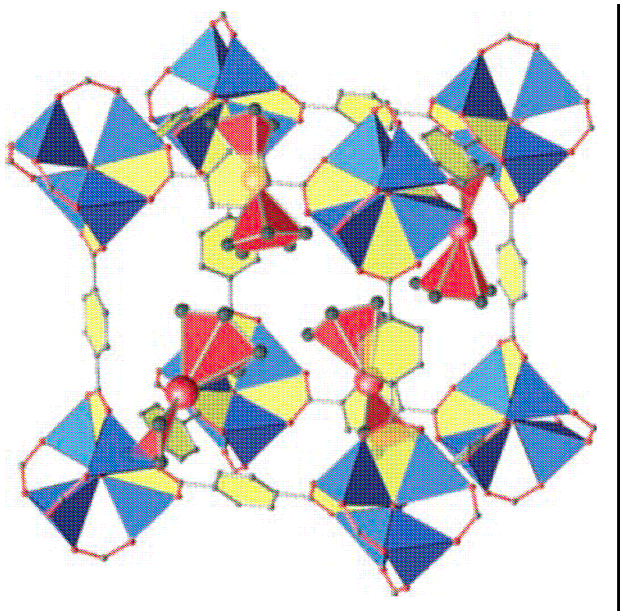

Figure 11: MOF-5 cage (blue/yellow) with four incorporated $[(\eta^5\text{-}C_5H_5)\ Pd(\eta^3\text{-}C_3H_5)]$ precursors (red).

It was found that the three-dimensional crystalline order of the MOF-host lattice remains unchanged after loading with the guest species. Further, incorporation

of nanoparticles of various metals such as Cu, Pd, Ag and metal oxide such as ZnO in the cavity of MOF-5 were also well demonstrate, highlighting the significance of host-guest chemistry of coordination polymers with porous networks.[83-85]

1.5.3 Electronic and magnetic properties

Making use of the knowledge of the electronic and magnetic properties of coordination complexes, efforts have been extended to the incorporation of these properties into porous molecular lattices.[86] A strong impetus for such efforts is the elucidation of structure–property relationships, since variation of sorbed guests provides a convenient method for systematically perturbing the host framework structure and, this in turn, their property. [87]

Spin crossover is a well known form of molecular switch in which the *d*-electron configuration of certain first-row transition metal ions (d^4-d^7) changes between high- and low-spin forms in response to external stimuli such as variations in temperature, pressure and irradiation.[88] Physical consequences of this transition include pronounced changes in color, magnetism and coordination bond distances. Guest-exchange in nanoporous spin crossover systems provides a new approach for investigating features such as the ligand field, electronic communication between spin crossover centres, and lattice dynamics.[89]

Spin crossover has recently been successfully incorporated directly into porous molecular lattices through the bridging of iron(II) spin crossover centers to form open frameworks. For example, the nanoporous phase $[Fe_2(trans\text{-}4,4'\text{-}azopyridine)_4(NCS)_4].(EtOH)$, displays a broad half spin crossover transition that depends on guest inclusion. Desorption of the unbound ethanol guests from this interpenetrated phase leads to a reversible single crystal to single crystal structural transformation in which the 1D pore channels collapse partially (see Figure 12).

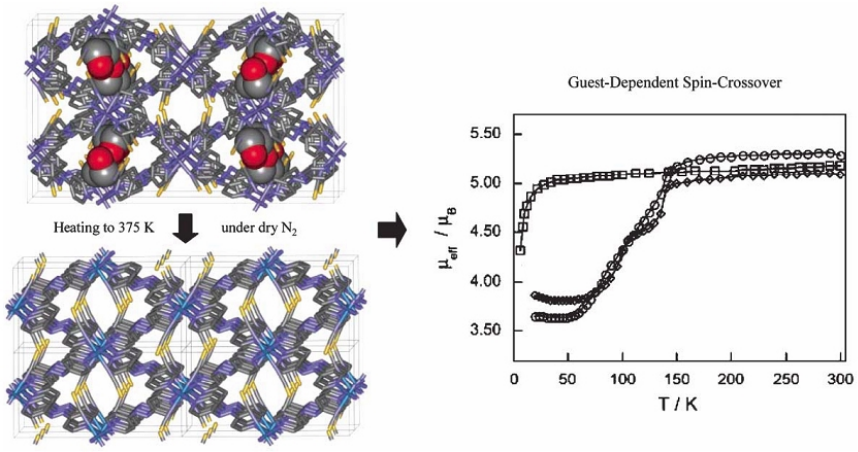

Figure 12: Representation of the guest-dependent spin-crossover nanoporous $[Fe_2(trans\text{-}4,4'\text{-}azopyridine)_4(NCS)_4]_n.(EtOH)$. Crystal structures of the as-synthesized at 150 K and evacuated sample at 375 K.

In contrast to the ethanol loaded material, the desorbed phase remains high spin to low temperature, which in turn may be due to the weakening of the ligand field with distortion of the coordination geometries following the guest removal, brought about by the structural changes in the vicinity of the iron(II) site, by the rotation of pyridyl donors and the loss of hydrogen bonding interactions between the ethanol

guest and the thiocyanate ligand bound at the iron(II) crossover site. Sorption of other alcohol guests, like 1-propanol '*switches back on*' the spin crossover sites, with subtle differences in behavior attributed to the steric influence of the guest on local iron(II) coordination geometry.[90]

In 2003, Real and co-workers reported the metal-organic framework, $[Fe^{II}(pyrimidine)(H_2O)\{Ag^{I}(CN)_2\}_2].H_2O$ and its Au analogue, that display spin crossover properties. The complex contain two independent iron(II) centres with differing coordination environment. Each of these phases undergo sharp half spin crossover transitions with appreciable hysteresis. Following the removal of both coordinated and uncoordinated water with reversible dehydration, a remarkable topochemical conversion occurs in which the pyrimidine molecules, previously bound only through one nitrogen atom, now bridge the two independent iron(II) centres, to form an extended assembly. The schematic representation of the variation in the coordination environment of the metal centre is shown in Figure 13. This conversion results in a change in the framework topology from the interpenetration of three separate three-dimensional networks to a single three-dimensional network and to large accompanying changes to the spin crossover properties.[91]

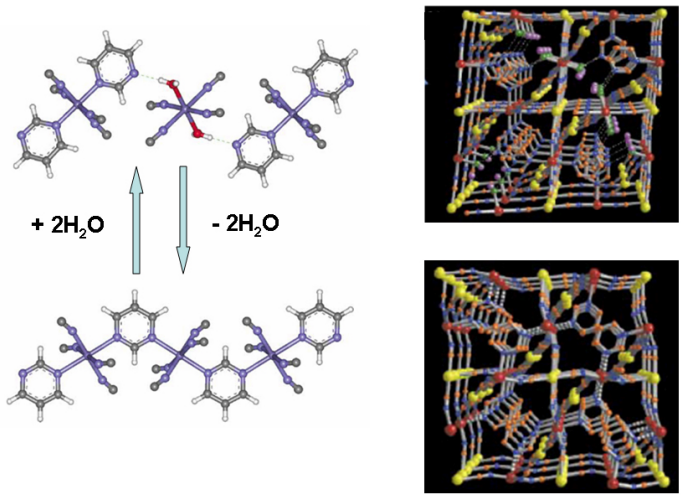

Figure 13: Reversible desorption of bound and unbound water molecules from the spin crossover frameworks $[Fe^{II}(pyrimidine)(H_2O)\{Ag^{I}(CN)_2\}_2]$ $.H_2O$. The three-dimensional packing arrangements are shown besides the corresponding metal-organic assemblies.

The magnetic properties of metal-organic frameworks opened new dimensions in the research of materials chemistry. Since the first report of open-framework complex, $[Cu_3(BTC)_2(H2O)_3]_n$, (wherein BTC = 1,3,5-benzene tricarboxylate ligand), with novel magnetic properties, emphasis towards utilization of metal ions as magnetic centres, become contemporary research frontier to develop metal-organic host networks with unprecedented magnetic properties.

Further, switching of the magnetic behavior of the metal-organic assemblies, with the sorption/desorption of the guest species – *solvato-magnetism* – have gained a lot of interest, as this property can be utilized in various applications like data transfer and storage. A highly pronounced solvato-magnetic effect has recently been observed

in a robust nanoporous framework, in which no change in metal coordination occurs with guest desorption.

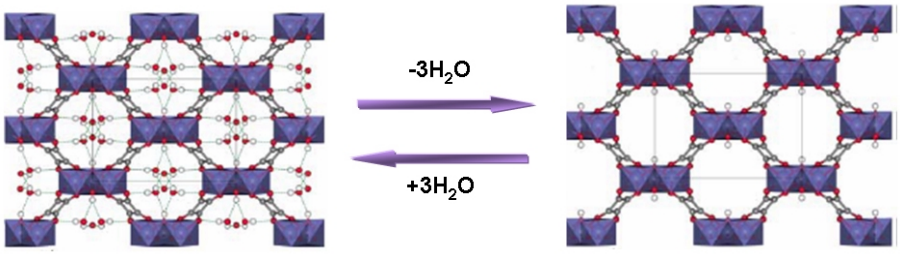

Figure 14: The schematic representation of the reversible dehydration of the coordination framework $[Co^{II}_3(OH)_2(C_4O_4)_2].3H_2O$ to $[Co^{II}_3(OH)_2(C_4O_4)_2]$.

Further, the reversible dehydration/rehydration of $[Co^{II}_3(OH)_2(C_4O_4)_2].\ 3H_2O$ leads to a reversible interconversion from antiferromagnetic to ferromagnetic ordering at low temperature. The host lattice, which consists of 1D $[Co^{II}_3(\mu 3\text{- } OH)_2]^{4+}$ ribbons linked by squarate anions to form a porous three dimensional network, undergoes only minimal changes with dehydration, suggesting that significant magnetic exchange coupling may occur through the hydrogen-bonded water molecules in the cavity of the hydrated phase (see Figure 14).[92]

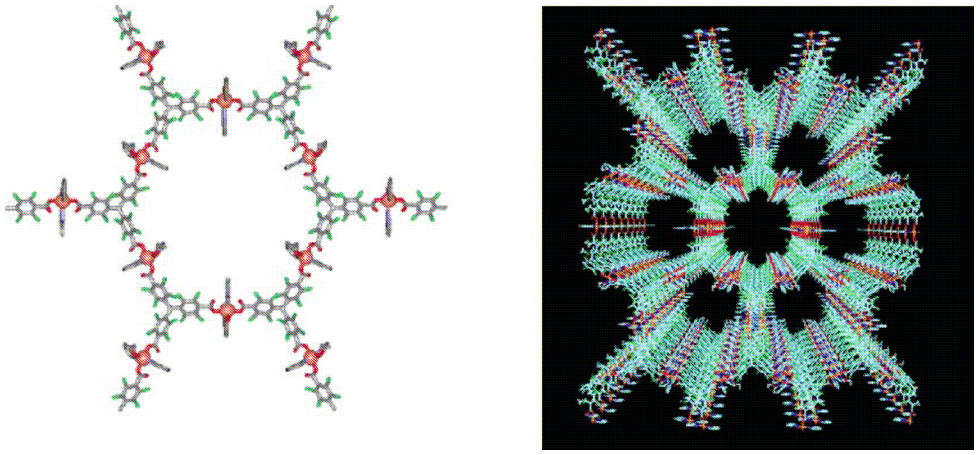

(a) **(b)**

Figure 15: (a) The two dimensional hexagonal layers of the nanoporous magnet Cu_3(*tris*-(4-carboxyphenyl)methyl)$_2$ (pyridine)$_6$(CH_3CH_2OH)$_2$ (H_2O) and (b) Channels formed in the crystal lattice.

In addition to the neutral ligands, radical bridging ligands are also employed for the preparation of metal-organic frameworks with solvate-magnetic behavior. A well cited example is the highly flexible nanoporous magnet Cu_3(*tris*-(4-carboxyphenyl)methyl)$_2$(pyridine)$_6$ (CH_3CH_2OH)$_2$ (H_2O), a two dimensional layered structure that contains Cu(II) centres bridged by polychlorinated *tris*-(4-carboxyphenyl)methyl radicals, as shown in Figure 15. This material shrinks and expands, up to 30% volume, with ethanol desorption/sorption and displays subtle solvato-magnetic effects associated with framework collapse and the removal of coordinated guests.[93]

Thus, the metal-organic frameworks find utility in the magnetic and electronic applications, as these materials can be fine-tuned by varying the guest species,

coordination environment of the metal centers and the ligands employed for the preparation of the frameworks.[94]

1.5.4 Optical properties

Coordination polymers are also known for the luminescence properties, owing to their higher thermal stability and the ability of affecting the emission wavelength of the organic material by metal coordination centre, usually through ligand-to-metal charge transfer (LMCT).[95] The combination of organic spacers and transition-metal centers in coordination polymers is seen as an efficient method for obtaining new types of electroluminescent materials for potential applications as light-emitting diodes (LEDs).[96] Further, the preparation of non-centrosymmetric coordination assemblies has exhibited its ability to be a potential candidate to the utilize in non-linear optical studies.

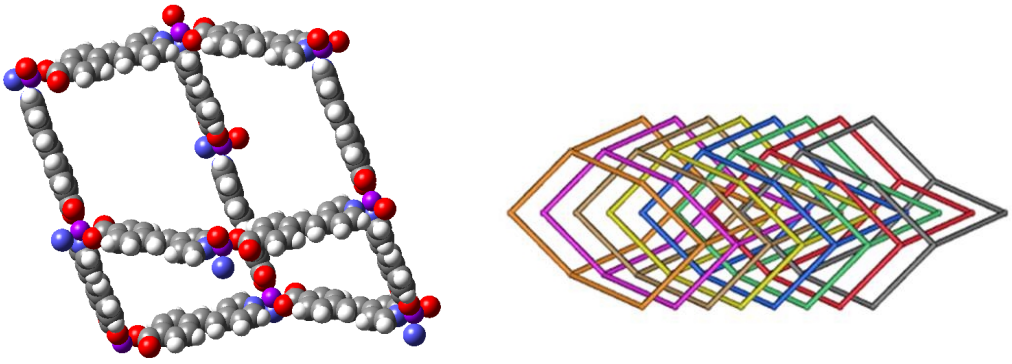

(a) **(b)**

Figure 16: (a) Diamondoid network structure of bis{4-[2-(4-pyridyl)ethenyl] benzoato}-zinc(II) complex. (b) Eight-fold interpenetration of the independent diamondoid nets in the complex.

For example, the coordination assemblies of bis{4-[2-(4-pyridyl) ethenyl]benzoato}-zinc(II) and cadmium(II) with 8-fold diamondoid network structures, as shown in Figure 16, prepared under hydrothermal conditions exhibit second harmonic generation efficiencies comparable to that of technologically important lithium niobate.[97]

As functional metal centers, rare earth metal ions are very attractive, due to their unusual coordination and chemical properites arising from 4f-electrons and the propensity to form isostructural complexes. Many coordination polymers based on rare earths have been synthesized and most of them exhibit amazing optical and magnetic properties, enabling them as fluorescent probes and IR-emitters.[98]

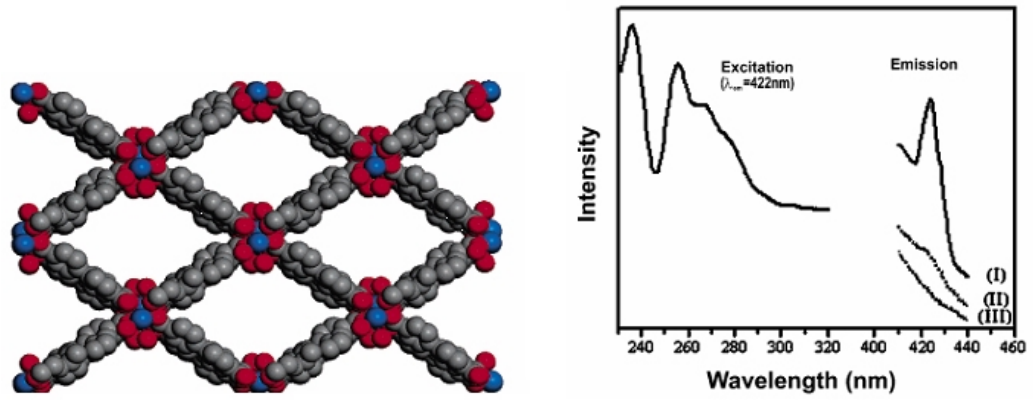

(a) **(b)**

Figure 17: (a) Large channels formed in the complex, [Tb(4,4'-biphenyl dicarboxylic acid)1.5(H2O)]0.5DMF. (b) Excitation and emission spectra of the complex excited at (I) 236 nm, (II) 285 nm and (III) 320 nm.

The recently reported, [M(4,4'-biphenyldicarboxylic acid)1.5(H2O)] 0.5DMF (M = Tb, Er, Ho, Yb), synthesized using a low-temperature solvent evaporation

method are the representative examples of rare earth based metal complexes in the optical property application studies. These coordination polymers are constructed from paddle-wheel building bocks, and form 25.15×17.09Å rhombic channels, without interpenetration, as shown in Figure 17a. These complexes exhibit strong fluorescence in the visible region, as shown in Figure 17b, while the Er-complex shows an Er^{3+} characteristic emission in the range 1450-1650 nm at room temperature. Thus, these complexes could be represented as potential fluorescent probes and an IR emitter, respectively.[99]

In addition, metal-organic frameworks with diamondoid and other non-centrosymmetric networks have been prepared and studied, in order to enable their utility in various opto-electronic applications. Recently, efforts are made to incorporate optical and electro-magnetic properties to metal-organic frameworks, by making use of hetero-bimetallic 3d-4f metal units, so that they can be utilized for novel applications like sensors, data storage and data transmission.[100-101]

1.5.5 Structural dynamic properties

The research in the area of metal-organic frameworks have developed a lot since it was first reviewed in 1964,[102] from the development of metal-organic assemblies that collapse after the removal of the guest species to those frameworks that adjust with the external stimuli or the incoming guest species. Porous coordination compounds were classified in the three categories, by Kitagawa.[103]

1) **Microporous frameworks**: They are sustained only with guest molecules and show irreversible framework collapse on removal of guest molecules.
2) **Stable and robust porous frameworks**: They show permanent porosity even without any guest molecules in the pores.
3) **Dynamic frameworks**: They respond to external stimuli, such as light, electric field, guest molecules, and change their channels or pores reversibly.

However, porous materials that exhibit both high framework stability and flexibility are comparatively rare.[104]

One of the best example of the dynamic behavior of coordination assemblies reported in the literature is the guest dependent behavior exhibited by the metal–organic assembly, [Zn_2(1,4-benzenedicarboxylic acid)$_2$(1,4-diazabicyclo[2.2.2]octane)]·4DMF·½H_2O, which shows unusual guest-dependent dynamic behavior – the framework shrinks upon guest inclusion and expands upon guest release, which is schematically represented in Figure 18. This was demonstrated by the guest absorption and desorption studies of the complex with benzene as the guest molecules, in which the square channels of the complex upon guest adsorption changes to the rhombic channels, brought about by the variation in the orientation of the dicarboxylic acid linker molecules.[105]

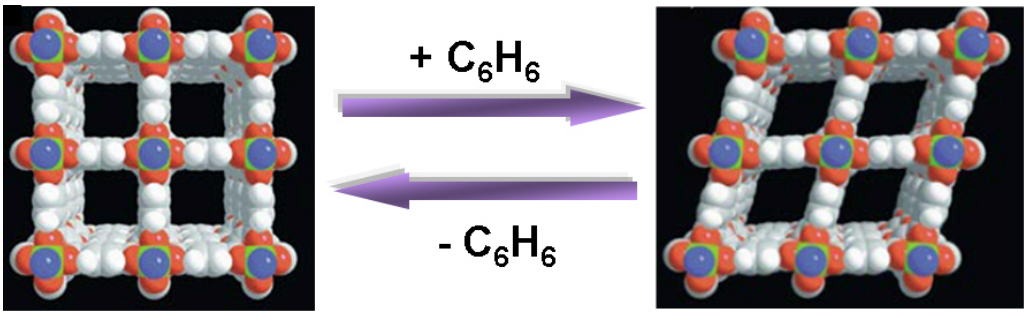

Figure 18: The schematic representation of the variation of the channel dimension upon adsorption and desorption of benzene guest molecules.

The guest induced structural transformation in the framework solids, was well demonstrated in a recent report of a Cr(III) assembly, {[Cr(OH)(1,4-benzenedicarboxylic acid)]. The transition between the hydrated form and the anhydrous solid is fully reversible and followed by a very high breathing effect; the pores being clipped in the presence of water molecules and reopened when the channels are empty, as shown in Figure 19.

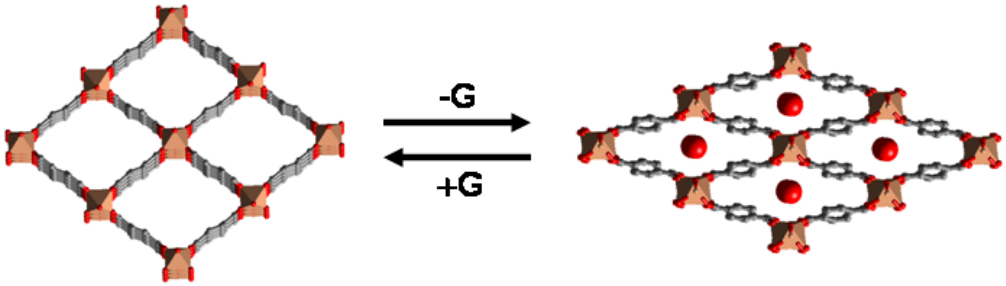

Figure 19: The structural representation of the complex, {[Cr(OH)(1,4-benzenedicarboxylic acid)], exhibiting reversible guest dependent dynamic response.

Further, it was observed that the water in the pores could be replaced on by DMF, but not topologically similar molecules like acetone or ethanol. This selectivity is attributed to the higher capability of DMF toward the formation of strong hydrogen bonds with the hydroxyl groups of the framework.[106]

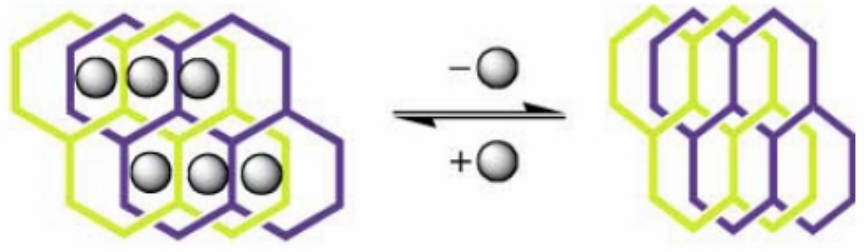

Figure 20: Schematic representation of the contraction and expansion of the 3D network on the removal or addition of guest molecules.

Another exotic example is a zinc complex, $[\{(ZnI_2)_3$ (2,4,6-tris(4-pyrdyl)triazine$)_2.6C_6H_5NO_2\}_n]$, that was reported to form an interpenetrated 3D network, with 60% of open space being occupied by the nitrobenzene molecules. A remarkable feature of the complex is the compression of the network without destroying the crystalline nature and network topology, as shown in Figure 20, when the guest molecules are released from the crystal lattice. The re-adsorption of the guest molecule yields the native complex. Further, the complex was utilized for the guest exchange reactions with various molecules like benzene, mesitylene, *cis*-stilbene and chloroform efficiently.[107]

1.6 Conclusions

Thus the ultimate goal in supramolecular chemistry is not only the design of specific structures, but also, engineering functional materials for practical applications such as nonlinear optics, magnetic materials, microporous solids, data storage, optical lasers and drug delivery. It has grown into an interdisciplinary field that seeks to develop the protocols for predicting and controlling the structures and thus the functional properties of solids. Some of the key research areas under the purview of this field include catalysis, optical materials, conducting and magnetic materials, nanotechnology electronic materials and sensors, protein-receptor binding, nano and microporous materials, supramolecular devices and molecular modeling.

1.7 References

(1) Carey, F. A.; Sundberg, R. J. *Advanced Organic Chemistry*, Plenum Press: New York, 1990.

(2) *Comprehensive Supramolecular Chemistry*; (Eds. Atwood, J. L.; Davies, J. E. D.; MacNicol, D. D.; Vögtle, F.) Pergamon: Oxford, 1996.

(3) (a) Lehn, J.-M. *Angew. Chem. Int. Ed.* **1988**, *27*, 89-112.

(4) Lehn, J.-M. *Supramolecular chemistry: concepts and perspectives*; VCH: Weinheim, 1995.

(5) Glusker, J. P. *Top. Curr. Chem.* **1998**, *198*, 1-56.

(6) Pauling, L. *The Nature of the Chemical Bond*; Cornell Univ. Press: New York, 1960.

(7) Latimer, W. M.; Rodebush, W. H. *J. Am. Chem. Soc.* **1920**, *42*, 1419-1433.

(8) Pimentel, G. C.; McClellan, A. L. *The Hydrogen Bond*; Freeman: San Francisco, 1960.

(9) Taylor, R.; Kennard, O. *J. Am. Chem. Soc.* **1982**, *104*, 5063-5070.

(10) Etter, M. C. *Acc. Chem. Res.* **1990**, *23*, 120-126.

(11) Leiserowitz, L. *Acta Crystallogr., Sect.B* **1976**, *B32*, 775-802.

(12) Schmidt, G. M. J. *J. Chem. Soc.* **1964**, 2014-2021.

(13) Desiraju, G. R. *Angew. Chem. Int. Ed.* **1995**, *34*, 2311-2327.

(14) Steiner, T. *Angew.Chem.Int.Ed.* **2002**, *41*, 48-76.

(15) Jeffrey, G. A.; Saenger, W. *Hydrogen bonding in biological structures*; Springer-Verlag: Berlin, 1991.

(16) Etter, M. C.; MacDonald, J. C.; Bernstein, J. *Acta Crystallogr., Sect.B* **1990**, *B46*, 256-262.

(17) Lehn, J.-M. *Angew. Chem. Int. Ed.* **1990**, *29*, 1304-1319.

(18) Tecilla, P.; Dixon, R. P.; Slobodkin, G.; Alavi, D. S.; Waldeck, D. H.; Hamilton, A. D. *J. Am. Chem. Soc.* **1990**, *112*, 9408-9410.

(19) Whitesides, G. M.; Simanek, E. E.; Mathias, J. P.; Seto, C. T.; Chin, D. N.; Mammen, M.; Gordon, D. M. *Acc.Chem.Res.* **1995**, *28*, 37-44.

(20) Ludwig, R. *Angew. Chem. Int. Ed.* **2001**, *40*, 1808-1827.

(21) Watson, J. D.; Crick, F. H. C. *Nature* **1953**, *171*, 964-967.

(22) Maeda, K.; Yashima, E. *Top. Curr. Chem.* **2006**, *265*, 47-88.

(23) (a) Xu, J.; Raymond, K. N. *Angew. Chem. Int. Ed*. **2006**, *45*, 6480-6485. (b) Pfeil, A.; Lehn, J. –M. *Chem. Commun.* **1992**, 838-840.

(24) Michl, J.; Magnera, T. F., *Proc. Natl. Acad. Sci*. **2002**, *99*, 4788-4792.

(25) Cantrill, s. J.; Pease, A. R.; Stoddart, F. J. *Dalton Trans*. **2000**, 3715-3734.

(26) Wuest, J. D. *Chem. Commun.* **2005**, 5830-5837.

(27) Ahn, S.; PrakashaReddy, J.; Kariuki, B. M.; Chatterjee, S.; Ranganathan, A.; Pedireddi, V. R.; Rao, C. N. R.; Harris, K. D. M. *Chem. Eur. J.* **2005**, *11*, 2433-2439.

(28) Whitesides, G. M.; Mathias, J. P.; Seto, C. T. *Science*, **1991**, *254*, 1312-1319.

(29) Ranganathan, A.; Pedireddi, V. R.; Rao, C. N. R. *J. Am. Chem. Soc.* **1999**, *121*, 1752-1753.

(30) Hosseini, M. W. *Acc. Chem. Res.* **2005**, *38*, 313-323.

(31) Gillard, R. E.; Raymo, F. M.; Stoddart, J. F. *Chem. Eur. J.* **1997**, *3*, 1933-1940 and references within.

(32) (a) *The crystal as a supramolecular entity, Perspectives in supramolecular chemistry*; Wiley: Chichester, 1995; Supramolecular organization and Material Design; (Eds. Jones, W.; Rao, C. N. R.); Cambridge University Press: Cambridge, 2002; (b) Metrangolo, P.; Resnati, G. *Chem. Eur. J.* **2001**, *7*, 2511-2519.

(33) Dunitz, J. D.; Gavezzotti, A. *Angew. Chem. Int. Ed.* **2005**, *44*, 1766-1787.

(34) Dunitz, J. D. *Pure Appl. Chem.* **1991**, *63*, 177-185.

(35) Desiraju, G. R. *Crystal Engineering. The design of organic solids*; Elsevier: Amsterdam, 1989.

(36) Braga, D. *Chem. Commun.* **2003**, 2751-2754.

(37) Hollingsworth, M. D. *Science* **2002**, *295*, 2410-2413.

(38) Bregman, J.; Osaki, K.; Schmidt, G. M. J.; Sonntag, F. I. *J. Chem. Soc.* **1964**, 2021-2030.

(39) Fan, E.; Vicent, C.; Geib, S. J.; Hamilton, A. D. *Chem. Mater.* **1994**, *6*, 1113-1117.

(40) Aakeröy, C. B. *Acta Crystallogr., Sect. B* **1997**, *B53*, 569-586.

(41) Bernstein, J.; Etter, M. C.; Leiserowitz, L. The Role of Hydrogen Bonding in Molecular Assemblies; In *Structure Correlations*; (Eds. Dunitz, J. D., Burgi, H.-B.); VCH: Weinheim, 1994; pp 431-507.

(42) (a) Subramanian, S.; Zaworotko, M. J. *Coord. Chem. Rev.* **1994**, *137*, 357-401. (b) Braga, D.; Grepioni, F. *Angew. Chem. Int. Ed.* **2004**, *43*, 4002-4011.

(43) (a) Fyfe, M. C. T.; Stoddart, J. F. *Acc. Chem. Res.* **1997**, *30*, 393-401; (b) Bishop, R. *Synlett*, **1999**, *9*, 1351-1358.

(44) Lehn, J.-M. *Angew. Chem. Int. Ed.* **1990**, *29*, 1304-1319

(45) Cotton, F. A.; Wilkinson, G. *Advanced Inorganic Chemistry*; Wiley: NewYork, 1988.

(46) Kitagawa, S.; Kitaura, R.; Noro, S. *Angew. Chem. Int. Ed.* **2004**, *43*, 2334-2375.

(47) Swiegers, G. F.; Malefetse, T. J. *Chem. Rev.* **2000**, *100*, 3483-3537.

(48) (a) Abourahma, H.; Moulton, B.; Kravtsov, V.; Zaworotko, M. J. *J. Am. Chem. Soc.* **2002**, *124*, 9990-9991. (b) Hennigar, T. L.; MacQuarrie, D. C.; Losier, P.; Rogers, R. D.; Zaworotko, M. J. *Angew. Chem. Int. Ed.* **1997**, *36*, 972-973. (c)

Holmes, K. E.; Kelly, P. F.; Elsegood, M. R. J. *Dalton Trans.* **2004**, 3488-3494. (d) Masaoka, S.; Tanaka, D.; Nakanishi, Y.; Kitagawa, S. *Angew. Chem. Int. Ed.* **2004**, *43*, 2530-2534; (e) Moulton, B.; Zaworotko, M. J. *Chem. Rev.* **2001**, *101*, 1629-1658.

(49) Long, D.; Blake, A. J.; Champness, N. R.; Wilson, C.; Schröder, M. *Chem. Eur. J.* **2002**, *8*, 2026-2033.

(50) Férey, G.; Mellot-Draznieks, C.; Serre, C.; Millange, F.; Dutour, J.; Surblé, S.; Margiolaki, I. *Science* **2005**, *309*, 2040-2042.

(51) (a) Abourahma, H.; Moulton, B.; Kravtsov, V.; Zaworotko, M. J. *J. Am. Chem. Soc.* **2002**, *124*, 9990-9991. (b) Wang, X.; Qin, C.; Wang, E. *Cryst. Growth Des.* **2006**, *6*, 439-443.

(52) Kitaura, R.; Kitagawa, S.; Kubota, Y.; Kobayashi, T. C.; Kindo, K.; Mita, Y.; Matsuo, A.; Kobayashi, M.; Chang, H.; Ozawa, T. C.; Suzuki, M.; Sakata, M.; Takata, M. *Science* **2002**, *298*, 2358-2361.

(53) Batten, S. R.; Robson, R. *Angew. Chem. Int. Ed.* **1998**, *37*, 1460-1494.

(54) (a) Ockwig, N. W.; Friedrichs, O. D.; O'Keeffe, M.; Yaghi, O. M. *Acc. Chem. Res.* **2005**, *38*, 176-182. (b) Perry, J. J.; McManus, G. J.; Zaworotko, M. J. *Chem. Commun.* **2004**, *10*, 2534-2535. (c) Wang, Z.; Kravtsov, V. C.; Zaworotko, M. J. *Angew. Chem. Int. Ed.* **2005**, *44*, 2877-2880.

(55) (a) Jun, Y. L.; Sung, J. H.; Kim, C.; Kim, S. J.; Kim, Y. *Inorg. Chem. Commun.* **2005**, *8*, 692-696. (b) Janiak, C. *Dalton Trans.* **2003**, 2781-2804.

(56) Amabilino, D. B.; Veciana, J. *Top. Curr. Chem.* **2006**, *265*, 253-302.

(57) Armaroli, N.; Accorsi, G.; Holler, M.; Moudam, O.; Nierengarten, J.; Zhou, Z.; Wegh, R. T.; Welter, R. *Adv. Mater.* **2006**, *18*, 1313-1316.

(58) Kitaura, R.; Fujimoto, K.; Noro, S.; Kondo, M.; Kitagawa, S. *Angew. Chem. Int. Ed.* **2002** , *41*, 133-135.

(59) Lu, J. Y. *Coord. Chem. Rev.* **2003**, *246*, 327-347 and references within.

(60) Lin, Z.; Wragg, D. S.; Morris, R. E. *Chem. Commun.* **2006**, 2021-2023.

(61) Rajic, N.; Stojakovic, D.; Logar, N. Z.; Kaucic, V. *J. Por. Mater.* **2006**, *13*, 153-156.

(62) Trask, A. V.; Motherwell, W. D. S.; Jones, W. *Cryst. Growth Des.* **2005**, *5*, 1013-1021.

(63) (a) Braga, D.; D'Addario, D.; Giaffreda, S. L.; Maini, L.; Polito, M.; Grepioni, F. *Top. Curr. Chem.* **2006**, *254*, 71-94. (b) Braga, D.; Grepioni, F. *Angew. Chem. Int. Ed.* **2004**, *43*, 4002-4011.

(64) Kitagawa, S.; Noro, S.; Nakamura, T. *Chem. Commun.* **2006**, 701-707.

(65) Langley, P. J.; Hulliger, J. *Chem. Soc. Rev.* **1999**, *28*, 279-291.

(66) Terpin, A. J.; Ziegler, M.; Johnson, D. W.; Raymond, K. N. *Angew. Chem. Int. Ed.* **2001**, *40*, 157-160.

(67) Wu, C. D.; Hu, A.; Zhang, L.; Lin, W. *J. Am. Chem. Soc.* **2005**, *127*, 8940-8941.

(68) Eddaoudi, M.; Moler, D. B.; Li, H.; Chen, B.; Reineke, T. M.; O'Keeffe, M.; Yaghi, O. M. *Acc. Chem. Res.* **2001**, *34*, 319-330.

(69) Chen, B.; Ockwig, N. W.; Millward, A. R.; Contreras, D. S.; Yaghi, O. M. *Angew. Chem. Int. Ed.* **2005**, *44*, 4745-4749.

(70) Ohmori, O.; Fujita, M. *Chem. Commun*. **2004**, 1586-1587.

(71) Uemura, T.; Horike, S.; Kitagawa, S. *Chem. Asian J*. **2006**, *1*, 36-44.

(72) Rosi, N. L.; Eckert, J.; Eddaoudi, M.; Vodak, T.; Kim, J.; O'Keeffe, M.; Yaghi, O. M. *Science* **2003**, *300*, 1127-1129.

(73) Li, H.; Eddaoudi, M.; O'Keeffe, M.; Yaghi, O. M. *Nature* **1999**, *402*, 276-279.

(74) (a) Rowsell, J. L. C.; Spencer, E. C.; Eckert, J.; Howard, J. A. K.; Yaghi, O. M. *Science* **2005**, *309*, 1350-1354. (b) Rowsell, J. L. C.; Eckert, J.; Yaghi, O. M. *J. Am. Chem. Soc*. **2005**, *127*, 14904-14910.

(75) Férey, G.; Mellot-Draznieks, C.; Serre, C.; Millange, F.; Dutour, J.; Surblé, S.; Margiolaki, I. *Science* **2005**, *309*, 2040-2042.

(76) Rowsell, J. L. C.; Yaghi, O. M. *Micropor. Mesopor. Mater.* **2004**, *73*, 3-14.

(77) Sudik, A. C.; Millward, A. R.; Ockwig, N. W.; Côte, A. P.; Kim, J.; Yaghi, O. M. *J. Am. Chem. Soc*. **2005**, *127*, 7110 -7118.

(78) Rowsell, J. L. C.; Yaghi, O. M. *Angew. Chem. Int. Ed.* **2005**, *44*, 4670-4679.

(79) (a) Xiong, R.; Tou, X.; Abrahams, B. F.; Xue, Z.; Che, C. *Angew. Chem. Int. Ed.* **2001**, *40*, 4422-4425. (b) Notestein, J. M.; Katz, A. *Chem. Eur. J.* **2006**, *12*, 3954-3965. (c) Brammer, L. *Chem. Soc. Rev.* **2004**, *33*, 476-489.

(80) Wu, C. D.; Hu, A.; Zhang, L.; Lin, W. *J. Am. Chem. Soc.*, **2005**, *127*, 8940-8941.

(81) Uemura, T.;Kitaura, R.; Ohta, Y.; Nagaoka, M.; Kitagawa, S. *Angew. Chem. Int. Ed.* **2006**, *45*, 4112-4116.

(82) Pan, L.; Olson, D. H.; Ciemnolonski, L. R.; Heddy, R.; Li, J. *Angew. Chem. Int. Ed.* **2006**, *45*, 616-619.

(83) Hermes, S.; Schrter, M.; Schmid, R.; Khodeir, L.; Muhler, M.; Tissler, A.; Fischer, R. W.; Fischer, R. A. *Angew. Chem. Int. Ed.* **2005**, *44*, 6237-6241.

(84) Kitaura, R.; Fujimoto, K.; Noro, S.; Kondo, M.; Kitagawa, S. *Angew. Chem. Int. Ed.* **2002**, *41*, 133-135.

(85) (a) Song, Y.; Zhou, T.; Wang, X.; Li, X.; Xiong, R. *Cryst. Growth Des.* **2006**, *6*, 14-17: (b) Tynan, E.; Jensen, P.; Kelly, N. R.; Kruger, P. E.; Lees, A. C.; Moubaraki, B.; Murray, K. S. *Dalton Trans.* **2004**, 3440-3447.

(86) Douglas, B. E.; McDaniel, D. H.; Alexander, J. J. *Concepts and Models of Inorganic Chemistry*, Wiley: New York, 1994.

(87) Sato, Y.; Ohkoshi, S.; Arai, K.; Tozawa, M.; Hashimoto, K. *J. Am. Chem. Soc.*, **2003**, *125*, 14590-14595.

(88) Kepert, C. J. *Chem. Commun.* **2006**, 695-700 and references within.

(89) Gaspar, A.B., Ksenofontov, V.; Seredyuk, M.; Gütlich, P. *Coord. Chem. Rev.* **2005**, *249*, 2661-2676 and references within.

(90) Halder, G. J.; Kepert, C. J.; Moubaraki, B.; Murray, K. S.; Cashion, J. D. *Science*, **2002**, *298*, 1762-1765.

(91) Neil, V.; Thompson, A. L.; Muñoz, M. C.; Galet, A.; Goeta, A. E.; Real, J. A. *Angew. Chem. Int. Ed.* **2003**, *42*, 3760-3763.

(92) Kurmoo, M.; Kumagai, H.; Chapman, K. W.; Kepert, C. J. *Chem. Commun.* **2005**, 3012-3014.

(93) Maspoch, D,; Ruiz-Molina, D.; Wurst, K.; Domingo, N.; Cavallini, M.; Biscarini, F.; Tejada, J.; Rovira, C.; Veciana, J. *Nat. Mater.*, **2003**, *2*, 190-195.

(94) Aumüller, A.; Erk, P.; Klebe, G.; Hünig, S.; von Schütz, J. U.; Werner, H. P. *Angew. Chem. Int. Ed.*, **1986**, *25*, 740-741.

(95) Owen, S. M.; Brooker, A. T. *A Guide to Modern Inorganic Chemistry*, Longman Group: London, 1991.

(96) Coe, B. J.; Curati, N. R. M. *Comm. Inorg. Chem.* **2004**, *25*, 147-184.

(97) Lin, W.; Ma, L.; Evans, O. R. *Chem. Commun.* **2000**, 2263-2264.

(98) (a) Bunzli, J. –C. G.; Piquet, C. *Chem. Soc. Rev*. **2005**, *34*, 1048-1077. (b) Tissue, B. M. *Chem. Mater*. **1998**, *10*, 2837-2845.

(99) Guo, X.; Zhu, G.; Fang, Q.; Xue, M.; Tian, Ge.; Sun, J.; Li, X.; Qiu, X. *Inorg. Chem.* **2005**, *44*, 3850-3855.

(100) (a) Liu, F.-C.; Zeng, Y.-F.; Jiao, J.; Li, J.-R.; Bu, X.-H.; Ribas, J.; Batten, S. R. *Inorg. Chem*. **2006**, *45*, 6129-6131. (b) Yue, Q.; Yang, J.; Li, G.-H.; Li, G.-D.; Xu, W.; Chen, J.-S.; Wang, S.-N. *Inorg. Chem*. **2005**, *44*, 5241-5246.

(101) (a) Trembley, M. S.; Sames, D. *Chem. Commun.* **2006**, 4116-4118. (b) Wong, W.; Liang, H.; Wong, W.; Cai, Z.; Li, K.; Cheah, K. *New J. Chem*., **2002**, 275-278.

(102) Bailar, Jr., J. C. *Prep. Inorg. React*. **1964**, 1-16.

(103) Kitagawa, S.; Kondo, M. *Bull. Chem. Soc. Jpn*. **1998**, *71*, 1739-1753.

(104) (a) Miyata, M.; Shibakami, M.; Chirachanchai, S.; Takemoto, K.; Kasai, N.; Miki, K. *Nature*, **1990**, *343*, 446-446. (b) Lipkowski, J. in *Inclusion Compounds*

1984-1991, ed. Atwood, J. L.; Davies, J. E. D.; MacNicol, D. D. 1984, vol.1, pp 59-103.

(105) Dybtsev, D. N.; Chun, H.; Kim, K. *Angew. Chem. Int. Ed.* **2004**, *43*, 5033-5036.

(106) Serre, C.; Millange, F.; Thouvenot, C.; Nogues, M.; Marsolier, G.; Louer, D.; Férey, G. *J. Am. Chem. Soc.* **2002**, *124*, 13519-13526.

(107) Biradha, K.; Fujita, M. *Angew. Chem. Int. Ed.* **2002**, *41*, 3392-3395.

Chapter-2

Role of Solvent of Crystallization and Aza-donor Ligands in the Self-assembly of Coordination Polymers

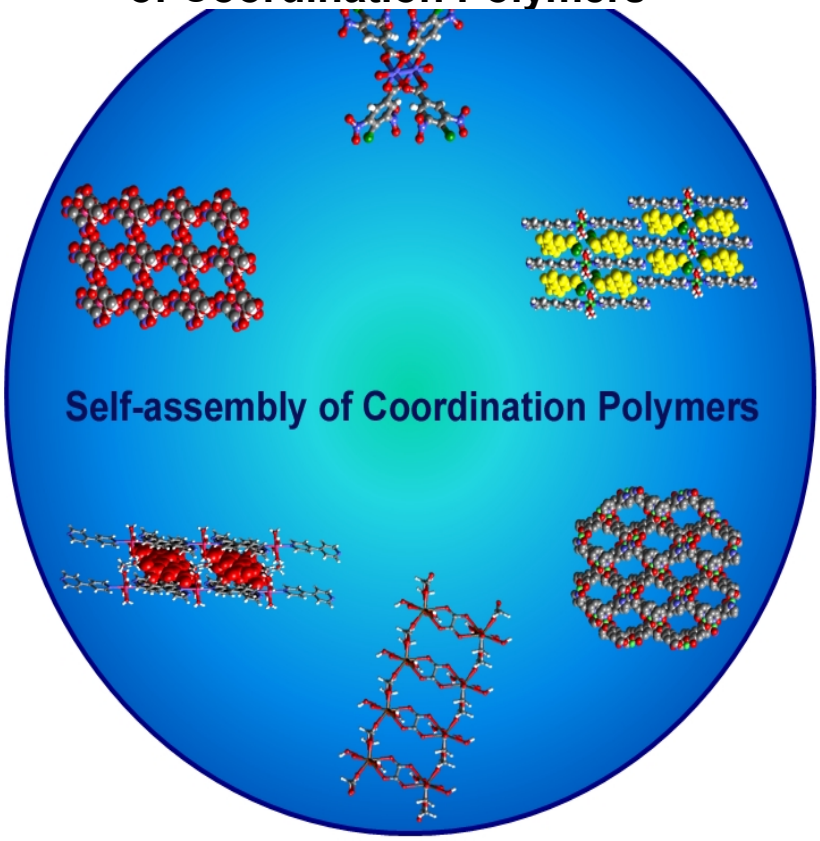

If I have seen further than others, it is by standing upon the shoulders of giants

-Sir Isaac Newton-

2.1 Introduction

Design and synthesis of coordination polymer networks through a rational combination of organic linkers and metal nodes is an area of contemporary research interest, owing to their potential applications in different fields such as catalysis, molecular separation, gas storage, etc.[1-4] Thus, efforts were devoted to the synthesis of desired targets through the controlled reaction of transition metal ions and multifunctional bridging ligands.[5,6] Towards this, various multifunctional ligands were used as linkers, forming extended networks exhibiting various architectures such as grids, honeycombs, etc., with an emphasis to obtain host-guest assemblies.[7,8] Since the stereochemistry of the ligands has profound effect on the resultant assembly of a coordination polymer, the selection or design of a suitable ligand is crucial to the construction of coordination polymers.

Further, there is also a growing interest in the study of supramolecular isomerism in coordination polymers, which are the superstructures that consist of the same molecular building blocks but exhibit different intermolecular connectivity and/or spatial organization.[9] The study of supramolecular isomerism is not only important in producing novel materials with interesting properties, but may also be helpful in developing a fundamental understanding of the factors influencing crystal growth. The structural diversity existing in the supramolecular isomers has been recently categorized into four different classes: structural (different networks formed from same components), conformational (arrays of identical composition that reveal

different conformational features), catenane (inter-weaved vs. noninterpenetrating networks), and optical (chiral supramolecular constructs).[10]

In general, the studies of the coordination polymers were mainly focused upon the design and preparation of coordination assemblies that mimic porous inorganic materials like zeolites,[11,12] utilizing the strength and directionality of the coordinate bonds formed between the organic ligands and the metal species.[13-15] Recently, Kitagawa, Puddephatt, Fujita, etc., have paid greater attention to incorporate, weaker interactions like hydrogen bonds in the coordination frameworks, to enhance the flexibility of the resulting networks.[16, 17] In order to gain a perfect control over the design of assemblies, which are stable and are capable of responding to the environment, a thorough understanding of various factors that control the self-assembly processes is required as described below.

2.1.1 Stimuli of external factors on the preparation of targeted coordination assemblies

The self-assembly processes and the resulting three-dimensional architecture of the coordination complexes are dependent on various factors such as i) the coordination number and geometry of the metal ions employed, ii) coordination behavior, flexibility and isomerism of the ligand, iii) reaction conditions like, pH, temperature and pressure, iv) counter ions present in the system, etc. Contributions of various research groups, illustrating the effects of some of these factors on the self-

assembly of coordination assemblies are discussed below, with some representative examples.

Kitagawa et al. made systematic attempts to evaluate the effect of concentration in conjunction with temperature on the supramolecular isomerism of coordination complexes based on *p*-benzoquinone, while, Zhou and coworkers reported novel temperature-controlled supramolecular stereoisomerism in porous copper coordination networks, possessing PtS and NbO net topologies.[18,19] Further, Cheetham and coworkers evaluated the influence of temperature in the self-assembly of coordination polymers, based on cobalt succinate materials synthesized from an identical starting mixture using temperature as the only independent variable.[20]

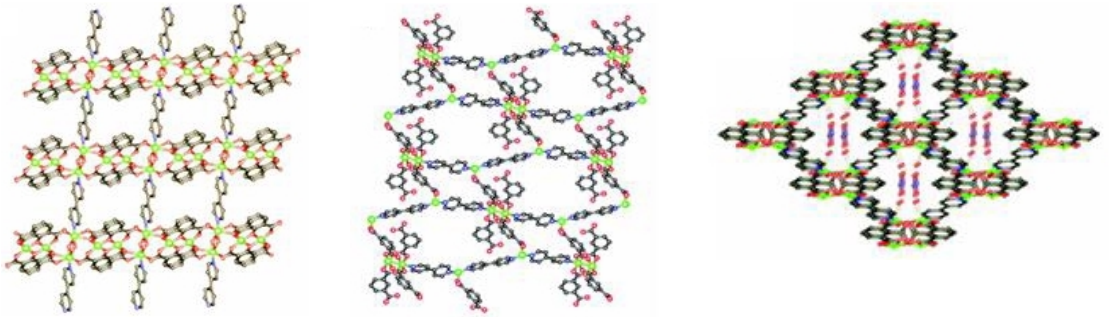

Figure 1: The networks formed by $Cu(NO_3)_2$, 4,4'-bipyridine and (a) 2-hydroxy-isophthalate (with 2 Equiv. NaOH) (b) isophthalate (with 4 Equiv. NaOH) and 1,2,3-benzenetricarboxylate (with no NaOH), formed in situ by the variation in the pH of the reaction medium

Evaluation of the influence of pH of the reaction medium is well documented in the literature.[21] One of the illustrative example is the three coordination polymers synthesized from a mixture of $Cu(NO_3)_2$, NaOH, 4,4'-bipyridine and 1,2,3-benzenetricarboxylic acid under various pH conditions. With the variation in pH,

brought about by the variation of equivalence of NaOH present in the reaction mixture, the 1,2,3-benzenetricarboxylic acid forms three different types of complexes as shown in Figure 1.[22]

The counterions effect in the self-assembly process is exemplified in the reactions of AgX, [X = trifluoroacetate ($CF_3CO_2^-$, tfa), nitrate (NO_3^-), trifluoromethanesulfonate (triflate, $CF_3SO_3^-$, OTf), hexafluorophosphate (PF_6^-), or perchlorate (ClO_4^-)], with 2,2',3"-tripyridylamine (tpa), yielding five novel silver(I) complexes, which have been structurally characterized.[23]

However, another important factor that is of considerable interest in the preparation of coordination assemblies is the solvent of crystallization. Although its influence is well documented in the preparation of organic assemblies as polymorphism,[24] such studies are limited in the case of coordination assemblies despite its impact is known in some examples as described in the reaction of 1-methyl-1A-(4-pyridyl)-2-(4-pyrimidyl)ethylene and $Co(NCS)_2$, in which, two pseudo-isomeric coordination polymer architectures - $[Co(1\text{-methyl-1A-(4-pyridyl)-2-(4-pyrimidyl)ethylene})_2(NCS)_2]_n$ and $[\{[Co(1\text{-methyl-1A-(4-pyridyl)-2-(4-pyrimidyl)ethylene})_2(NCS)_2]\cdot 2[Co(1\text{-methyl-1A-(4-pyridyl)-2-(4-pyrimidyl) ethylene})_2(NCS)_2]\}\cdot 5CH_3OH]_n$ - were isolated by performing the reaction from methanol/water and methanol/nitromethane, respectively.[25]

Thus, to further evaluate the influence of solvent of crystallization and the flexibility of the coordination behavior of various organic ligands on the supramolecular architectures, reactions of metal salts with derivatives of 3,5-

dinitrobenzoic acid in different solvents have been carried out in the presence of various N-donor ligands. The resulting assemblies have been structurally evaluated as described in the following sections.

2.2 Effect of Solvent of Crystallization on Metal-Organic Assemblies

To begin with, the coordination complexes of 3,5-dinitrobenzoic acid, **1**, and 3,5-dinitro-4-methylbenzoic acid, **2**, with cobalt nitrate in the presence of 4,4'-bipyridine have been prepared. The choice of these acids lies with the fact that numerous organic assemblies of acids, **1** and **2** were well-known in the literature, but not well utilized in the preparation and the analysis of metal-organic assemblies.[26]

Scheme 1

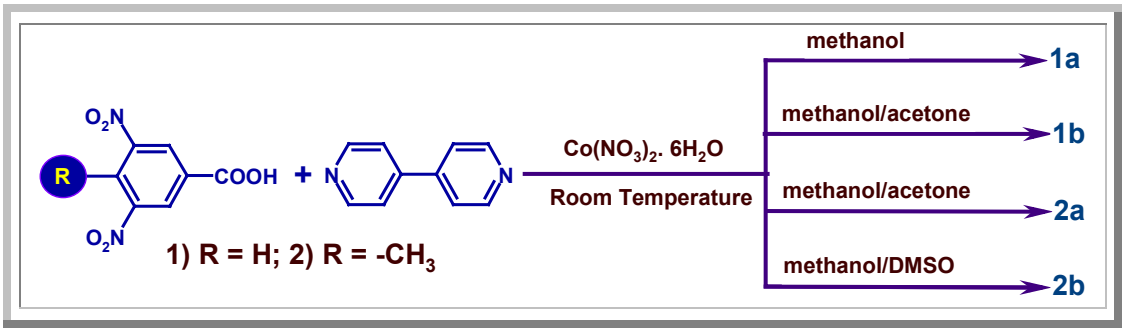

The reactions of **1** or the corresponding methyl derivative, **2** with 4,4'-bipyridine, ***bpy*** and cobalt nitrate hexahydrate gave different types of coordination polymers with the variation of solvent of crystallization and the obtained complexes

are denoted as **1a**, **1b**, **2a**, and **2b**, as illustrated in Scheme 1. The salient features of all the four complexes are discussed in the following sections.

2.2.1 Experimental Section

Synthesis of Complexes by Cocrystallization Methods

All the chemicals were obtained commercially, and the crystallization experiments were carried out at room temperature by dissolving the constituent reactants in spectroscopic-grade solvents, as the case may be. The synthesis of each complex is described below.

$[Co(C_7H_3N_2O_6)_2(C_{10}H_8N_2)_2(CH_3O)_2]$, 1a

A solution of **1** (0.106g, 0.5 mmol) in methanol (10 mL) was slowly added to a warm solution of $Co(NO_3)_2.6H_2O$ (0.146 g, 0.5 mmol) in methanol (10 mL) with constant stirring over a period of 5 minutes. To this mixture was added drop wise 4,4'-bipyridine (0.078 g, 0.5 mmol) in methanol (5 mL). The reaction mixture was warmed for a while and allowed to evaporate slowly under ambient conditions. Pale pink needles suitable for X-ray analysis were obtained within 2 days.

$[Co_4(C_7H_3N_2O_6)_8(C_{10}H_8N_2)_8(CH_3O)_2].CH_3COCH_3$, 1b

To a warm solution of $Co(NO_3)_2.6H_2O$ (0.146 g, 0.5 mmol) in methanol (10 mL) was added slowly with constant stirring the methanolic solution (5 mL) of **1** (0.106 g, 0.5 mmol). To the mixture was added drop wise over a period of 5 minutes, 4,4'-bipyridine (0.078 g, 0.5 mmol) in methanol (5 mL). Acetone (5 mL) was allowed

to diffuse slowly through the reaction mixture. Pale pink needles of X-ray quality were obtained over a period of 3 days.

$[Co_2(\mu_2\text{-}C_8H_5N_2O_6)_2(\mu_2\text{-}C_8H_5N_2O_6)_2(C_{10}H_8N_2)_4]$, 2a

$Co(NO_3)_2.6H_2O$ (0.146 g, 0.5 mmol) in methanol (15 mL) was added drop wise to a solution of acid **2** (0.113 g, 0.5 mmol) in methanol (5 mL). To this stirred solution was added slowly over a period of 5 minutes, 4,4'-bipyridine (0.078 g, 0.5 mmol) in a 1:1 mixture of methanol and acetone (10 mL). Pale pink needles were obtained over a period of 2 days and were found to be suitable for X-ray analysis.

$[Co(C_8H_5N_2O_6)_2(C_{10}H_8N_2)_2(H_2O)_2].(CH_3)_2SO$, 2b

A solution of **2** (0.113 g, 0.5 mmol) in methanol (10 mL) was added drop wise with constant stirring to a warm solution of $Co(NO_3)_2.6H_2O$ (0.146 g, 0.5 mmol) in methanol (5 mL). To this reaction mixture was added over a period of 5 minutes, 4,4'-bipyridine (0.078 g, 0.5 mmol) in methanol (10 mL). This reaction mixture was warmed for a while, and DMSO (2 mL) was allowed to diffuse slowly to yield pale pink X-ray-quality crystals.

2.2.2 X-ray Crystallography

Good-quality single crystals of **1a**, **1b**, **2a**, and **2b** were carefully chosen after they were viewed through a Leica microscope supported by a rotatable polarizing stage and a CCD camera. The crystals were glued to a thin glass fiber using an adhesive (cyano acrylate) and mounted on a diffractometer equipped with an APEX CCD area detector. The data collection was smooth in all the cases, and no extraordinary methods were employed, except that the crystals were smeared in cyano

acrylate to protect them from ambient laboratory conditions. The intensity data were processed using Bruker's suite of data processing programs (SAINT), and absorption corrections were applied using SADABS. The structure solution of all the complexes was carried out by direct methods, and refinements were performed by full-matrix least-squares on F^2 using the SHELXTL-PLUS suite of programs.[27] All the structures converged to good *R* factors. All the non-hydrogen atoms were refined anisotropically, and the hydrogen atoms obtained from Fourier maps were refined isotropically. All the refinements were smooth in all the structures. Intermolecular interactions were computed using the PLATON program.[28]

2.2.3 Complex $[Co(C_7H_3N_2O_6)_2(C_{10}H_8N_2)_2(CH_3O)_2]$, 1a

Reaction of **1,** with 4,4'-bipyridine, ***bpy*** and cobalt nitrate hexahydrate, in a methanol solution and subsequent slow evaporation over a period of two days at ambient conditions yielded pink crystals of complex, **1a**. The crystals thus obtained were analyzed using single crystal x-ray diffraction technique and the structure determination revealed that complex **1a** crystallizes in a noncentrosymmetric space group, $P4_32_12$. Complete details of the crystallographic information are given in Table 2.1.

In the complex **1a**, ***bpy*** units interact with Co(II) in a *trans*-mode, forming the Co–N (2.171, 2.187 Å) coordinate bonds, as shown in Figure 2a. Further, two molecules of **1**, in its carboxylate form, interact with the Co(II) metal centre in monodentate mode. In addition, two methanol molecules coordinated to each metal

center through Co–O dative bonds. Thus, each Co(II) is connected to two ***bpy*** molecules and two carboxylate units of **1** and two methanol molecules and the coordination environment details are tabulated in Table 2.2. Thus, in a typical octahedron, while ***bpy*** molecules lie at the axial positions, carboxylates and methanol units occupy the equatorial sites. These octahedral units constitute polymeric chains in the direction of Co–N bonds, utilizing the bis-monodentate bridging coordination mode exhibited by ***bpy*** molecules.

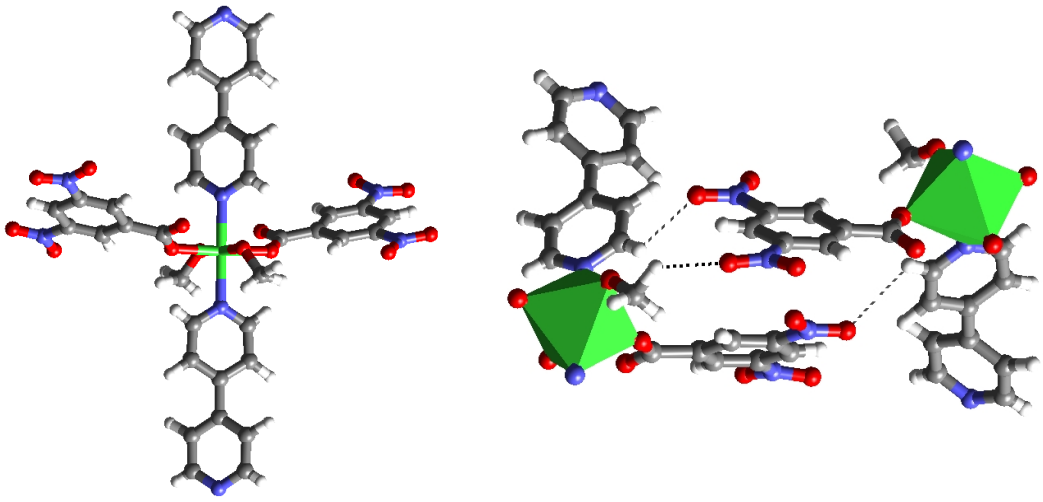

(a) **(b)**

Figure 2: (a) A typical metal coordination centre in complex **1a**. (b) A pictorial representation of the C-H···O hydrogen bonds, formed between the polymer units. Dashed lines represent the hydrogen bonds.

In three-dimensional arrangement, the polymer chains thus formed are arranged in a crossed manner and interact with the adjacent units through C–H···O hydrogen bonds, formed between the $–NO_2$ group of **1** and hydrogen atoms of the ***bpy*** (H···O, 2.85 and 2.90 Å) and methanol molecules (H···O, 2.73 Å). The detailed view of

the hydrogen bonds established between the adjacent polymer chains is shown in Figure 2b.

2.2.4 Complex $[Co_4(C_7H_3N_2O_6)_8(C_{10}H_8N_2)_8(CH_3O)_2].CH_3COCH_3$, 1b

Reaction of **1** with ***bpy*** and Co(II) in a methanol/acetone mixture, however, gave a coordination polymer, **1b,** which is entirely different from that of **1a**, as revealed by the crystal x-ray diffraction studies. The structure analysis reveals the presence of methanol and acetone, in the crystal lattice. A representative supramolecular unit of the coordination complex is shown in Figure 3.

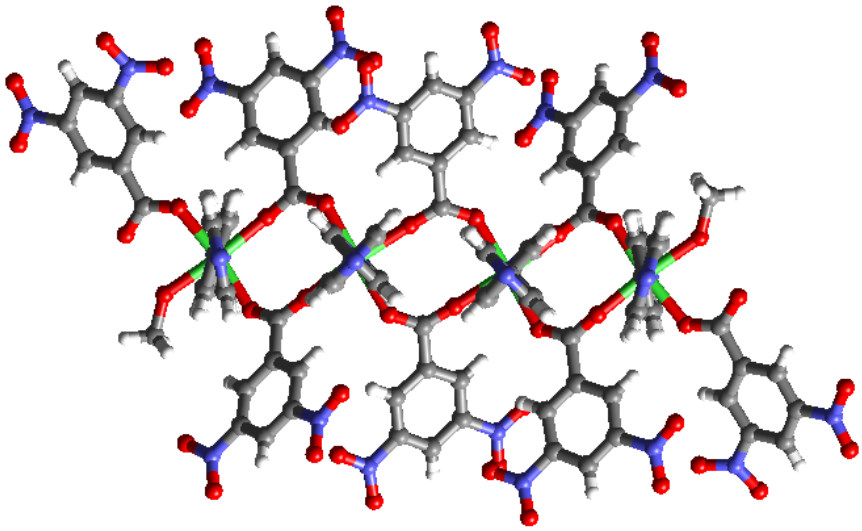

Figure 3: Representation of the tetrameric polymer unit in the crystal structure of **1b.**

In a typical unit, all Co(II) centres are attached to the carboxylate units and ***bpy*** through Co-O and Co-N coordinate bonds, respectively. The structure analysis of the complex reveals the formation of a unique tetrameric coordination unit, with four

Co(II) atoms, eight molecules of **1** and ***bpy*** each, and two molecules of methanol. In this complex, the ***bpy*** molecules act as bis-monodentate ligand connecting two metal centres, through Co-N coordinate bonds, with an average distance of 2.147 Å.

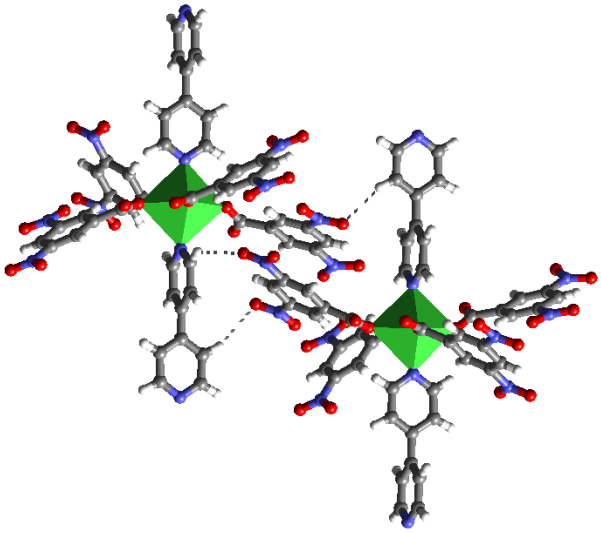

Figure 4: C-H···O hydrogen bonds formed between the adjacent polymer blocks. Dashed lines represent C-H···O hydrogen bonds.

The carboxylate group in complex **1b** exhibit two different modes of interaction with Co(II) - monodentate and bridging bidentate mode. While carboxylate units form single Co-O bond (in a monodentate fashion) with terminal Co(II) metal centres, it act as bridging ligands with the two intermediate Co(II) ions. Further, the hexa-coordination of the two terminal Co(II) is fulfilled by coordinating methanol molecules. The tetrameric cobalt-centered units, thus formed, constitute a polymer block-type structure by joining the adjacent tetramers through coordinated ***bpy*** units. These blocks, further, are held together by C-H···O hydrogen bonds formed between the -NO_2 groups of **1** and pyridyl hydrogen of ***bpy***, as shown in Figure 4, and the H···O

distances are in the range 2.49-2.89 Å. The details of the hydrogen bond are tabulated in Table 2.3.

In the crystal lattice, the acetone molecules are inserted as guest species between the adjacent blocks, as shown in Figure 5a, and are held to the host framework through C-H···O hydrogen bonds, established between the methyl groups of acetone and the uncoordinated oxygen atom of a terminal carboxylate. The H···O distances are found to be in the range of 2.52-2.87 Å (see Figure 5b).

(a)

(b)

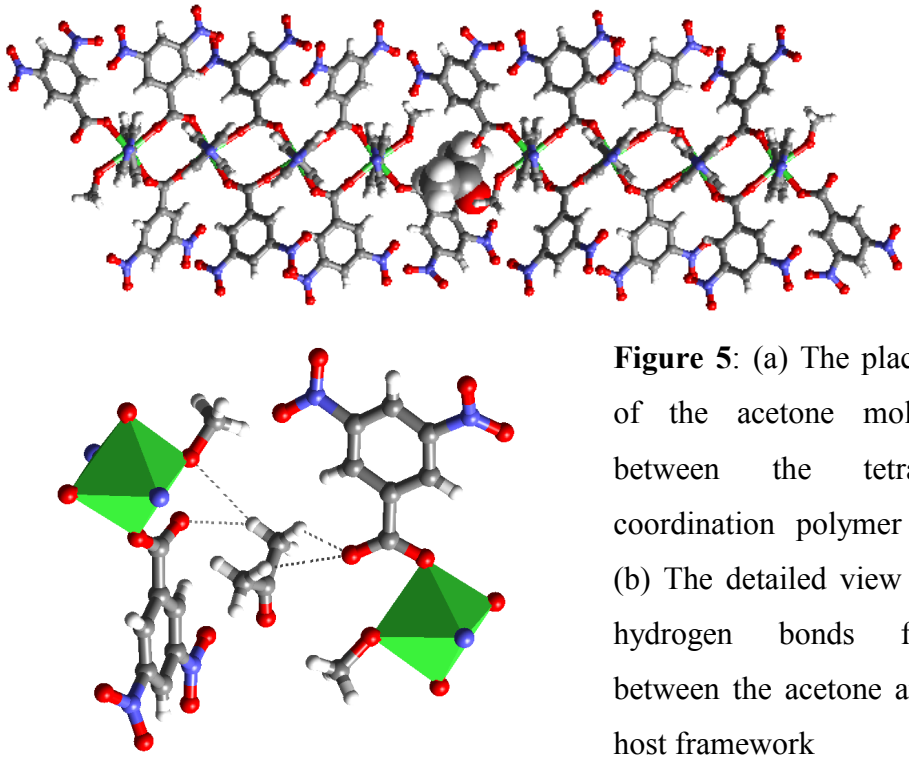

Figure 5: (a) The placement of the acetone molecules between the tetrameric coordination polymer units. (b) The detailed view of the hydrogen bonds formed between the acetone and the host framework

In order to study further the influence of the solvent of crystallization on the coordination modes and the three-dimensional architectures of the coordination assemblies, acid **1** was replaced by its methyl derivative, 3,5-dinitro-4-methylbenzoic

acid, **2**. Thus, reactions were carried out in various solvents, but good quality single crystals for the x-ray diffraction studies were obtained only in the case of methanol-acetone mixture and methanol-dimethylsulfoxide solution. The structural details and the variation in the three-dimensional architectures of these complexes are discussed in the following sections.

2.2.5 Complex $[Co_2(\mu_2\text{-}C_8H_5N_2O_6)_2(\mu_2\text{-}C_8H_5N_2O_6)_2(C_{10}H_8N_2)_4]$, 2a

A reaction of cobalt nitrate with **2** and ***bpy*** from a methanol-acetone solution mixture, yielded a complex, **2a** in a 1:2:1 stoichiometry of the reagents, as determined by x-ray analysis. In this complex, ***bpy*** molecules act as bis-monodentate ligand and coordinate to Co(II) centres, through the formation of Co-N coordinate bonds, with distances of 2.159 and 2.163 Å. Further, these units extend in one-dimension to form an infinite one dimensional coordination polymer. In this complex, the acid molecules exhibit, two coordination modes – bridging and chelating. Two adjacent metal centres are bound together by carboxylates through the bridging mode, with Co-O distances of 2.040 and 2.075 Å, thus forming a dinuclear metal building unit. The remaining coordination sites of the metal centres are fulfilled by the molecules of **2** bound in the chelating mode, with Co-O distances of 2.219 and 2.223 Å. A representative dinuclear metal unit, with novel coordination arrangement and observed hydrogen bonding patterns are shown in Figure 6. The topological arrangement of organic ligands around Co(II) is very much similar to that of **1a** and **1b**, with the carboxylates occupying equatorial positions while the ***bpy*** molecules the axial positions of the octahedron.

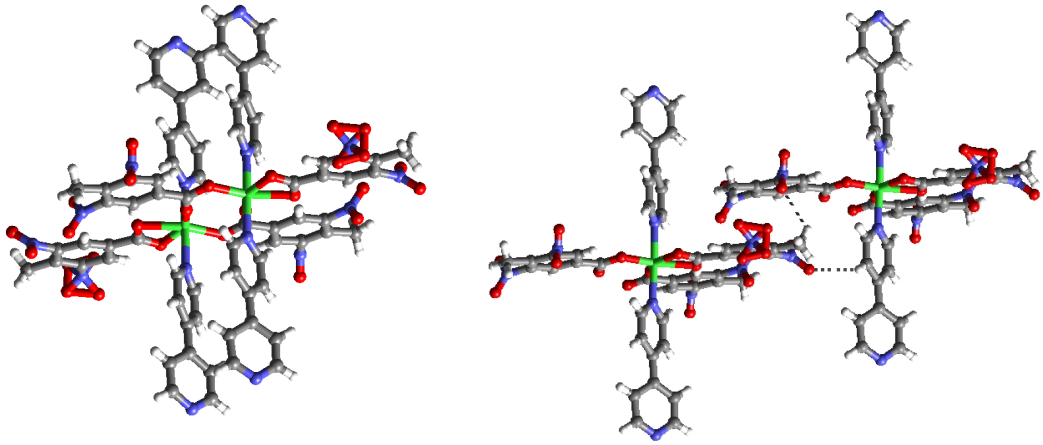

(a) **(b)**

Figure 6: (a) The dinuclear metal coordination unit in complex **2a**. (b) The C-H···O hydrogen bonds formed between the adjacent bimetallic units.

The polymer chains thus formed, undergo self-assembly, making use of the C-H···O hydrogen bonds, to yield a channel structure in the three-dimensional arrangement as shown in Figure 7. A noteworthy feature of the channels observed in the complex **2a** is that, the channels are the resultant of the C-H···O hydrogen bonds, (H···O distance 2.44-2.95 Å) formed between the one-dimensional polymer chains, unlike the similar channel structures known in the literature wherein the channels are created exclusively due to the coordinate bonds formed between the metal and organic ligands.

However, the occupants of the channels, most probably the solvent molecules (methanol or acetone), could not be determined by single crystal X-ray diffraction methods, unequivocally, as complex **2a** is unstable. Another noteworthy and

interesting feature of complex **2a** is that, no solvent molecule is coordinated to Co(II) metal centre, unlike the complex **1a** and **1b**.

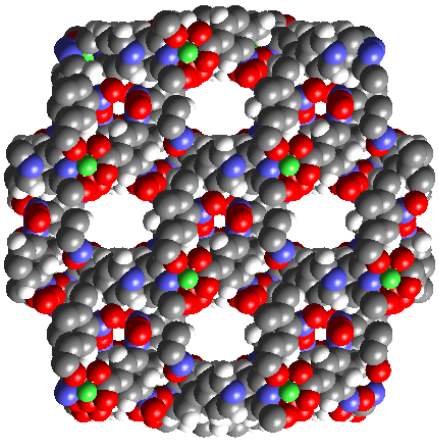

Figure 7: The channel structure formed by the self-assembly of coordination polymers.

2.2.6 Complex $[Co(C_8H_5N_2O_6)_2(C_{10}H_8N_2)_2(H_2O)_2].(CH_3)_2SO$, 2b

The crystal structure determination of the pale pink crystals obtained from a methanol-DMSO solution of **2** and bpy with Co(II), reveals the inclusion of the solvent of crystallization in the crystal lattice, with asymmetric unit consisting of the reactants in a 2:1:1 ratio. As in the case of other coordination complexes, **1a**, **1b** and **2a**, discussed above, the molecules of ***bpy*** interact with Co(II) through Co-N bonds with a distance of 2.174 Å and form infinite polymeric chains. The arrangement of molecules around each metal center and their packing in the three-dimensional arrangement are shown in Figure 8. In this complex, the two carboxylates of **2** interact with Co(II) in a monodentate mode, with a Co-O distance of 2.080 Å. But, unlike the arrangement of carboxylates in **1a**, **1b**, and **2a**, the two carboxylates in **2b** arrange in a *cisoid*-manner in the equatorial plane.

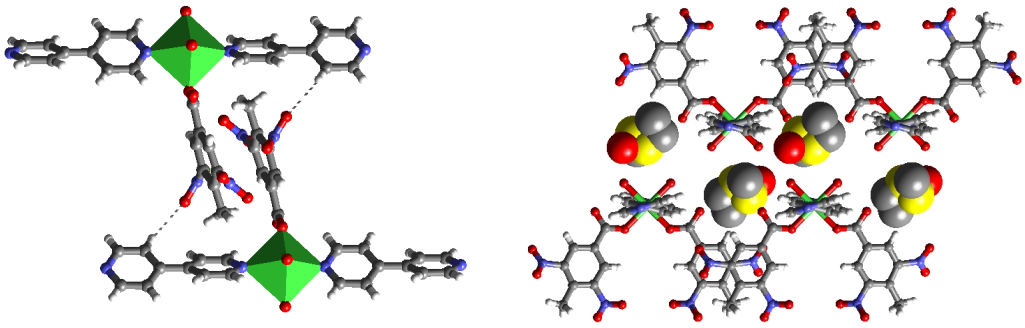

(a) **(b)**

Figure 8: Representation of bilayers formed by the coordination polymers, with the coordinated acid molecules between the layers. The C-H···O hydrogen bonds are represented as dotted lines. (b) Three-dimensional arrangement of coordination polymers in the crystal structure of complex **2b**. The DMSO molecules are represented in space filling mode.

Further, the hexa-coordination around Co(II) is completed with the coordination of two water molecules. Thus an octahedral geometry around the Co(II) metal centre is achieved with ***bpy*** molecules at the apices, while acid and water molecules occupying the equatorial positions. Further, the adjacent coordination polymers interact through C-H···O hydrogen bonds, formed between the $-NO_2$ groups of **2** and the aromatic hydrogen of ***bpy*** molecules, yielding bilayer architecture. In three-dimensional arrangement, these bilayers stack, forming a clay-like architecture, with DMSO molecules being inserted between the layers.

Thus, it is evident from the study of the solid state structures of **1a**, **1b**, **2a** and **2b** that, the solvent of crystallization can bring about subtle variation in the coordination behavior of ligands, especially, ligands like carboxylates, which can exhibit flexible coordination modes. In all the above complexes, **1a**, **1b**, **2a** and **2b**,

formation of infinite one-dimensional coordination polymer chains were established making use of the Co(II) – ***bpy*** linkage. Although this linkage is common in all the complexes, differences in the coordination modes exhibited by the carboxylates, influenced by solvent of crystallization, resulted in the formation of different types of three-dimensional architectures. Further, the topographic analysis of the metal-carboxylate bonds revealed a similarity of the metal coordination with the hydrogen bonded dimer and catemer of carboxylic acids. The topographic analysis of the coordinate bonds observed in the complexes **1a**, **1b**, **2a** and **2b** are schematically represented in Scheme 2.

Scheme 2:

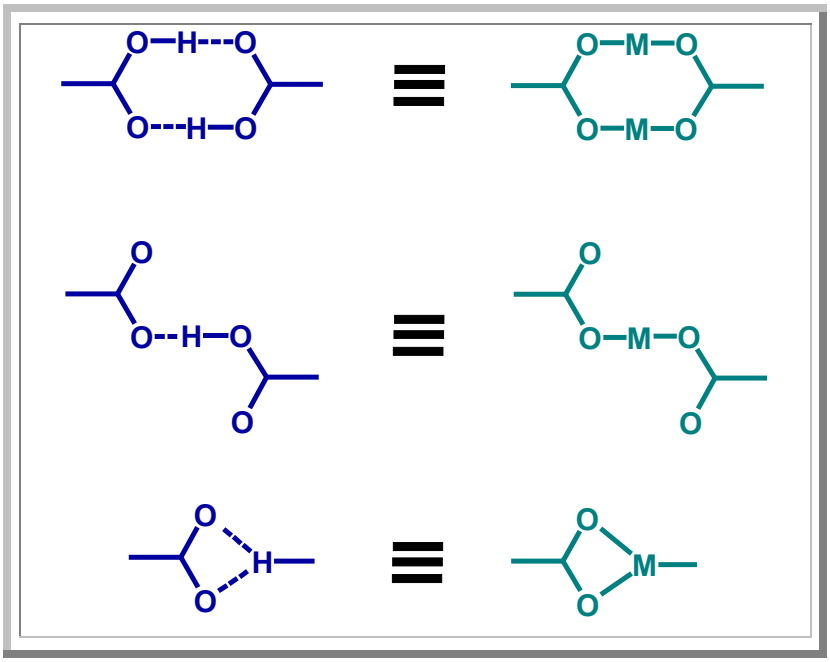

While **1a** forms a square grid network, the other complexes, **1b, 2a** and **2b** form host-guest type structures with the incorporation of solvent molecules. The

variations in the packing arrangement of the complexes **1a**, **1b**, **2a** and **2b** are schematically represented in the Scheme 3. Further, complexes **1b** and **2b** are closely related, with the insertion of solvent molecules between the polymer chains. In all the complexes, the major binding force between the polymer chains is the C-H···O hydrogen bonds formed between the -NO_2 groups and hydrogen atoms of ***bpy***.

Scheme 3

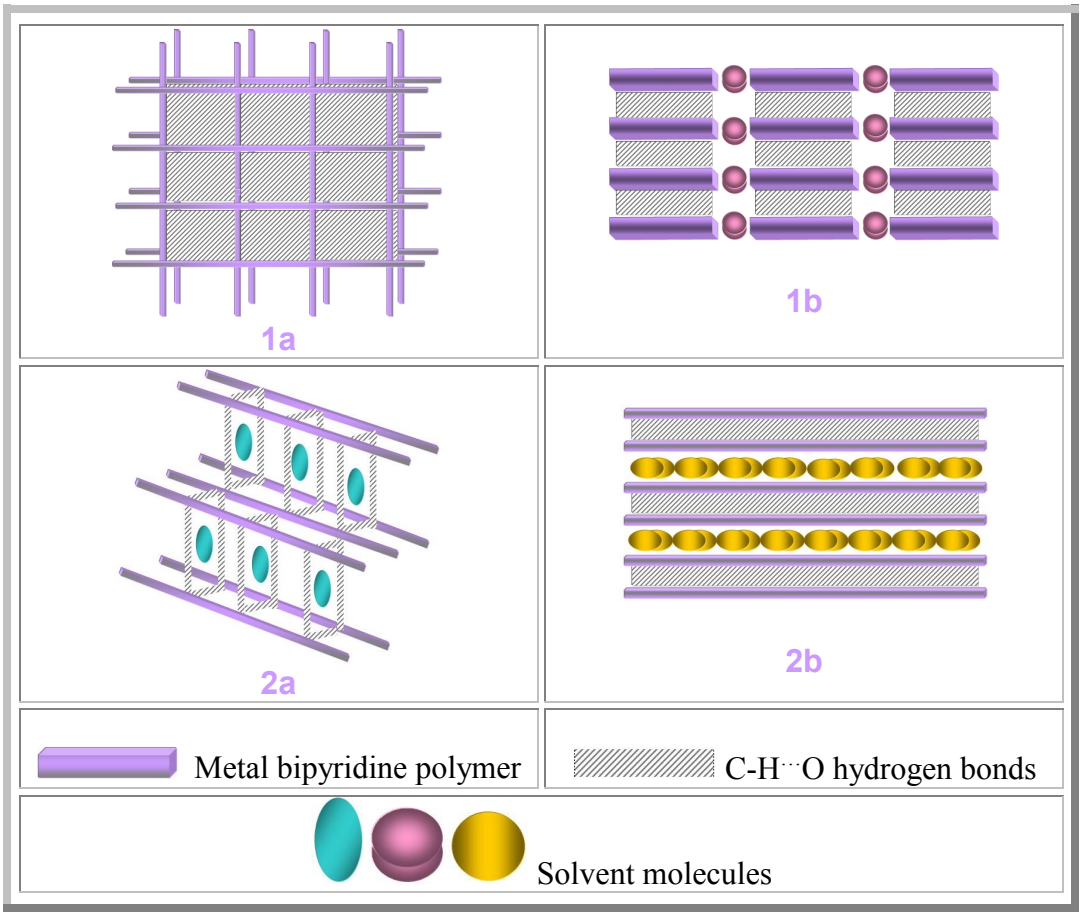

Observing such an effective influence of solvent of crystallization on the structural diversity of the coordination assemblies, irrespective of the nature of the acid molecules, further experiments were carried out to study the structural variations

by varying the N-donor ligands. Towards this, successful results of the preparation and structural analysis of coordination assemblies of 3,5-dinitrobenzoic acid, **1** with $Mn(CH_3COO)_2.4H_2O$ in the presence of different N-donor ligands (listed in Chart 1) are compiled in the following sections.

2.3 Effect of Aza-donor Ligands on the Self-assembly of Metal-Organic Assemblies

The use of conformationally flexible ligands with multiple donor sites to engineer coordination polymer arrays has a number of inherent challenges. Conformational flexibility and different binding modes could enhance the possibility of forming supramolecular isomers. Thus, N-donor ligands that are differentiated by both coordination ability and conformational flexibility, as listed in Chart 1, are employed in the reactions with Mn(II) and acid, **1**.

Chart-1:

	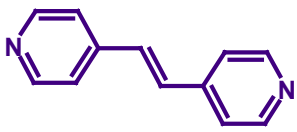	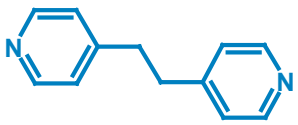
4,4'-bipyridine (*bpy*)	**1,2-bis(4-pyridyl)ethane (*bpyee*)**	**1,2-bis(4-pyridyl)ethane (*bpyea*)**
	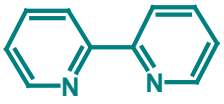	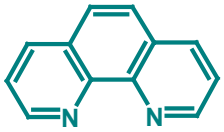
1,3-bis(4-pyridyl)propane (*bpypa*)	**2,2'-bipyridine (*22bpy*)**	**1,10-phenanthroline (*110phe*)**

In all the cases, the reactions were carried out at ambient conditions and the crystals were obtained by the slow evaporation technique. The crystals thus obtained were analyzed using single crystal x-ray diffraction technique to evaluate their solid state structures. The reaction conditions and the reagents involved in the reactions are given in Scheme 4.

Scheme 4

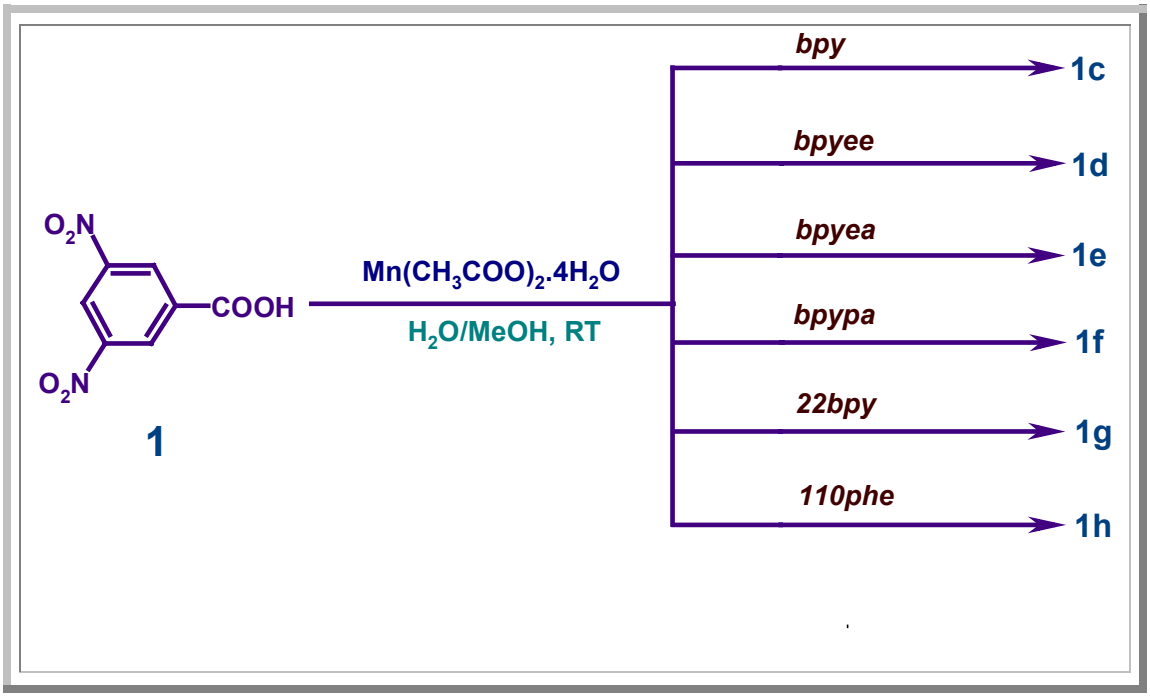

2.3.1 Experimental Section

A General procedure for the synthesis of complexes 1c – 1h

To an aqueous solution (15 mL) of $Mn(CH_3COO)_2.4H_2O$ (0.1mmol), a methanolic solution (5 mL) of 3,5-dinitrobenzoic acid, **1** (0.021g, 0.1mmol) was added drop wise at room temperature. This mixture was heated on a water bath for five minutes and to

this hot solution, the N-donor ligand, (***bpy***, ***bpyee***, ***bpyea***, ***bpypa***, ***22bpy*** or ***110phe***) (0.1mmol) in methanol (5 mL) was added carefully to avoid precipitation. After heating further for 15 minutes, the solution was diluted by adding further 5 mL methanol. The clear solution thus obtained was filtered and the filtrate was kept for slow evaporation. Colorless crystals were obtained over a period of one week. The crystals thus, obtained were washed thoroughly using cold distilled water and dried.

2.3.2 X-ray Crystallography

Good-quality single crystals of **1c**-**1h** were carefully chosen after they were viewed through a Leica microscope supported by a rotatable polarizing stage and a CCD camera. The crystals were glued to a thin glass fiber using an adhesive (cyano acrylate) and mounted on a diffractometer equipped with an APEX CCD area detector. The data collection was carried out at 120 K in all the cases except that of **1d** and the data collection was smooth in all the cases, and no extraordinary methods were employed, except that the crystals were smeared in cyano acrylate to protect them from ambient laboratory conditions. The intensity data were processed using Bruker's suite of data processing programs (SAINT), and absorption corrections were applied using SADABS. The structure solution of all the complexes was carried out by direct methods, and refinements were performed by full-matrix least-squares on F^2 using the SHELXTL-PLUS suite of programs.[27] All the structures converged to good *R* factors. All the non-hydrogen atoms were refined anisotropically, and the hydrogen atoms obtained from Fourier maps were refined isotropically. All the refinements were

smooth in all the structures. Intermolecular interactions were computed using the PLATON program.[28]

2.3.3 Complex $[Mn(C_7H_3N_2O_6)_2(C_{10}H_8N_2)]$, 1c

Reaction of manganese acetate tetrahydrate and **1** with 4,4'-bipyridine, ***bpy***, in a methanol/water mixture and subsequent slow evaporation over a period of two days at ambient conditions yielded a 1:2:1 complex, **1c**. The crystal structure determination reveals that the complex **1c** crystallizes in centrosymmetric space group, *P*2/*c*, and the complete details of the crystallographic information are given in Table 2.4.

In the complex **1c**, ***bpy*** units interact with Mn(II) in a *trans*-mode, forming Mn–N coordinate bonds, with an average distances of 2.269 Å. Further, four acid units (in bridging mode) interact with the Mn(II) metal centre, yielding hexa-coordination environment around each metal centre. A typical metal centre in the complex **1c** is shown in Figure 9a. The details of the coordination environment are given in Table 2.5.

In the octahedral arrangement, while ***bpy*** molecules lie at the axial positions, carboxylates occupy the equatorial sites. Further, the structure analysis reveals that, adjacent octahedra are held together by Mn-N coordinate bonds, making use of ***bpy*** spacer ligand, constituting polymer chains, while the carboxylates exhibiting bridging mode hold the adjacent Mn(II)-***bpy*** polymers together to form a grid-like network as shown in Figure 9c.

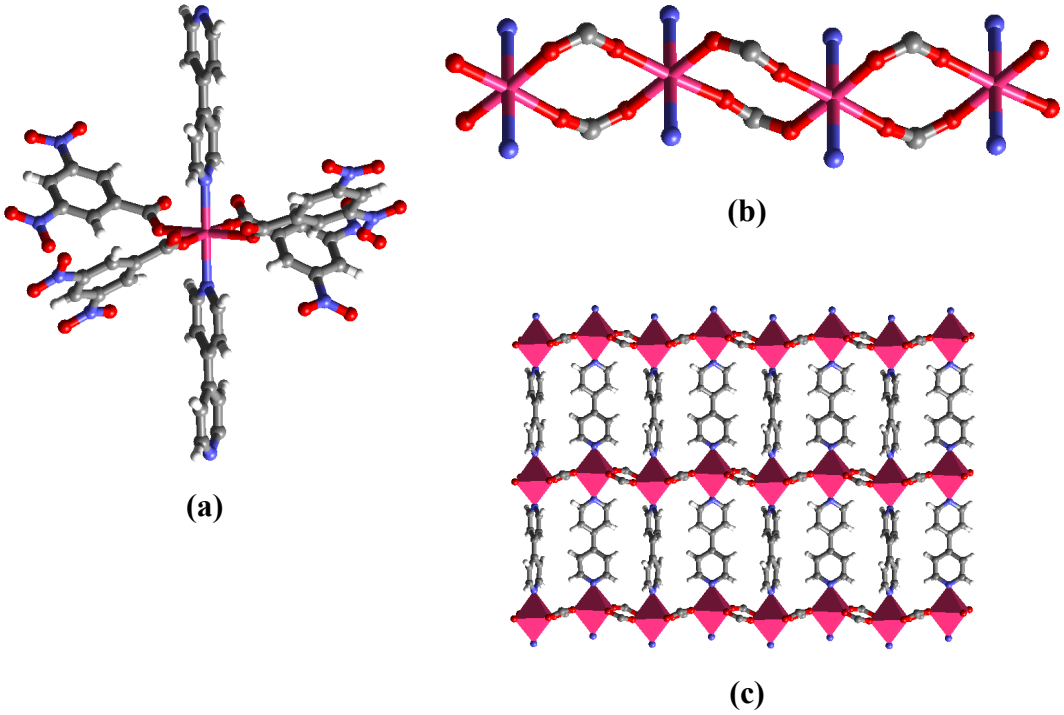

Figure 9: (a) The coordination environment of the metal centre in complex, **1c**. (b) The schematic representation of the coordination mode of the ligands. (Color scheme: blue – N-atoms of the pyridyl ligand, red – O-atoms of the carboxylate) (c) The grid-like network formed by the interconnected metal-bipyridyl one-dimensional coordination polymers.

The grid-like networks thus formed, interact further with each other through C-H···O and C-H···N hydrogen bonds formed between the $–NO_2$ groups of **1** and the aromatic hydrogen of the ***bpy*** molecules, with H···O distances in the range 2.57-2.84Å, while the H···N distance is being 2.84Å. The detailed view of the hydrogen bonds formed between the adjacent polymer chains is shown in Figure 10. The details of the hydrogen bonds are tabulated in Table 2.6.

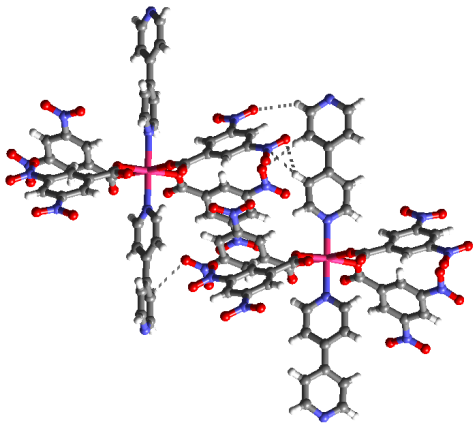

(a)

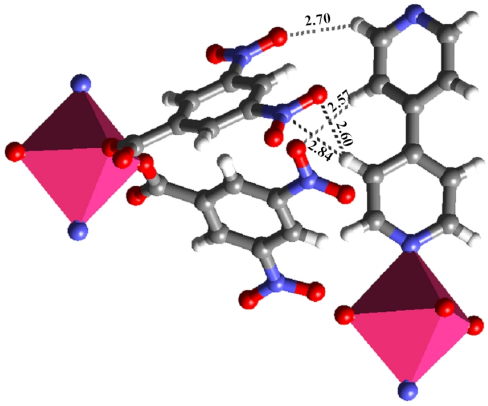

(b)

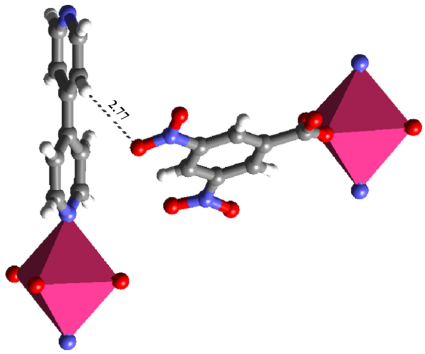

(c)

Figure 10: (a) The representation of the hydrogen bonds formed between the adjacent grid networks observed in the complex, **1c**. The interactions shown in (a) are represented more vividly in (b) and (c).

2.3.4 Complex [$Mn(C_7H_3N_2O_6)(C_{12}H_{10}N_2)$], 1d

Upon crystallization from a methanol-water solution mixture, manganese acetate and **1** in the presence of 1,2-bis(4-pyridyl)ethene, ***bpyee*** gave a complex, **1d** in a 1:1:1 stoichiometry of the reagents. The stoichiometry was determined from the structure determination by single-crystal x-ray diffraction methods and the elementary analysis. Structure analysis reveals that one of the olefinic carbon atoms of ***bpyee*** molecule is disordered, as shown in Figure 11a.

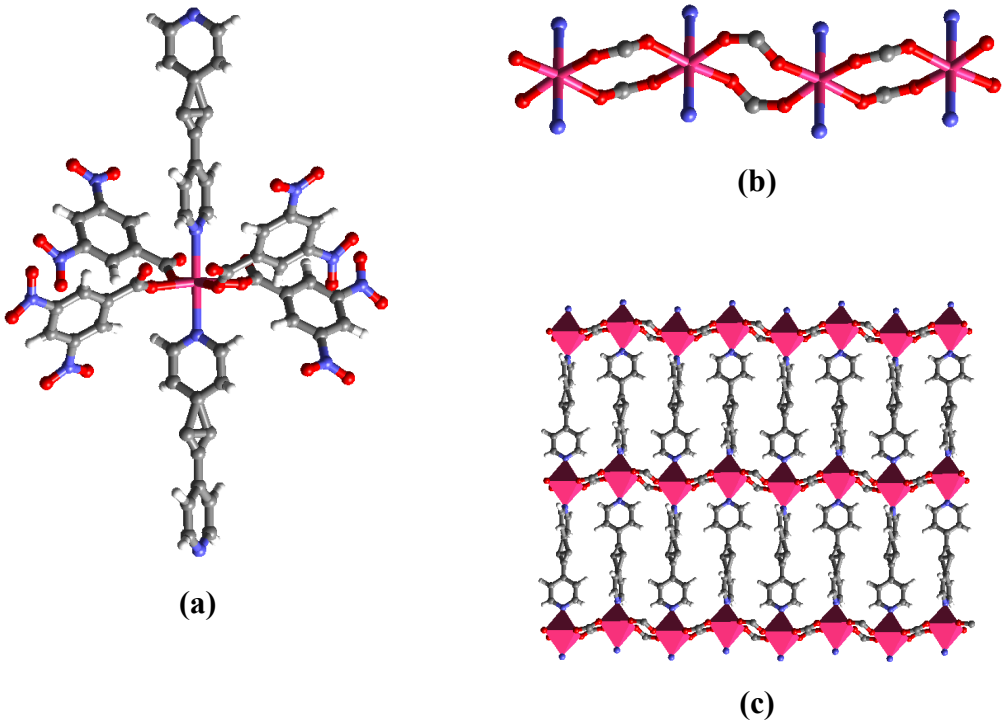

Figure 11: (a) A typical metal centre in the complex, **1d**. (b) The schematic representation of the coordination mode of the ligands. (c) The grid-like network formed in the complex, **1d**.

In this complex, the ***bpyee*** molecules act as bis-monodentate ligand and coordinate to Mn(II) metal centres, through the formation of Mn-N coordinate bonds, with distances of 2.268 and 2.298 Å. Further, these units extend to form an infinite one-dimensional coordination polymers. As in the case of the complex, **1c**, in this complex also, the acid molecules exhibit bridging mode of coordination. Two adjacent metal centres are bound together by the bridging mode of carboxylates, with Mn-O distance of 2.152 Å (see Figure-11b). Thus, each Mn(II) is bonded to two ***bpyee***

molecules and four carboxylate units of **1**, yielding a slightly distorted octahedral arrangement.

In a typical octahedron, while ***bpyee*** molecules lie at the axial positions, carboxylates occupy the equatorial sites. Further, two-dimensional grid-like networks are formed, making use of the bridging mode of the carboxylate, as shown in Figure 11c. Such adjacent grids interact through C-H···O hydrogen bonds, as observed in **1c**, involving $-NO_2$ groups of the acid and the aromatic hydrogen of ***bpyee*** molecules, with a H···O distance of 2.90 Å. These interactions are further supplemented by the formation of C-H···π interactions with an average H···π distance of 3.16 Å, as shown in Figure 12b.

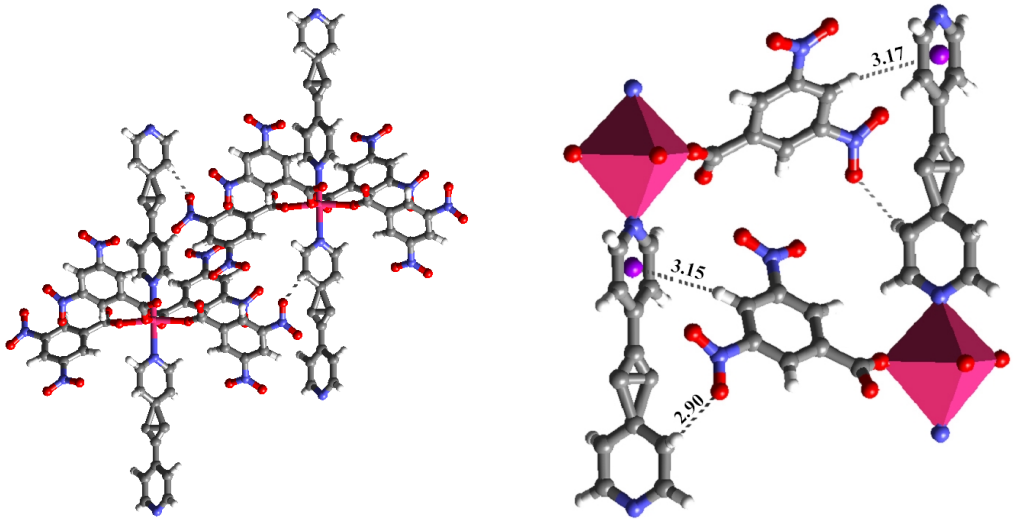

(a) **(b)**

Figure 12: (a) The inter-grid interactions present in the complex, **1d**. (b) Annotations of C-H···O and C-H···π interactions in the complex **1d**.

In continuation of the experiments to augment the conformational flexibility as well in the creation of exotic supramolecular architectures, the reactions of Mn(II)

acetate and **1** were studied in conjunction with flexible ligands, 1,2-bis(4-pyridyl)ethane, ***bpyea*** and 1,3-bis(4-pyridyl) propane, ***bpypa***.

2.3.5 Complex $[Mn(C_7H_3N_2O_6)(C_{12}H_{12}N_2)]$, 1e

The reaction of **1**, Mn(II) and 1,2-bis(4-pyridyl)ethane, ***bpyea***, in a methanol/water mixture and subsequent slow evaporation over a period of five days at ambient conditions yielded colorless needles. The crystal structure determination reveals that complex **1e** crystallizes in centrosymmetric space group, $P\bar{1}$ and the asymmetric unit contents are in the ratio 1:1:1.

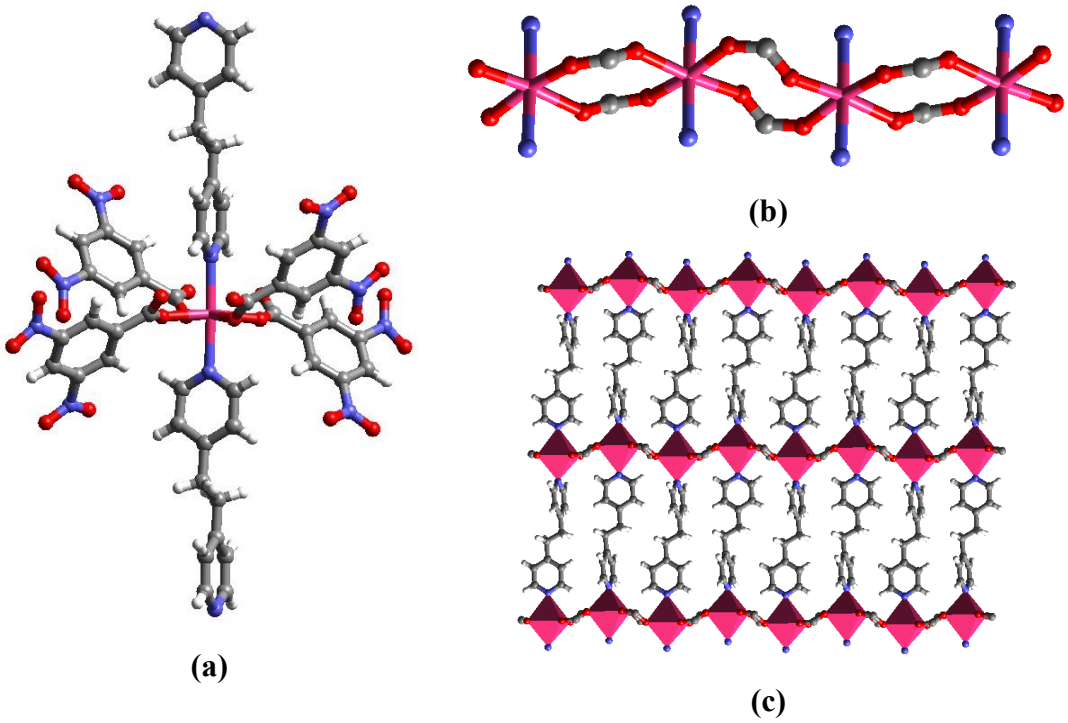

Figure 13: (a) The coordination environment around the metal centre in the complex, **1e**. (b) A view of the coordination mode of the ligands in the complex. (c) The grid-like network formed.

In the complex, **1e**, the ***bpyea*** molecule also forms a similar assembly as the rigid and linear molecules, ***bpy*** and ***bpyee***, as observed in **1c** and **1d**. A typical metal centre is bound to two ***bpyea*** molecules and four carboxylates, thus, giving a hexa-coordinated Mn(II) species, as shown in Figure 13a. While, ***bpyea*** molecules form coordinate bonds in a *trans*-mode with Mn(II) metal centre, through Mn(II)–N (2.262 and 2.300 Å) bonds, the metal-carboxylate bonds are of the distances, 2.148 and 2.151 Å. The infinite one-dimensional coordination polymers formed by making use of Mn(II) – ***bpyea*** coordinate bonds are held together by the bridging mode of carboxylates, thus leading to the formation of grid-like networks, as observed in **1c** and **1d** (see Figure 13c).

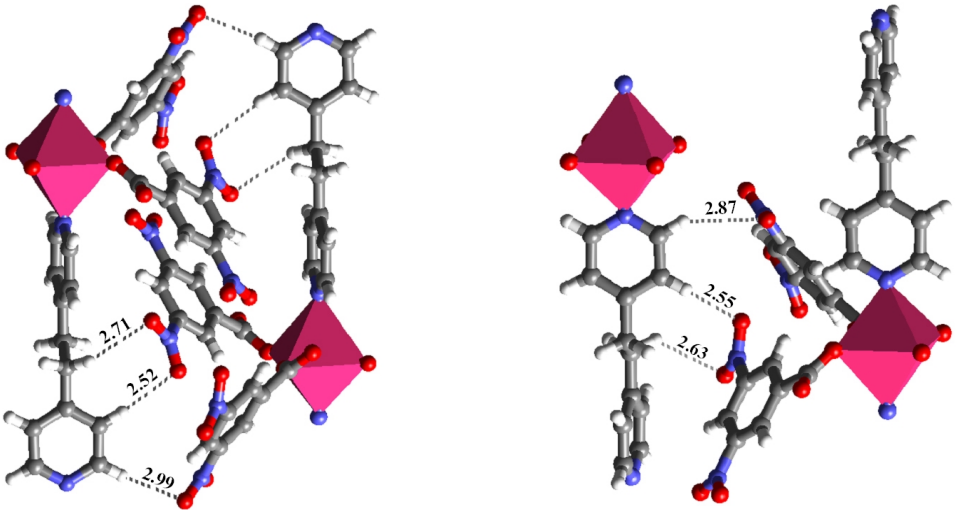

Figure 14: (a) and (b) The inter-grid interactions present in the complex, **1e**.

In addition, the interactions between the adjacent grids is also very much similar to those observed in the structures of **1c** and **1d**, forming C-H···O and C-H···N hydrogen bonds by making use of $–NO_2$ groups of **1** and the aromatic hydrogen of the

bpyea molecules. The detailed view of the hydrogen bonds formed between the adjacent grid networks, is shown in Figure 14. While, the H···O distances of the hydrogen bonds formed by the involvement of ***bpyea*** units are in the range 2.42 and 3.02 Å, the average H···N distance is 2.99 Å.

2.3.6 Complex $[Mn(C_7H_3N_2O_6)_2(C_{13}H_{14}N_2)]$, 1f

The crystal structure determination of the colorless crystals, obtained from a reaction of **1** and Mn(II) acetate with 1,3-bis(4-pyridyl) propane, ***bpypa*** in a methanol-water solution mixture, reveals the formation of complex **1f**, with the reactants in a 2:1:1 ratio.

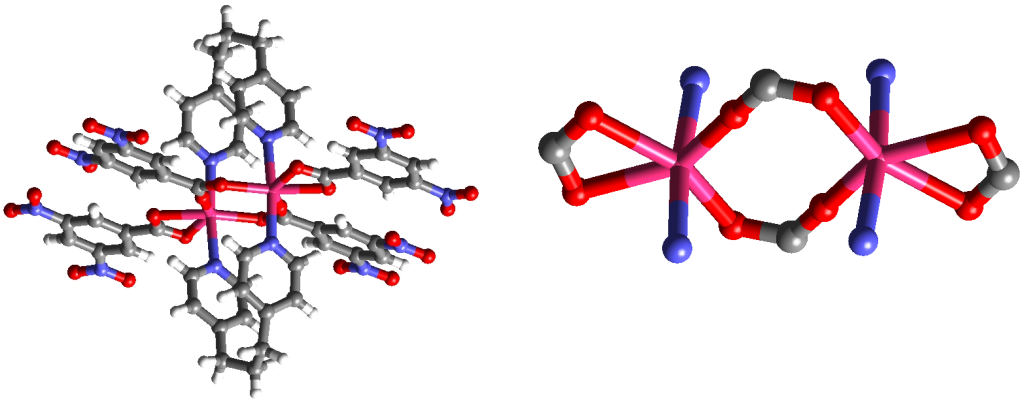

Figure 15: (a) A view of the metal centre in the complex, **1f** and (b) the coordination mode of the ligands.

In this complex, the acid molecules exhibit two different coordination modes – bridging and chelating. The two adjacent metal centres are bound together by the bridging mode of the carboxylate, with Mn–O distances of 2.150 Å, forming a dinuclear metal building unit. Further, the flexible ***bpypa*** molecules exhibit a *magic*

U-conformation connecting to both the metal centres in the dinuclear metal building units, thus leading to the formation of a capsule-like topology, as shown in Figure 15.

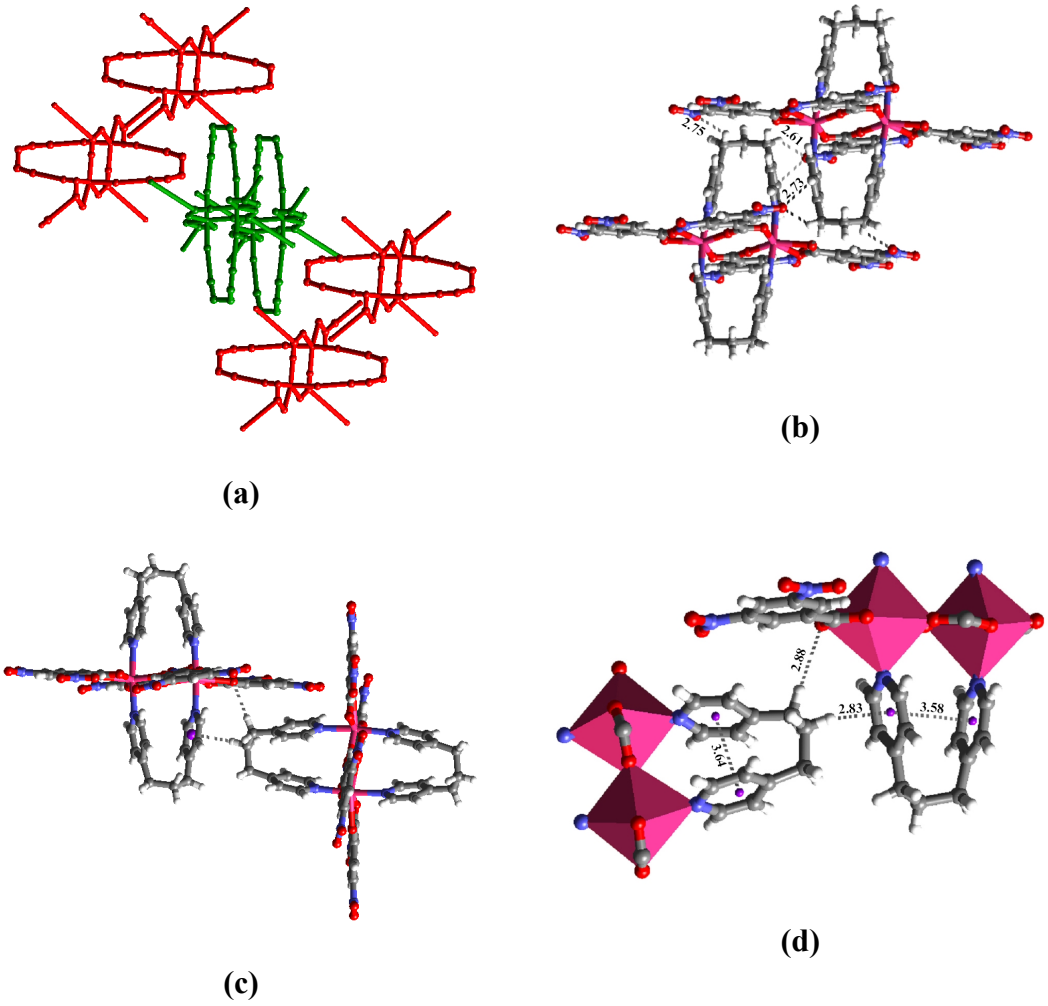

Figure 16: (a) A schematic representation of the three-dimensional packing of the bimetallic units in the complex **1f**. The green and red defines two modes of arrangement in the lattice. (b) The interactions between the parallel units. (c) The interactions existing between the perpendicular units. (d) A vivid view of the interactions existing between the perpendicular units.

In three-dimensional arrangement, the individual capsule-like building units are arranged in two modes. A schematic representation of the three dimensional packing arrangement exhibited by complex, **1f** is shown in Figure 16a. In one of the arrangements, in which the adjacent capsules lie parallel to each other, the dinuclear metal units are held together by C-H···O hydrogen bonds, formed between the $-NO_2$ groups of the acid and the methylene as well as the aromatic hydrogen of ***bpypa*** molecules. In this case, the average H···O distance is of the range, 2.70 Å.

But in the other mode, wherein, the capsules are arranged perpendicularly, the adjacent coordination units are held together by the C-H···O bond formed between the methylene hydrogen of ***bpypa*** and the carboxylate O-atom of the acid molecule, exhibiting the chelating mode of coordination. The hydrogen bonds, thus formed is further strengthened by the C-H···π interactions (H···π, 2.83Å) present between the ***bpypa*** molecules on the adjacent units, as shown in Figure 16d. Within a typical dinuclear metal units, face to face π ···π interactions (π ···π, 3.64 and 3.58 Å) exist between the two aromatic rings of individual ***bpypa*** molecule.

In the further evaluation of the coordination behavior of the ligands in the supramolecular coordination assemblies, chelating ligands like, 2,2'-bipyridine, ***22bpy*** and 1,10-phenanthroline, ***110phe***, were utilized in conjunction with Mn(II) and **1**, to evaluate structural differences in the resulting complexes, in comparison with the flexible ligands discussed earlier.

2.3.7 Complex $[Mn(C_7H_3N_2O_6)_2(C_{10}H_8N_2)]$, 1g

Reaction of manganese acetate tetrahydrate and **1** in the presence of 2,2'-bipyridine, ***22bpy*** from a methanol-water solution mixture, yielded a complex, **1g** in a 1:2:1 of the constituents in the reactions respectively, as determined by single-crystal x-ray diffraction methods. Complete details of the crystallographic information are given in Table 2.4.

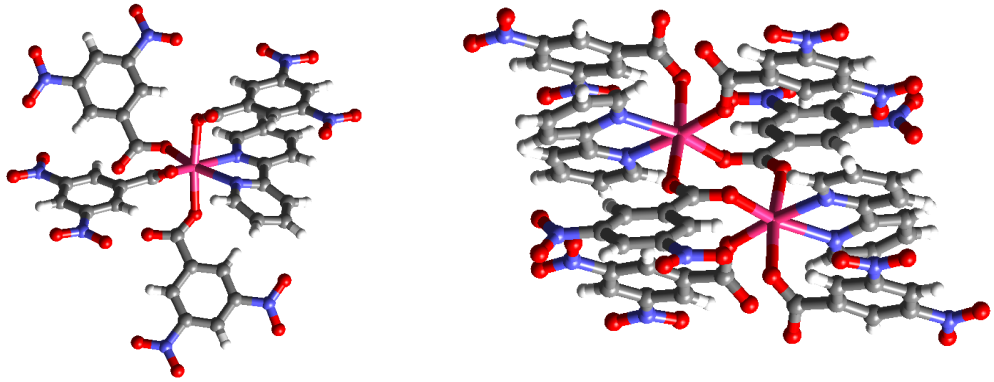

(a) **(b)**

Figure 17: (a) A typical metal coordination centre in complex **1g**. (b) The view of the helical arrangement, established in the complex **1g**, formed by the bridging mode of the carboxylate.

In this complex, the carboxylate exhibit the bridging mode coordination, with an average Mn–O distance of 2.130 Å. The ***22bpy*** molecules act as chelating ligand, as expected, through the formation of Mn–N coordinate bond, with distances, 2.314 and 2.285 Å. A representative metal coordination centre is shown in Figure 17a.Further, the adjacent metal centres are held together by carboxylates, as shown in Figure 17b, constitutes helical assembly. The helices, thus formed interact with the adjacent units through the formation of C-H···O hydrogen bonds, as shown in Figure 18, with the

–NO_2 group of **1** acting as the hydrogen bond acceptor and the donor species being the aromatic hydrogen atoms of ***22bpy*** and **1**.

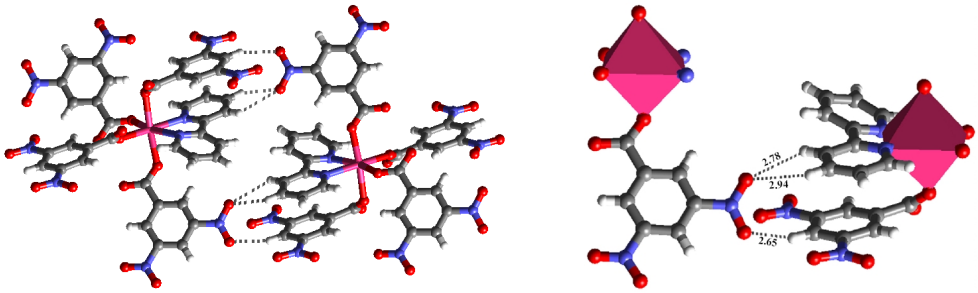

Figure 18: The C-H···O hydrogen bonds existing between the adjacent helices in the complex **1g**.

2.3.8 Complex $[Mn(C_7H_3N_2O_6)_2(C_{12}H_8N_2)(CH_3OH)]$, 1h

The crystal structure determination on the pale pink crystals obtained by the reaction of **1** and Mn(II) acetate in the presence of 1,10-phenanthroline, ***110phe***, from a methanol-water solution mixture, reveals the presence of the solvent of crystallization, methanol, in the asymmetric unit. The structure analysis further discloses that the asymmetric unit contains Mn(II), **1** and ***110phe*** in a 1:2:1 ratio respectively.

In this complex, ***110phe*** molecule functions as a chelating ligand and forms Mn–N (2.303 and 2.295 Å) coordinate bonds, with the metal center. In this complex, the carboxylate exhibits two different modes of coordination – bridging and monodentate. The bridging mode of coordination leads to the formation of a bimetallic building unit. Further, the hexa-coordination of the metal centre is fulfilled by a methanol molecule and a carboxylate unit, with monodentate coordination bonds.

Thus, each metal centre is coordinated to one ***110phe*** ligand, three carboxylates and one methanol molecule, yielding a distorted octahedral coordination sphere. The bimetallic unit formed and the schematic representation of the coordination environment of the metal centres is shown in Figure 19.

(a)

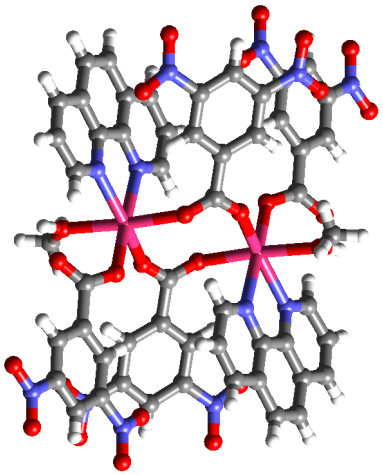

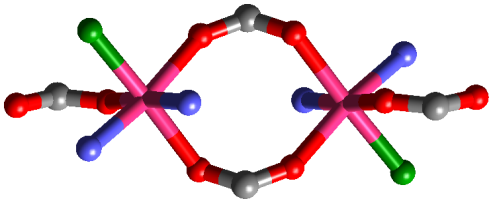

(b)

Figure 19: (a) The bimetallic unit formed and (b) the schematic representation of the coordination environment of the metal centres in the complex **1h**.

The bimetallic units, thus, formed interact with the adjacent units through the formation of O-H···O hydrogen bonds, with a H···O distance of 1.92Å, formed between the –OH group of methanol and the free O-atom of the carboxylate units (see Figure 20a). In addition, the assembly is stabilized by the C-H···O hydrogen bonds present between the adjacent units with H···O distance in the range of 2.33 to 2.83 Å. Further, these dinuclear metal units interact in the lateral direction also by forming C-H···O hydrogen bonds with the neighboring coordination units. This is established by making use of the aromatic hydrogen of ***110phe*** ligand and the $-NO_2$ group of the acid molecules, as shown in Figure 20b.

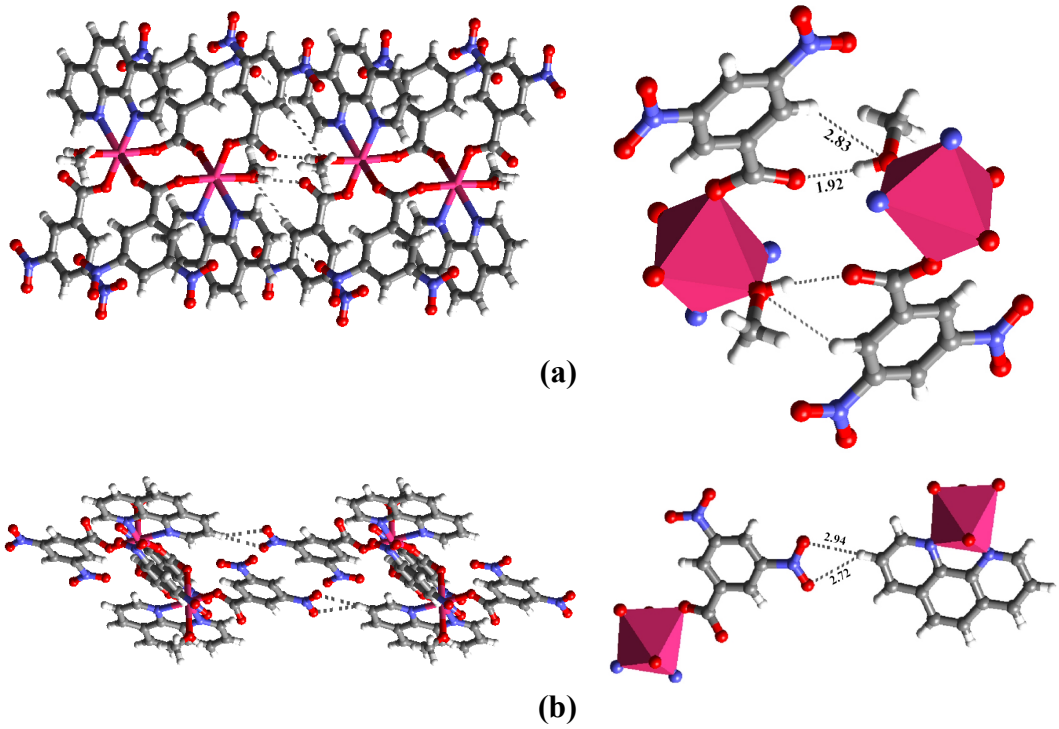

Figure 20: (a) The hydrogen bonds formed between the adjacent bimetallic units in the complex **1h**. (b) The interactions existing between the coordination units in the lateral direction.

Thus, this study reveals that, the different aza-donor ligands with varying dimensions and flexibility in coordination mode bring about subtle variation in the coordination behavior of functional groups with dynamic coordination modes, as shown in Scheme 5. While **1c, 1d** and **1e** formed grid-like networks, the complex **1f,** prepared by making use of flexible ***bpypa*** ligand yielded a bimetallic capsule like topology. Further, the complexes **1g** and **1h**, formed in the presence of chelating ligands ***22bpy*** and ***110phe***, respectively, gave helical assembly and bimetallic complexes. In all the complexes, the major binding force between the polymer chains is the C-H···O hydrogen bonds formed by making use of the $-NO_2$ groups on **1**.

Scheme 5

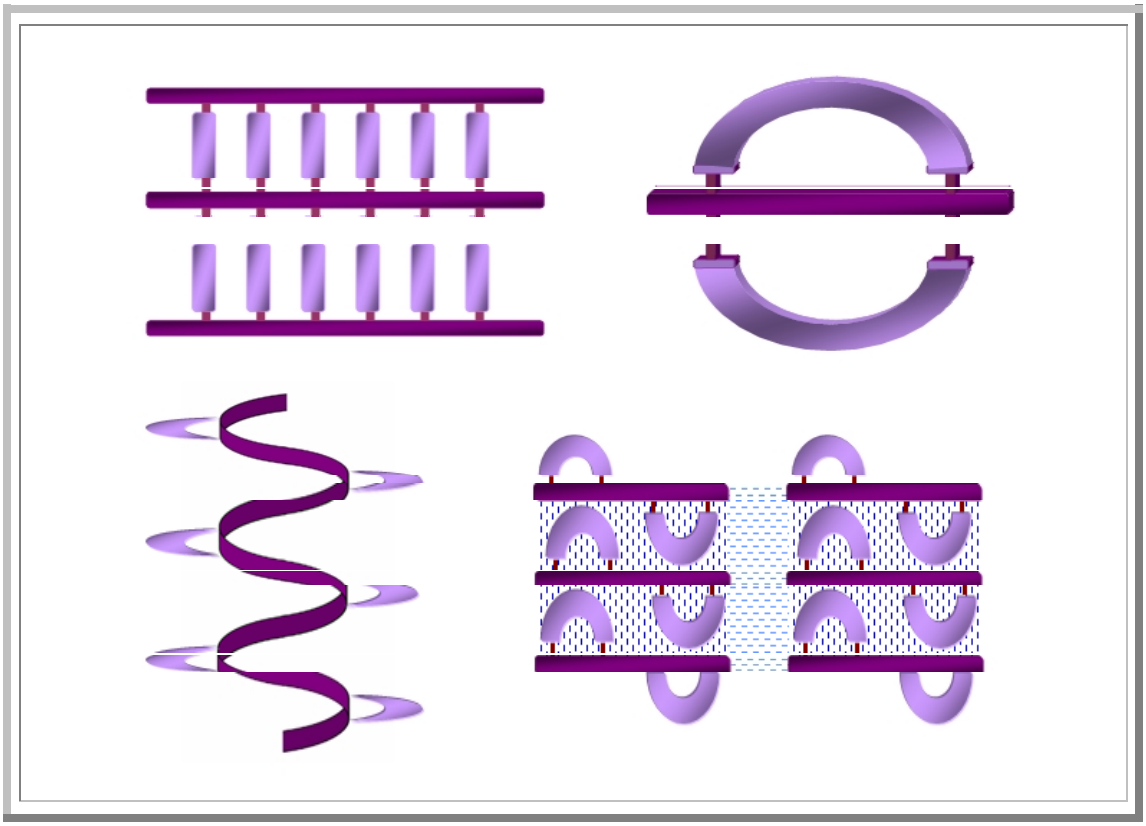

2.4 Conclusions

The structural evaluation of the metal-organic assemblies obtained by the variation of reaction conditions and different aza-donor ligands, reveals that the conditions like, solvent of crystallization and the flexibility and the coordination modes of the spacer ligands bring about notable variation in the coordination behavior of dynamic functional groups like carboxylate, which can take part in coordination bond formation in a variety of ways. This in turn can influence the self-assembly and the three-dimensional architecture of the resulting assemblies. Further, the presence of the other functional groups like $-NO_2$ facilitated the stabilization of the resultant

architectures through hydrogen bonds such as C-H···O bonds as observed in all the complexes discussed in this Chapter. Thus, this study also reveals the synergetic effect of coordinate bonds and hydrogen bonds to yield a variety of supramolecular assemblies with the variation of simple experimental conditions like solvent of crystallization and functionality of the aza-donor ligands.

Tables

Table 2.1: Crystallographic information of Co(II) complexes of **1** and **2**.

Complex	1a	1b	2a	2b
Formula	$[Co(C_7H_3N_2O_6)_2(C_{10}H_8N_2)(CH_3O)_2]$	$[Co_2(C_7H_3N_2O_6)_4(C_{10}H_8N_2)_2(CH_3O)]C_3H_6O$	$[Co(C_8H_5N_2O_6)_2(C_{10}H_8N_2)]$	$[Co(C_8H_5N_2O_6)_2(C_{10}H_8N_2)(H_2O)_2]2(C_2H_6S0)$
Formula Wt.	699.41	1363.80	664.39	841.55
Crystal system	Tetragonal	Monoclinic	Monoclinic	Monoclinic
Space group	$P4_32_12$	$P2_1/c$	$C2/c$	$P2/n$
***a* (Å)**	8.095(1)	22.774(2)	17.675(6)	11.025(5)
b *(•)*	8.095(1)	*11.375(1)*	18.709(4)	*15.139(4)*
***c* (Å)**	46.283(6)	22.533(2)	21.044(6)	11.443(4)
α (deg)	90	90	90	90
β (deg)	90	104.15(1)	108.68(3)	97.48(3)
γ (deg)	90	90	90	90
***V* (Å^3)**	3033.0(7)	5660.2(9)	6592(3)	1893.8(1)
Z	4	*4*	8	*2*
D_{calc} (g cm^{-3})	1.532	1.600	1.339	1.579
***T* (K)**	298(2)	298(2)	298(2)	298(2)
μ (Mo K_α) (mm^{-1})	0.646	0.687	0.586	1.064
2θ range (deg)	46.52	46.60	46.36	46.60
Total Reflns.	12826	23238	5005	7728
Unique Reflns.	2169	8158	3085	2726
R(int)				
Reflns. used	1957	3933	2318	1972
No. of Parameters	250	830	420	262
GOF on F^2	1.229	1.121	1.353	1.062
Final R1, wR2	0.0500, 0.1136	0.1041, 0.2152	0.0997, 0.2860	0.0522, 0.1400

Table 2.2: Coordination environment of Co(II) metal center in the complexes **1a, 1b, 2a** and **2b.** (Bond lengths in Å)

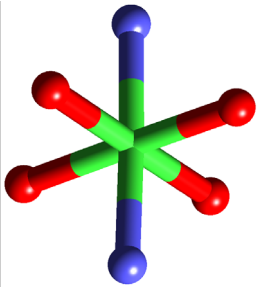

				Co-O(carboxylate)		
	Co-N(pyridyl)	Co-O(water)	Co-O(MeOH)	monodentate	bridging	chelating
1a	2.171(5) 2.187(5)		2.139(4)	2.070(3)		
1b[a]	2.143(9) 2.153(9)		2.162(8)	2.103(8)	2.053(8) 2.040(8)	
1b[b]	2.140(9) 2.153(9)				2.106(8) 2.087(9) 2.119(8) 2.094(9)	
2a	2.163(9) 2.159(9)				2.040(8) 2.075(8)	2.219(7) 2.223(8)
2b	2.174(4)	2.139(3)		2.080(3)		
a-Terminal metal centre			***b-Middle metal centre***			

Table 2.3: Characteristics of hydrogen bonds (distances/Å and angles/deg) [#]

	1a	1b	2a	2b
C-H···O	2.725 3.725 139 2.852 3.360 127 2.899 3.505 126	2.487 3.341 153 2.520 3.445 173 2.524 3.327 141 2.599 3.514 168 2.671 3.523 153 2.753 3.557 145 2.835 3.756 161 2.843 3.730 160 2.864 3.746 159 2.886 3.648 140 2.930 3.781 153 2.955 3.809 149	2.436 3.204 137 2.661 3.260 121 2.898 3.803 165 2.954 3.668 135 2.983 3.668 140	2.684 3.596 167 2.717 3.325 124 2.810 3.460 128 2.783 3.624 147
O-H···O				2.68

[#] The three numbers in each column indicate H···A, D···A and angles, respectively

Table 2.4: Crystallographic information of the complexes, **1c**-**1h**.

Complex	1c	1d	1e
Formula	$[Mn(C_7H_3N_2O_6)_2(C_{10}H_8N_2)]$	$[Mn(C_7H_3N_2O_6)(C_{12}H_{10}N_2)]$	$[Mn(C_7H_3N_2O_6)(C_{12}H_{12}N_2)]$
Formula Wt.	633.35	659.37	661.40
Crystal system	Monoclinic	Monoclinic	Triclinic
Space group	*P*2/c	*C*2/*c*	$P\bar{1}$
***a* (Å)**	9.999(5)	20.510(3)	10.048(3)
b *(•)*	11.649(7)	*13.945(3)*	12.210(4)
***c* (Å)**	21.986(4)	10.016(2)	12.660(4)
α (deg)	90	90	68.02(2)
β (deg)	108.26(1)	113.13(4)	67.81(1)
γ (deg)	90	90	70.50(2)
***V* (Å^3)**	2432(2)	2634.4(12)	1299.7(7)
Z	4	*4*	2
D_{calc} (g cm^{-3})	1.730	1.657	1.690
***T* (K)**	120(2)	298(2)	120(2)
μ (Mo K_α) (mm^{-1})	0.627	0.582	0.591
2θ range (deg)	66.28	56.06	66.28
Total Reflns.	27009	11060	21162
Unique Reflns. R(int)	9172	3042	9843
Reflns. used	7298	2544	8476
No. of Parameters	407	235	414
GOF on F^2	1.014	1.111	1.044
Final R1, wR2	0.0357, 0.0913	0.0436, 0.1273	0.0342, 0.0913

Table 2.4 *(Contd…)*:

Complex	1f	1g	1h
Formula	$[Mn(C_7H_3N_2O_6)_2(C_{13}H_{14}N_2)]$	$[Mn(C_7H_3N_2O_6)_2(C_{10}H_8N_2)]$	$[Mn(C_7H_3N_2O_6)_2(C_{12}H_8N_2)(CH_3OH)]$
Formula Wt.	675.43	633.35	689.41
Crystal system	Monoclinic	Triclinic	Triclinic
Space group	$P2_1/c$	$P\bar{1}$	$P\bar{1}$
***a* (Å)**	12.432(3)	7.638(2)	9.545(3)
b *(•)*	*9.967(2)*	11.928(3)	*12.085(4)*
***c* (Å)**	23.566(5)	14.765(4)	12.453(3)
α (deg)	90	76.20(1)	96.85(2)
β (deg)	110.55(1)	75.88(1)	91.65(2)
γ (deg)	90	88.77(1)	102.88(2)
***V* (Å^3)**	2734.2(11)	1265.9(6)	1388.1(7)
Z	*4*	2	*2*
D_{calc} (g cm^{-3})	1.641	1.662	1.650
***T* (K)**	120(2)	120(2)	120(2)
μ (Mo K_α) (mm^{-1})	0.563	0.602	0.559
2θ range (deg)	66.28	66.32	46.50
Total Reflns.	44348	20955	10950
Unique Reflns.	10414	9559	3996
R(int)			
Reflns. used	8249	7159	3543
No. of Parameters	435	388	428
GOF on F^2	1.033	1.030	1.062
Final R1, wR2	0.0482, 0.1331	0.0420, 0.0939	0.0263, 0.0679

Table 2.5: Coordination environment of Mn(II) metal center in the complexes, **1c-1h** (Bond lengths in Å).

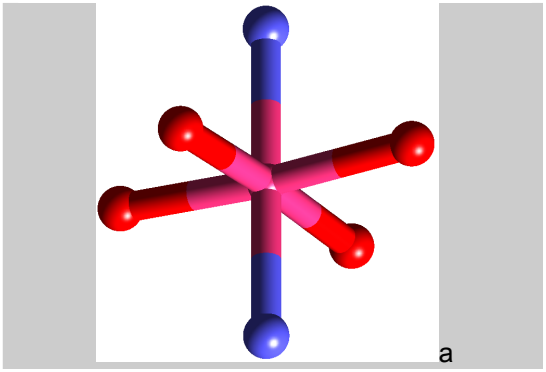
a

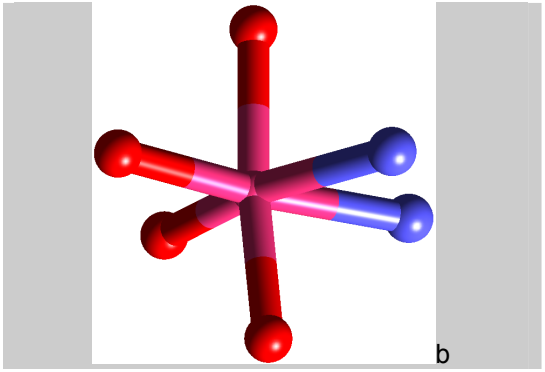
b

			Mn-O$_{(carboxylate)}$		
Complex	**Mn-N$_{(pyridyl)}$**	**Mn-O$_{(MeOH)}$**	**monodentate**	**bridging**	**chelating**
1c	2.268(2) 2.270(2)			2.198(1) 2.131(1) 2.159(1) 2.194(1)	
1d	2.268(2) 2.298(2)			2.152(1)	
1e	2.300(1) 2.262(1)			2.148(9) 2.151(9)	
1f	2.240(1) 2.272(1)			2.150(1)	2.342(2)
1g	2.314(1) 2.285(1)			2.160(1) 2.100(1)	
1h	2.303(2) 2.295(2)	2.217(2)	2.112(2)	2.119(1)	
a – metal center of complexes 1c, 1d, 1e and 1f			***b – metal center of complexes 1g and 1h***		

Table 2.6: Characteristics of hydrogen bonds for complexes **1c**-**1h**. (distances/Å and angles/deg)

	1c	**1d**	**1e**
O–H···O			
C–H···O	2.574 3.500 174 2.599 3.324 135 2.703 3.497 144 2.842 3.517 129	2.900 3.493 167 3.016 3.944 151	2.422 3.286 151 2.520 3.463 172 2.540 3.423 155 2.552 3.380 146 2.633 3.304 125 2.712 3.517 139 2.866 3.707 148 2.994 3.707 133 3.024 3.897 153
C–H···N	2.843 3.680 150		2.992 3.661 126 2.994 3.761 139 3.069 3.837 139

	1f	**1g**	**1h**
O–H···O			1.923 2.702 170
C–H···O	2.445 3.335 156 2.489 3.130 122 2.605 3.243 125 2.610 3.471 145 2.728 3.378 126 2.745 3.494 133 2.753 3.526 139 2.772 3.507 135 2.793 3.507 132 2.880 3.785 152 2.989 3.865 148 3.072 3.842 139	2.457 3.371 161 2.649 3.530 155 2.669 3.260 121 2.698 3.382 129 2.775 3.435 127 2.784 3.456 128 2.842 3.517 129 2.939 3.514 120	2.355 3.029 128 2.369 3.274 159 2.535 3.389 150 2.567 3.488 163 2.570 3.489 163 2.599 3.424 142 2.674 3.627 164 2.722 3.671 177 2.832 3.646 144 2.936 3.680 136 2.964 3.904 170
C–H···N	3.028 3.838 140		2.825 3.787 167

2.5 References

(1) (a) Gómez-Lor, B.; Gutiérrez-Puebla, E.; Iglesias, M.; Monge, M. A.; Ruiz-Valero, C.; Snejko, N. *Chem. Mater.* **2005**, *17*, 2568-2573. (b) Janiak, C. *Dalton Trans.* **2003**, 2781-2804. (c) Notestein, J. M.; Katz, A. *Chem. Eur. J.* **2006**, *12*, 3954-3965.

(2) (a) Brammer, L. *Chem. Soc. Rev.* **2004**, *33*, 476-489. (b) Chen, B.; Liang, C.; Yang, J.; Contreras, D. S.; Clancy, Y. L.; Lobkovsky, E. B.; Yaghi, O. M.; Dai, S. *Angew. Chem. Int. Ed.* **2006**, *45*, 1390-1393. (c) Cui, G. H.; Li, J. R.; Tian, J. L.; Bu, X. H.; Batten, S. R. *Cryst. Growth Des.* **2005**, *5*, 1775-1780. (d) Kitagawa, S.; Kitaura, R.; Noro, S. *Angew. Chem. Int. Ed.* **2004**, *43*, 2334-2375.

(3) (a) Chen, B.; Ockwig, N. W.; Millward, A. R.; Contreras, D. S.; Yaghi, O. M. *Angew. Chem. Int. Ed.* **2005**, *44*, 4745-4749. (b) Dybtsev, D. N.; Chun, H.; Kim, K. *Angew. Chem. Int. Ed.* **2004**, *43*, 5033-5036. (c) Panella, B.; Hirscher, M.; Pütter, H.; Müller, U. *Adv. Funct. Mater.* **2006**, *16*, 520-524. (d) Rowsell, J. L. C.; Yaghi, O. M. *Angew. Chem. Int. Ed.* **2005**, *44*, 4670-4679.

(4) Drechsler, U.; Erdogan, B.; Rotella, V. M. *Chem. Eur. J.* **2004**, *10*, 5570-5579.

(5) (a) Holmes, K. E.; Kelly, P. F.; Elsegood, M. R. J. *Dalton Trans.* **2004**, 3488-3494. (b) Ma, B.; Coppens, P. *Chem. Commun.* **2003**, 2290-2291. (c) Melendez, R. E.; Sharma, C. V. K.; Zaworotko, M. J.; Bauer, C.; Rogers, R. D. *Angew. Chem. Int. Ed.* **1996**, *35*, 2213-2215.

(6) (a) Sudik, A. C.; Côté, A. P.; Yaghi, O. M. *Inorg. Chem.* **2005**, *44*, 2998-3000. (b) Zhang, Z. H.; Shen, Z. L.; Okamura, T. A.; Zhu, H. F.; Sun, W. Y.; Ueyama, N. *Cryst. Growth Des.* **2005**, *5*, 1191-1197. (c) Abourahma, H.; Moulton, B.; Kravtsov, V.; Zaworotko, M. J. *J. Am. Chem. Soc.* **2002**, *124*, 9990-9991.

(7) (a) Batten, S. R.; Murray, K. S. *Aust. J. Chem.* **2001**, *54*, 605-609. (b) Blake, A. J.; Champness, N. R.; Hubberstey, P.; Li, W.; Withersby, M. A.; Schröder, M. *Coord. Chem. Rev.* **1999**, *183*, 117-138. (c) Chen, B.; Ockwig, N. W.; Fronczek, F. R.; Contreras, D. S.; Yaghi, O. M. *Inorg. Chem.* **2005**, *44*, 181-183. (d) Li, Y.; Zou, X. *Angew. Chem. Int. Ed.* **2005**, *44*, 2012-2015. (e) Maji, T. K.; Mostafa, G.; Changa, H.; Kitagawa, S. *Chem. Commun.* **2005**, 2436-2438.

(8) (a) Dybtsev, D. N.; Chun, H.; Kim, K. *Angew. Chem. Int. Ed.* **2004**, *43*, 5033-5036. (b) Nishikiori, S.; Yoshikawa, H.; Sano, Y.; Iwamoto, T. *Acc. Chem. Res.* **2005**, *38*, 227-234. (c) Tynan, E.; Jensen, P.; Kelly, N. R.; Kruger, P. E.; Lees, A. C.; Moubaraki, B.; Murray, K. S. *Dalton Trans.* **2004**, 3440-3447.

(9) (a) Carlucci, L.; Ciani, G.; Proserpio, D. M.; Spadacini, L. *CrystEngComm* **2004**, *6*, 96-101. (b) Hennigar, T. L.; MacQuarrie, D. C.; Losier, P.; Rogers, R. D.; Zaworotko, M. J. *Angew. Chem. Int. Ed.* **1997**, *36*, 972-973. (c) Moulton, B.; Zaworotko, M. J. *Chem. Rev.* **2001**, *101*, 1629-1658.

(10) (a) Kepert, C. J. *Chem. Commun.* **2006**, 695-700 and references within. (b) Cheetham, A. K.; Rao, C. N. R.; Feller, R. K. *Chem. Commun.* **2006**, 4780-4795.

(11) (a) Zaworotko, M. J. *Angew. Chem. Int. Ed.* **2000**, *39*, 3052-3054. (b) Ohmori, O.; Kawano, M.; Fujita, M. *Angew. Chem. Int. Ed.* **2005**, *44*, 1962-1964. (c) Xiong, R.; Tou, X.; Abrahams, B. F.; Xue, Z.; Che, C. *Angew. Chem. Int. Ed.* **2001**, *40*, 4422-4425.

(12) (a) Maji, T. K.; Mostafa, G.; Changa, H.; Kitagawa, S. *Chem. Commun.* **2005**, 2436-2438. (b) Rusanov, E. B.; Ponomarova, V. V.; Komarchuk, V. V.; Stoeckli-Evans, H.; Fernandez-Ibalez, E.; Stoeckli, F.; Sieler, J.; Domasevitch, K. V. *Angew. Chem. Int. Ed.* **2003**, *42*, 2499-2501.

(13) (a) Chen, B.; Eddaoudi, M.; Hyde, S. T.; O'Keeffe, M.; Yaghi, O. M. *Science* **2001**, *291*, 1021-1023. (b) Rosi, N. L.; Eckert, J.; Eddaoudi, M.; Vodak, T.; Kim, J.; O'Keeffe, M.; Yaghi, O. M. *Science* **2003**, *300*, 1127-1129. (c) Biradha, K.; Fujita, M. *Chem. Commun.* **2001**, 15-16. (d) Fujita, M.; Tominaga, M.; Hori, A.; Therrien, B. *Acc. Chem. Res.* **2005**, *38*, 371-380.

(14) (a) Serre, C.; Millange, F.; Thouvenot, C.; Nogues, M.; Marsolier, G.; Louer, D.; Férey, G. *J. Am. Chem. Soc.*, **2002**, *124*, 13519-13526. (b) Kitagawa, S.; Kondo, M. *Bull. Chem. Soc. Jpn.* **1998**, *71*, 1739-1753.

(15) (a) Amoore, J. J. M.; Hanton, L. R.; Spicer, M. D. *Supramol. Chem.* **2005**, *17*, 557-565. (b) Awaleh, M. O.; Badia, A.; Brisse, F. *Inorg. Chem.* **2005**, *44*, 7833-7845. (c) Cordes, D. B.; Bailey, A. S.; Caradoc-Davies, P. L.; Gregory, D. H.; Hanton, L. R.; Lee, K.; Spicer, M. D. *Inorg. Chem.* **2005**, *44*, 2544-2552. (d) Du,

M.; Li, C. P.; Zhao, X. J. *Cryst. Growth Des.* **2006**, *6*, 335-341. (e) Ska, L.; Raubenheimer, H. G.; Barbour, L. J. *Chem. Commun.* **2005**, 5050-5052. (f) Zhu, H. F.; Fan, J.; Okamura, T. A.; Zhang, Z. H.; Liu, G. X.; Yu, K. B.; Sun, W. Y.; Ueyama, N. *Inorg. Chem.* **2006**, *45*, 3941-3948.

(16) (a) Kitagawa, S.; Uemura, K. *Chem. Soc. Rev.* **2005**, *34*, 109-119. (b) Kitagawa, S.; Kitaura, R.; Noro, S. *Angew. Chem. Int. Ed.* **2004**, *43*, 2334-2375. (c) Burchell, T. J.; Eisler, D. J.; Puddephatt, R. J. *Chem. Commun.* **2004**, 944-945.

(17) (a) Biradha, K.; Fujita, M. *Angew. Chem. Int. Ed.* **2002**, *41*, 3392-3395. (b) Takaoka, K.; Kawano, M.; Tominaga, M.; Fujita, M. *Angew. Chem. Int. Ed.* **2005**, *44*, 2151-2154.

(18) Masaoka, S.; Tanaka, D.; Nakanishi, Y.; Kitagawa, S. *Angew. Chem. Int. Ed.* **2004**, *43*, 2530-2534.

(19) Sun, D.; Ke, Y.; Mattox, T. M.; Ooro, B. A.; Zhou, H. *Chem. Commun.* **2005**, 5447-5449.

(20) Forster, P. M.; Burbank, A. R.; Livage, C.; Férey, G.; Cheetham, A. K. *Chem. Commun.* **2004**, 368-369.

(21) (a) Dalgarno, S. J.; Hardie, M. J.; Raston, C. L. *Cryst. Growth Des.* **2004**, *4*, 227-234.

(22) Zheng, Y.; Tong, M. L.; Chen, X. *New J. Chem.* **2004**, 1412-1415.

(23) (a) Seward, C.; Chan, J.; Song, D.; Wang, S. *Inorg. Chem.* **2003**, *42*, 1112-1120. (b) Feazell, R. P.; Carson, C. E.; Klausmeyer, K. K. *Inorg.Chem.* **2005**, *44*, 996-1005. (c) Ren, Y.; Kong, X.; Long, L.; Huang, R.; Zheng, L. *Cryst.Growth Des.* **2006**, *6*, 572-576. (d) Sun, C.; Li, L.; Jin, L. *Polyhedron* **2006**, *25*, 3017-3024.

(24) (a) Bernstein, J.; Davey, R. J.; Henck, J.-O. *Angew. Chem. Int. Ed.* **1999**, *38*, 3440-3461. (b) Bernstein, J. *Polymorphism in Molecular Crystals*; Oxford Univ. Press: New York, 2002. (c) Caira, M. R. *Top. Curr. Chem.* **1998**, *198*, 163-208. (d) McCrone, W. C. Polymorphism; In *Physics and Chemistry of the Organic Solid State*; (Eds. Fox, D., Labes, M. M., Weissberger, A.); Interscience: New York, 1965. (e) Threlfall, T. L. *Analyst* **1995**, *120*, 2435-2460.

(25) Shin, D. M.; Lee, I. S.; Chung, Y. K.; Lah, M. S. *Chem. Commun.* **2003**, 1036-1037.

(26) (a) Varughese, S.; Pedireddi, V. R. *Tetrahedron Lett.* **2005**, *46*, 2411-2415. (b) Ranganathan, A.; Pedireddi, V. R. *Tetrahedron Lett.* **1998**, *39*, 1803-1806. (c) Pedireddi, V. R.; Ranganathan, A.; Chatterjee, S. *Tetrahedron Lett*. **1998**, *39*, 9831-9834. Pedireddi, V. R.; Jones, W.; Chorlton, A. P.; Dochery, R. *Chem. Commun.* **1996**, 987-988.

(27) (a) Sheldrick, G. M. SADABS, Area Detector Correction. 2002. Madison, WI, Siemens Industrial Automation, Inc. (b) Sheldrick, G. M. SAINT Area Detector Integration Software. 1998. Madison, WI, Siemens Industrial Automation, Inc.

(c) Sheldrick, G. M. SHELX97 programs for crystal Strucutre Analysis. (97-2). 1998. Institüt für Anorganische Chemie der Universität. (d) Sheldrick, G. M. XPREP. (V5.1). 1997. Madison, WI, Bruker Analytical X-Ray Systems.

(28) Speck, A. L. PLATON. Acta Crystallogr., Sect.A A46, C34. 1990.

Chapter-3

Hydrogen bond Mediated
Metal-Organic Open-frame Networks

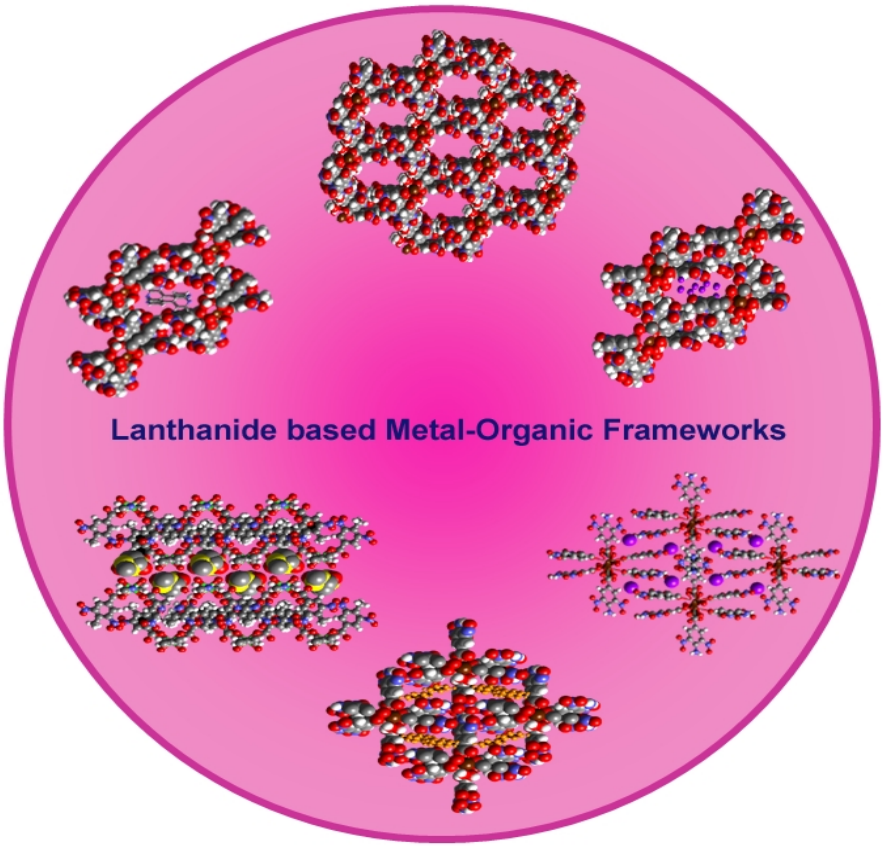

The way to get good ideas is to get lots of ideas, and throw the bad ones away

-Linus Pauling-

3.1 Introduction

The preparation of organic-inorganic hybrid materials with rigid and open frameworks have received a lot of attention, due to their potential applications in catalysis, gas storage, optics, luminescent materials and magnetics.[1-4] In this regard, versatile organic ligands and metal ions have been utilized for the preparation of numerous coordination polymers with exotic architectures and tailor-made properties.[5] While, the earlier studies of the coordination assemblies of metal carboxylate networks mostly centered on the *d*-block metal ions, the analogous chemistry of the lanthanide ions is not that well explored, except a few reports appeared in the recent literature.[6,7]

Lanthanides are attractive due to their unique nature of several physical characteristics such as large ionic radii, high and variable coordination numbers and the existence of multi-single electrons.[8] Thus, the assemblies of lanthanide complexes with novel structures and specific properties offer great challenges and opportunities in terms of controlling their shape and dimensionality. In addition to the attractive coordination properties, these metal species exhibit unique chemical characteristics arising from *4f*-electrons and also they show the propensity to form isostructural complexes, with different optical and magnetic properties, enabling them as fluorescent probes and IR-emitters.[9]

One of the major hurdles for the synthesis of metal-organic assemblies is the solubility of the resultant assemblies and it is more reflective while drifting from transition metal ions to lanthanides, which is perhaps one of the many reasons for the

limited research in the lanthanide based coordination assemblies. However recent developments in the exploration of novel synthetic strategies like hydrothermal technique, provided solution for a large number of complex problems often encountered in the supramolecular synthesis.[10]

Hydrothermal equipment is basically a steel vessel, closed at one end. The other end has a screw cap with a gasket of soft copper to provide a seal. Inside this vessel, a teflon container with a lid is placed. The reaction mixture and an appropriate amount of water are placed inside this container and sealed. The schematic representation is shown in Figure 1.

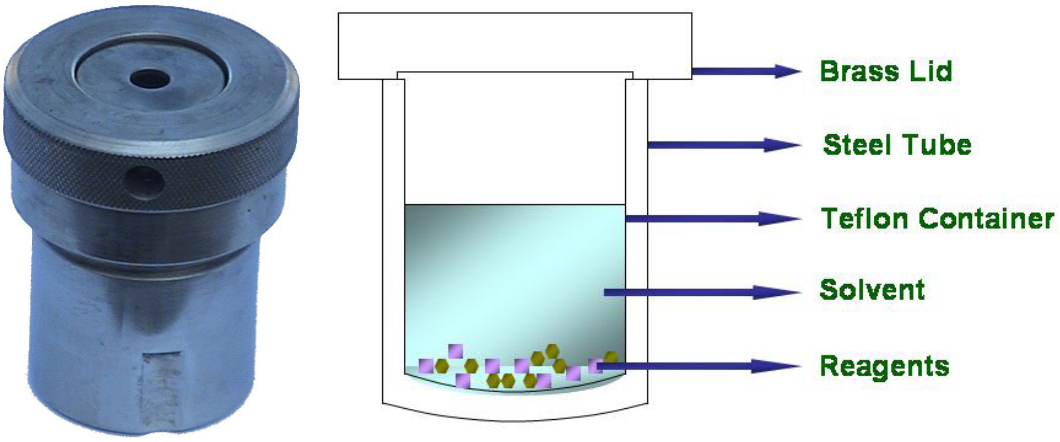

(a) **(b)**

Figure 1: (a) Photograph of a stainless steel hydrothermal bomb. (b) The schematic representation of a hydrothermal bomb.

Hydrothermal methods, which are basically dealing with high pressure and high temperature, are finding increasing applications in materials science and solid state chemistry.[11] Further, they are technologically important, both as an important

method of crystal growth and for the synthesis of new materials with useful properties. Thus, the proposed lanthanide assemblies have been prepared by using hydrothermal methods and the obtained supramolecular frameworks are discussed in the following sections.

3.2 Hydrogen bond mediated metal-organic assemblies

A large number of studies of coordination assemblies were not only aimed at the utilization of transition metal ions as discussed above, but also mainly focused on the preparation of 3-D frameworks possessing pores, making use of rigid building units linked by coordination bonds. But, since the realization of numerous advantages of dynamic assemblies, efforts were made to synthesize frameworks by the utilization of building units that can also afford intermolecular interactions such as hydrogen bonds, along with the coordination bonds.[12]

The generation of a host framework that interacts with exchangeable guest species in a switchable fashion has implications for the generation of advanced materials with applications in areas such as molecular sensing.[13] It is worth noting that, even weak interactions between guest and pore-wall molecules can induce a structural change because of a cooperative effect based on a large ensemble over an infinite framework. Hence, for the synthesis of dynamic porous coordination polymers, it is necessary to consider a large spectrum of intermolecular interactions such as hydrogen bonds, van der Waals forces, π-π stacking etc.[14]

Scheme 1

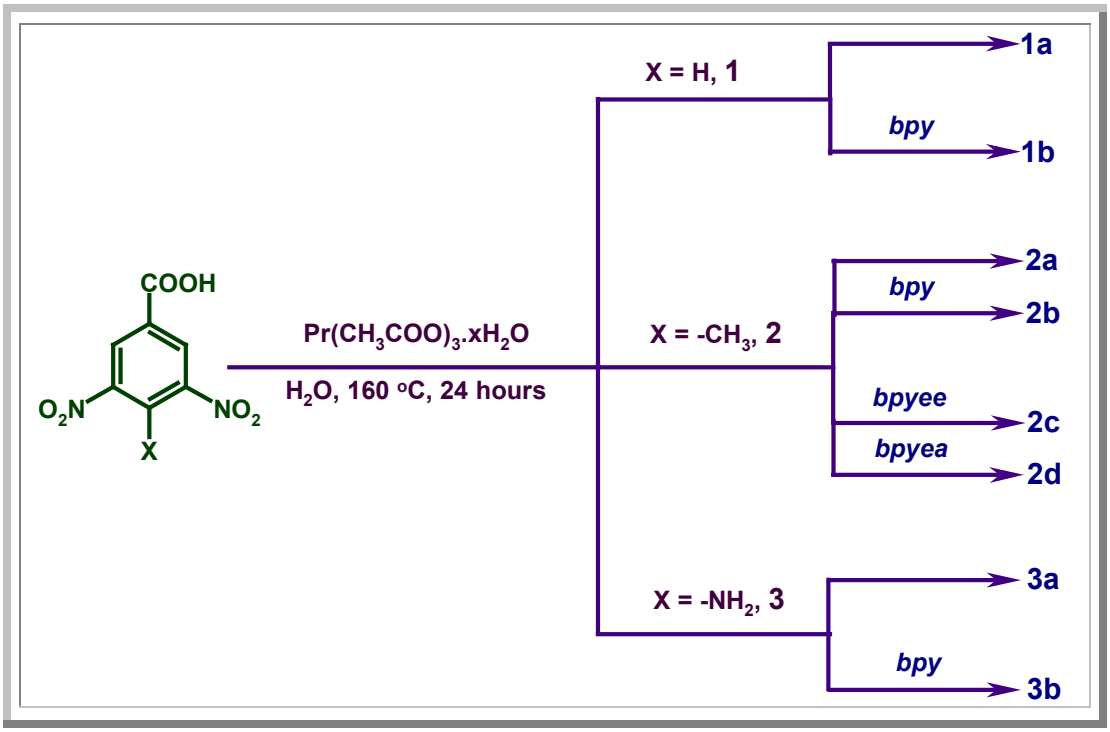

Since the hydrogen bond characteristics are well studied,[15] judicial choice of organic ligands in the synthesis of metal-organic framework solids would provide greater chances of yielding a wide range of dynamic functional solids. This can be achieved by making use of organic ligands having functional groups, such as $–NO_2$, $–NH_2$ etc., which are known to form well defined robust hydrogen bond networks and have less affinity towards metal ions. In this direction, taking advantage of the earlier success, as discussed in Chapter 2, the preparation of lanthanide based metal-organic assemblies of 3,5-dinitrobenzoic acid, **1** and its methyl-derivative, 3,5-dinitro-4-methylbenzoic acid, **2**, in the presence of various aza-donor spacer ligands, 4,4'-bipyridine, ***bpy***, 1,2-bis(4-pyridyl)ethane, ***bpyea***, 1,2-bis(4-pyridyl)ethene, ***bpyee***, have been carried out to expand the horizon of combination of coordinate bonds and

hydrogen bonds to lanthanide based assemblies. The detailed experimental conditions and the sequence of reaction process are given in Scheme 1. All the resulted complexes have been characterized by single crystal x-ray diffraction methods.

3.2.1 Experimental Section

A General procedure for the synthesis of complexes 1a - 3a

To an aqueous solution (15mL) of $Pr(CH_3COO)_3.\ xH_2O$ (0.1 mmol), was added the acid **1**, **2** or **3** (0.1 mmol), with stirring. After stirring for 15 minutes at room temperature, the mixture was transferred and sealed in a Teflon-lined stainless-steel autoclave of 23 mL capacity, under autogenous pressure, and heated to 160 ^oC for 24 h. The crystals obtained were washed with distilled water and dried at room temperature.

A General procedure for the synthesis of complexes 1b, 2b - 2d and 3b

To an aqueous solution (15mL) of praseodymium acetate hydrate (0.1 mmol), was added the acid (**1**, **2** or **3**) (0.1 mmol), with stirring, followed by the N-donor ligand (***bpy***, ***bpyea*** or ***bpyee***) (0.1 mmol), as the case may be. After stirring for 15 minutes at ambient conditions, the mixture was transferred and sealed in a Teflon-lined stainless steel autoclave of 23 mL capacity, under autogenous pressure and heated to 160 ^oC for 24 h. The crystals obtained were washed thoroughly with distilled water and dried at room temperature.

3.2.2 X-ray Crystallography

Good quality single crystals of **1a**, **1b**, **2a - 2d, 3a** and **3b** were carefully chosen after they were viewed through a Leica microscope supported by a rotatable polarizing stage and a CCD camera. The crystals were glued to a thin glass fiber using an adhesive (cyanoacrylate) and mounted on a diffractometer equipped with an APEX CCD area detector. The data collection was smooth in all the cases, and no extraordinary methods were employed, except that the crystals were smeared in cyanoacrylate to protect them from ambient laboratory conditions. The intensity data were processed using Bruker's suite of data processing programs (SAINT), and absorption corrections were applied using SADABS. The structure solution of all the complexes was carried out by direct methods, and refinements were performed by full-matrix least-squares on F^2 using the SHELXTL-PLUS suite of programs.[16] All the structures converged to good R factors. All the non-hydrogen atoms were refined anisotropically, and the hydrogen atoms obtained from Fourier maps were refined isotropically. All the refinements were smooth in all the structures. Intermolecular interactions were computed using the PLATON program.[17]

3.3 Complexes of Pr(III) and 3,5-dinitrobenzoic acid

3.3.1 Complex $[Pr_2(C_7H_3N_2O_6)_6(H_2O)_4].2H_2O$, 1a

The hydrothermal reaction of Pr(III) acetate and 3,5-dinitrobenzoic acid in a molar ratio of 1:1 gave pale green, block-like, crystals of coordination polymer $[Pr_2(C_7H_3N_2O_6)_6(H_2O)_4].2H_2O$ (**1a**). The crystallographic analysis revealed that the

complex **1a** consists of nine coordinated Pr(III) metal nodes, connected through the bridging mode of carboxylate of **1**, forming one-dimensional coordination polymers. The complete details of the crystallographic analysis are given in Table 3.1.

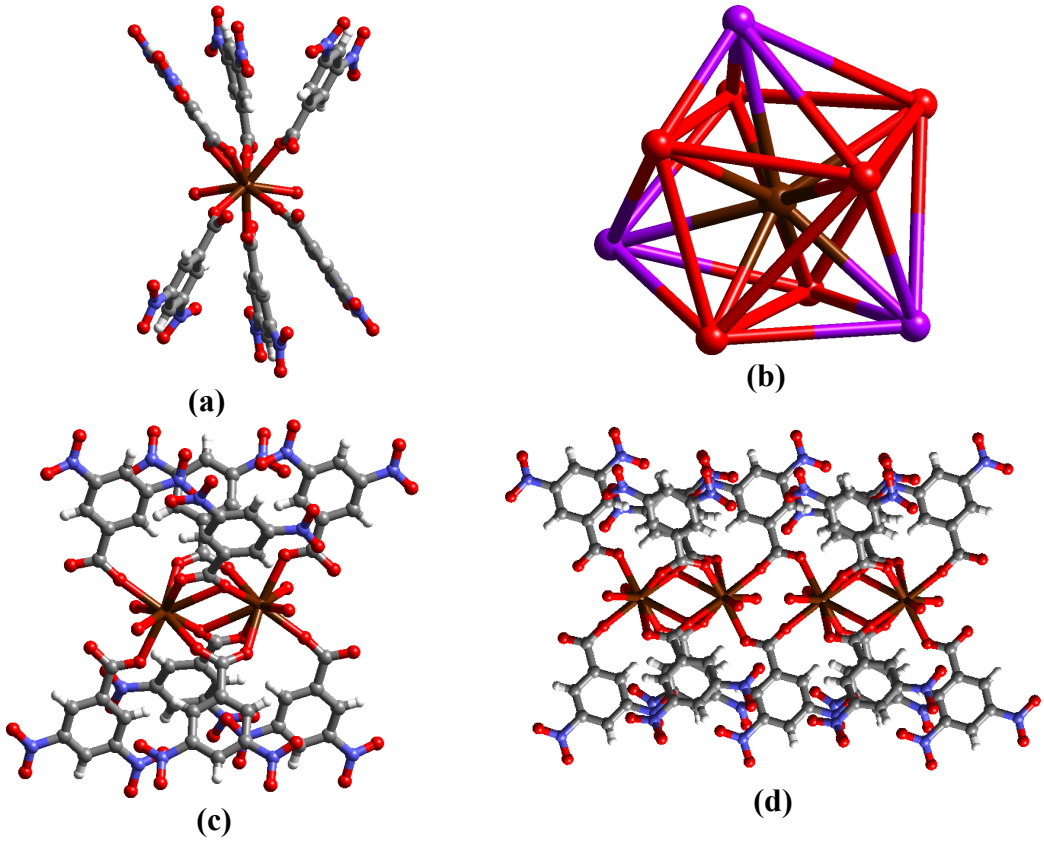

Figure 2: (a) The nine-coordinated Pr(III) in the complex **1a**. (b) The tricapped trigonal prismatic polyhedral geometry exhibited by the Pr(III) metal centre. (*The capping elements, two coordinated water and one of the O-atom of the chelating carboxylate, are shown in purple color*). (c) The bimetallic unit, resulted from the bridging and the tridentate mode of coordination of the carboxylate. (d) The one-dimensional coordination polymer formed in complex **1a**.

Each Pr(III) metal center is coordinated to seven oxygen atoms of six carboxylate units and two oxygen atoms of water molecules, as shown in Figure 2a. In

this complex, the acid moiety exhibits various coordination modes – bridging, chelating and μ-oxo bridging tridentate mode. Thus, each metal center exhibits tricapped trigonal prismatic coordination geometry, as shown in Figure 2b. The coordination environment around the Pr(III) metal centre in the complex **1a** is tabulated in the Table 3.2.

The bridging mode of the carboxylates binds the adjacent metal centres to yield one-dimensional polymers, as shown in Figure 2d. The self- assembly of the resulting one-dimensional coordination polymers yielded a hexagonal close-packed coordination assembly, as shown in Figure 3. The adjacent coordination polymers are stabilized by O-H···O hydrogen bonds, with an O···O distance of 2.97 Å, formed between the coordinated water molecules and the $-NO_2$ groups of the acid functionality. These interactions are further strengthened by the C-H···O hydrogen bonds, as listed in Table 3.3, formed between the aromatic hydrogen atoms and the $-NO_2$ groups present on **1**.

Further, the self-assembly of coordination polymers results in the formation of void spaces, which are occupied by the water molecules. The free water molecules are held to the host framework making use of the O-H···O hydrogen bonds, with O···O distance of 2.73 Å and C-H···O hydrogen bonds formed by utilizing the aromatic hydrogen atoms of the acid molecules. The average H···O distance for C-H···O hydrogen bonds is 2.86 Å.

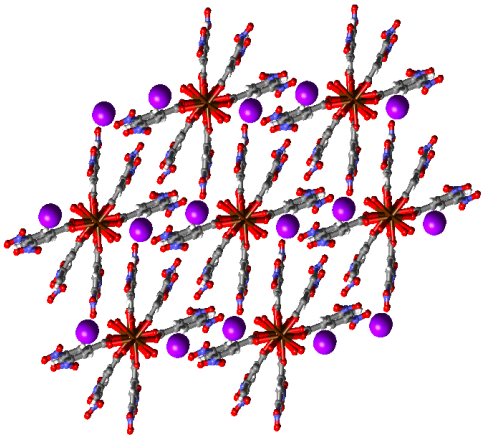

Figure 3: The three dimensional packing of the complex **1a**. The guest water molecules are represented in purple colored ball mode.

Further, to enhance the pore dimension of the coordination assembly observed in **1a** and to replace water molecules with molecules of larger dimensions, the complex of Pr(III) and **1** was prepared in the presence of 4,4'-bipyridine, ***bpy***, which is well known to interact with metal ions and also with the –COOH groups.

3.3.2 Complex $[Pr_2(C_7H_3N_2O_6)_4(C_2H_3O_2)_2(C_{10}H_8N_2)_2(H_2O)_2]$, 1b

Coordination polymers of the formula $[Pr_2(C_7H_3N_2O_6)_4(C_2H_3O_2)_2(C_{10}H_8N_2)_2(H_2O)_2]$ were synthesized from the hydrothermal reaction of praseodymium(III) acetate with 3,5-dinitrobenzoic acid, **1**, in the presence of 4,4'-bipyridine, ***bpy***, and were obtained in the form of needle-like crystals.

Structure analysis reveals that in a typical metal centre, Pr(III) is coordinated to four acid molecules, two acetates, one ***bpy*** molecule and one water molecule, as shown in Figure 4a. The details of the coordination bonds are given in Table 3.4. In this complex, ***bpy*** molecules are coordinated to the metal centre as monodentate ligands, making use of only one of its hetero-atom. The other N-atom is involved in

the hydrogen bond formation of O-H···N hydrogen bonds (O···N, 2.843Å) with the water molecules coordinated to metal centre. The bridging mode of the carboxylate of **1** holds two adjacent metal units thus, yielding a bimetallic unit. Further, the acetate molecules acting as a tridentate ligand also play a major role in the formation of the bimetallic units. A representative example of the bimetallic unit formed in the complex **1b** is shown in the Figure 4b. The bimetallic units thus formed, interact with neighboring units through the bridging carboxylates, thus forming a one-dimensional coordination polymer.

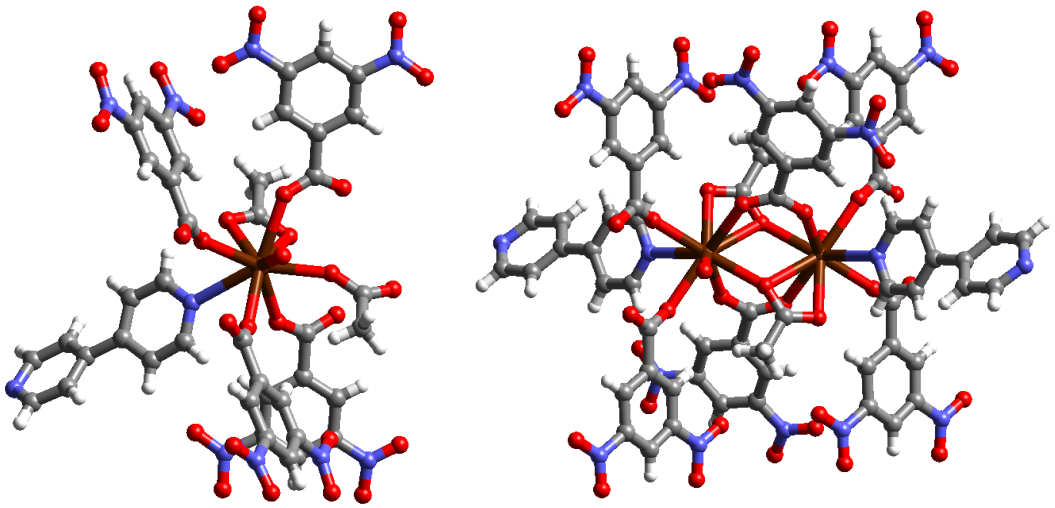

(a) **(b)**

Figure 4: (a) The coordination environment of Pr(III) in the complex, **1b**. (b) The bimetallic units formed by the bridging mode of coordination exhibited by the carboxylates.

In the ultimate crystal packing, the one-dimensional polymers undergo self-assembly to form a close-packed structure, as shown in Figure 5a. The polymer units are held together by the O-H···N hydrogen bonds formed between the coordinated water molecules and the hetero-atom of the ***bpy*** units. The detailed view of the

hydrogen bond pattern is shown in Figure 5b. Further, the assembly is stabilized by several C-H···O hydrogen bonds, making use of $–NO_2$ group of **1**. Although the spacer ligand, ***bpy***, is able to coordinate to metal centers as anticipated, the self-protrusion of bulky moieties from the adjacent polymer blocks constituted a close-packed structure, rather than forming a porous structure.

(a)

(b)

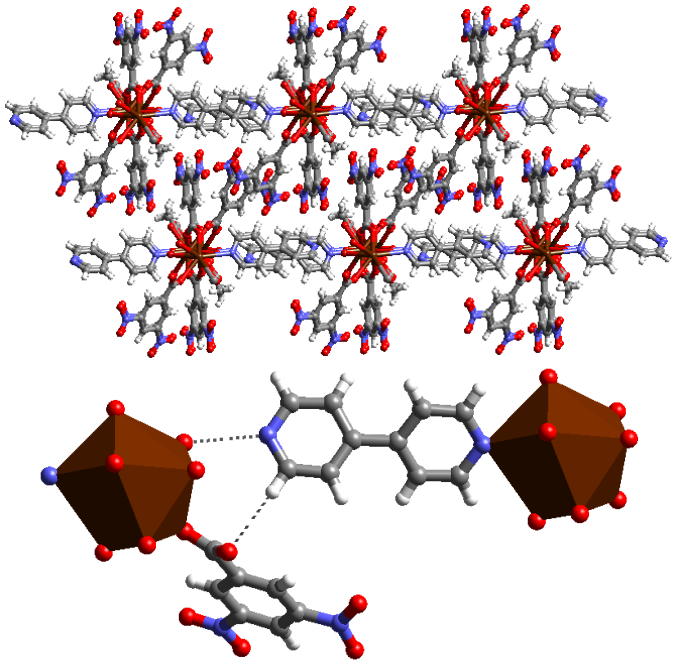

Figure 5: (a) The three-dimensional close-packed structure formed in the complex, **1b**. (b) The vivid view of the hydrogen bonds formed by ***bpy*** units.

Further efforts to analyze the structures obtained from ***bpyea*** and ***bpyee*** were not successful, as the crystals were unstable to characterize by single crystal x-ray diffraction methods. Thus, in search of preparing porous framework structures through the combination of coordinate and hydrogen bonds, efforts were made to prepare the metal-organic assemblies of methyl- and amino- derivatives of 3,5-dinitrobenzoic acids as these molecules are known to self-assemble through intermolecular

interactions formed by $–NO_2$ and $–NH_2$ groups, and such an environment may promote the formation of open-frame networks, while carboxylates interact through dative bonds.

3.4 Complexes of Pr(III) and 3,5-dinitro-4-methyl benzoic acid

3.4.1 Complex $[Pr_2(C_8H_5N_2O_6)_6(H_2O)_4].6H_2O$, 2a

A Coordination polymer of the formula $[Pr_2(C_8H_5N_2O_6)_6(H_2O)_4].6H_2O$ was synthesized from the hydrothermal reactions of praseodymium(III) acetate with 3,5-dinitro-4-methylbenzoic acid, **2** and was characterized by single crystal x-ray diffraction methods (see Table 3.5).

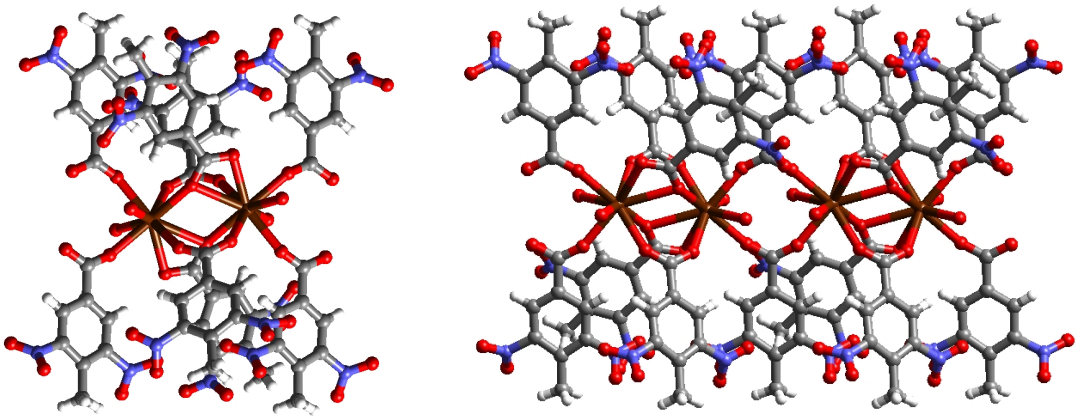

(a) **(b)**

Figure 6: (a) The bimetallic unit formed by the coordination behavior of the carboxylates. (b) The extended one-dimensional polymers formed by the bridging mode of the carboxylate, binding the adjacent bimetallic units.

Analysis of the coordination geometry reveals the formation of a bimetallic building unit with two Pr(III) ions being bridged by the carboxylate groups of two acid molecules with an average Pr–O distance of 2.400 Å, as shown in Figure 6a. The

coordination environment details of the Pr(III) metal centre is given in Table 3.6. The two Pr(III) ions in the complex, act as nine connected nodes with four carboxylate groups bridging to the nodes in bis-monodentate and tridentate modes thus, giving rise to a bimetallic unit. Further, each Pr(III) metal fulfills the nona-coordination with two water molecules, with an average Pr–O distances of 2.563 and 2.610 Å. The remaining two molecules of **2**, however, act as bis-monodentate ligands and bridge bimetallic units, with Pr–O distances of 2.418 and 2.495 Å (see Figure 6b), giving rise to one-dimensional polymers.

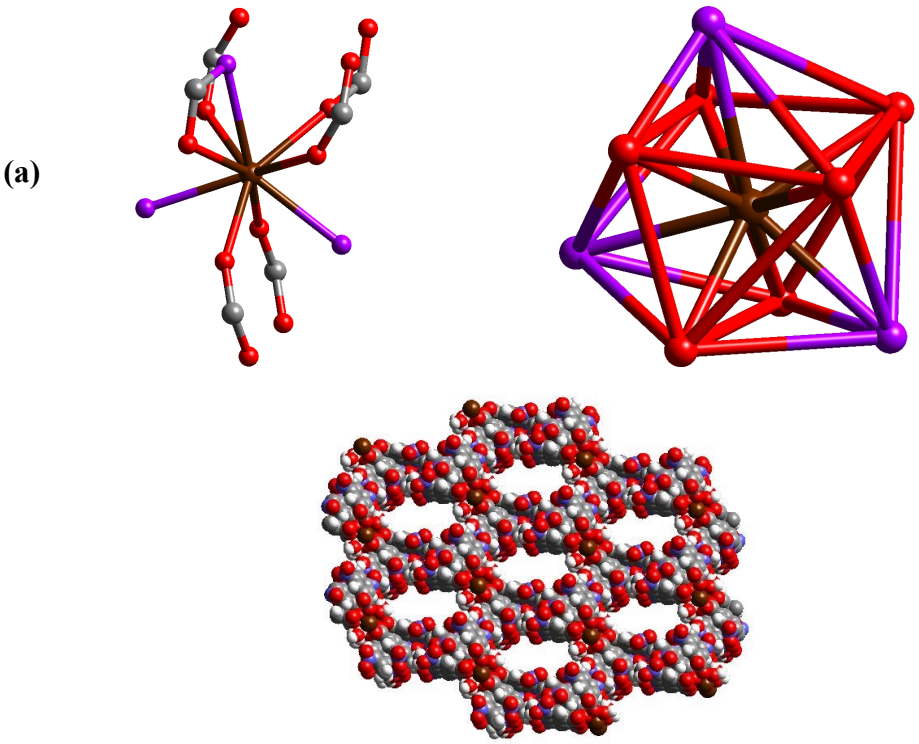

Figure 7: (a) The coordination environment of Pr(III) in the complex **2a**. (b) The tricapped trigonal prismatic polyhedral coordination geometry exhibited by Pr(III). (*The three capping elements are shown in purple color*). (c) Three- dimensional view of the porous network formed in complex **2a**.

Typical metal coordination environment in $[Pr_2(C_8H_5N_2O_6)_6(H_2O)_4]$. $6H_2O$ and the schematic representation of the coordination geometry around Pr(III) as a tricapped trigonal prism are shown in Figure 7a and 7b, respectively. The three-dimensional arrangement of the resultant coordination polymer, however, is quite intriguing as the one-dimensional polymers undergo self-assembly to form an open-frame network through the hydrogen bonds formed between the $–CH_3$ and $–NO_2$ groups. Viewed along the crystallographic *c*-axis, the resulting 3D network of the complex, **2a**, is reminiscent of the shape of a compressed honeycomb with channels. A typical arrangement of the framework is shown in Figure 7c.

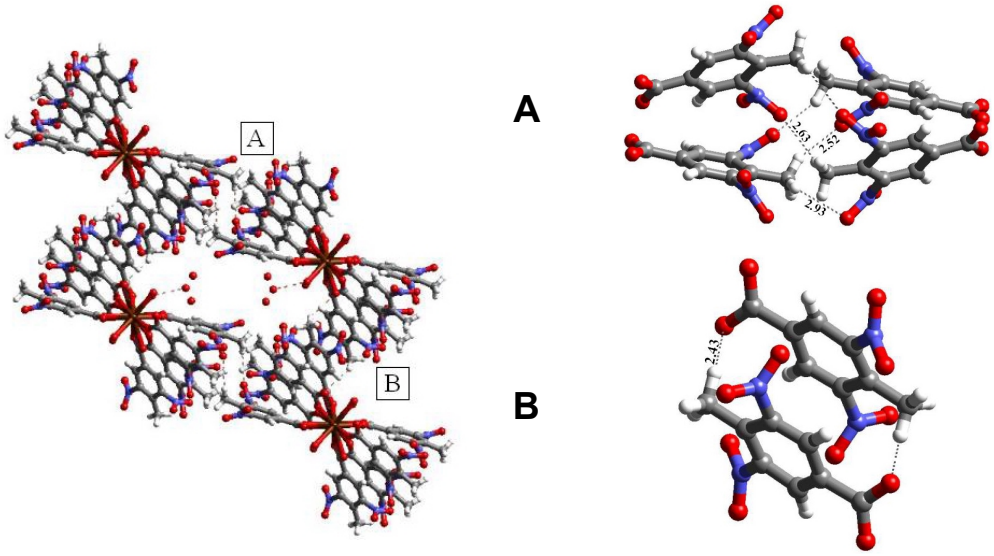

Figure 8: The cavity structure formed by the self-assembly of the coordination polymers in complex **2a**, along with the hydrogen bond details.

Each channel is created due to two different types of hydrogen bonding networks, as represented by 'A' and 'B' in Figure 8, by connecting four neighboring units by C–H···O hydrogen bonds with H···O distances in the range 2.43–2.95 Å (see

Table 3.7). Thus, the coordination units are aggregated making use of the C–H···O hydrogen bonds, resulting in the formation of channels, with a dimension of 6 × 15 $Å^2$ which are occupied by six water molecules.

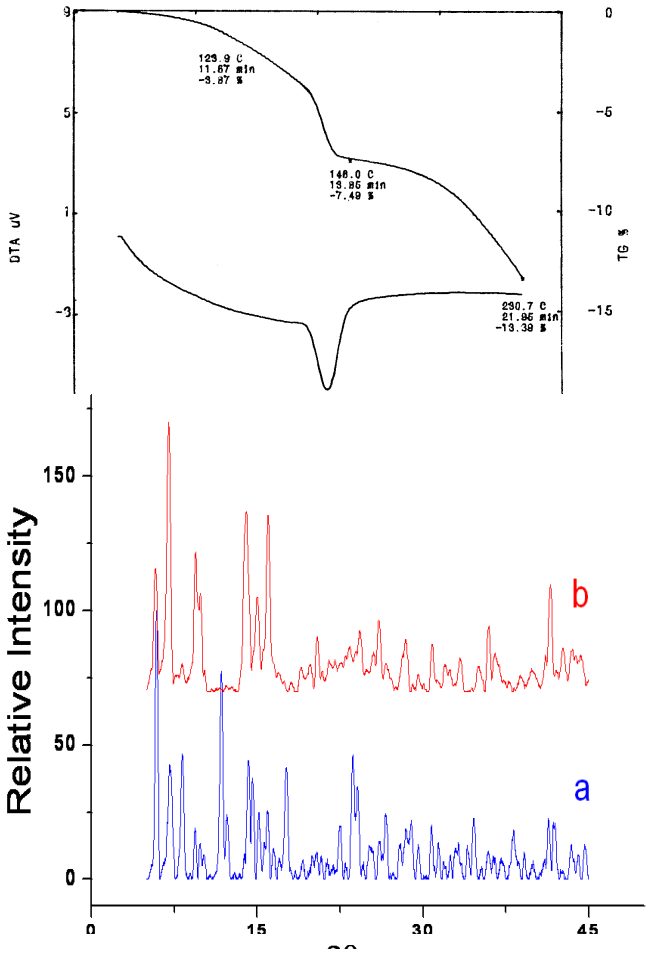

Figure 9: (a) The thermogravimetric plot and (b) The PXRD patterns of the complex **2a**. (Blue – as synthesized and Red – after heating at 120 ^oC for 8hrs.)

The thermogravimetric analysis of the complex, **2a** reveals that water molecules in the channels are being evacuated at around 130 ^oC, showing about 3% weight lose (Figure

9a) and the complex still remains crystalline and stable as confirmed by x-ray powder diffraction methods (Figure 9b).

Taking advantage of the formation of open-framework solid structure by **2** with Pr(III), further efforts were made to insert hydrocarbons like benzene, naphthalane and anthracene in such channels as these hydrocarbons are well known to form host-guest complexes. But, the experiments revealed that the components crystallized separately, perhaps due to incompatibility between the dimensions of the channels and the guests or may be due to the lack of hydrogen bond forming functionalities in the guest species. Hence, hydrothermal experiments have been carried out with N-donor ligands which are potentially good hydrogen donor acceptors as well as have different molecular dimensions than hydrocarbons.

3.4.2 Complex $[Pr_2(C_8H_5N_2O_6)_6(H_2O)_4].2C_{10}H_8N_2$, 2b

The hydrothermal reaction of **2**, ***bpy*** and Pr(III) acetate, at 160 ^oC for 24 hours, yielded complex **2b**, having the molecular formula $[Pr_2(C_8H_5N_2O_6)_6(H_2O)_4].2C_{10}H_8N_2$, in which the host network is formed by the self-assembly of coordination polymers formed by Pr(III) and carboxylate of **2**, with cavities of dimensions 7 **x** 14 $Å^2$.

Further, it was noted that the complexes **2a** and **2b** are isostructural, with similar aggregation patterns. In both cases the channels are formed by the association of the neighboring coordination units through C–H···O hydrogen bonds. The C–H···O

hydrogen bonds observed in **2b** with H···O distances in the range 2.53–2.92 Å are as shown in Figure 10.

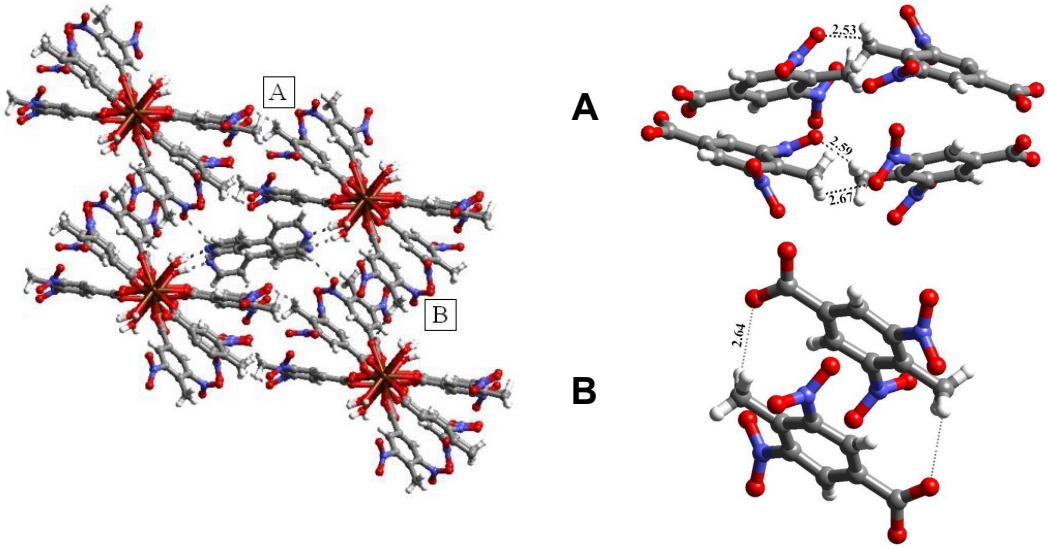

Figure 10: The porous assembly formed by the self-assembly of 1D coordination polymers and the detailed view of the hydrogen bonds stabilizing the assembly.

In such a channel structure, two molecules of ***bpy***, occupy the void space, thus, replacing all six water molecules, observed in complex, **2a**. Such a replacement apparently occurred as the ***bpy*** molecules in the channels are found to be interacting with the host network through the formation of O–H···N hydrogen bonds (N···O, 2.77 and 2.80 Å). Furthermore, the open-frame network observed in complexes **2a** and **2b** are as stable as generally observed in the structures mediated exclusively by coordinate bonds, such that, even, guest-exchange reactions could be performed, as we noted that a reaction between **2a** and ***bpy*** gave exclusively **2b**.

3.4.3 Complex $[Pr_2(C_8H_5N_2O_6)_6(H_2O)_4](C_{12}H_{10}N_2).\ 4H_2O$, 2c

Further, to evaluate the utility of the host framework in the guest exchange reaction with other organic molecules, a reaction was carried out between the complex **2a** and *trans*-1,2-bis(4-pyridyl)ethene, ***bpyee***, and obtained a host guest complex, **2c** in which only two water molecules, present in the channels of **2a**, were replaced by a ***bpyee*** molecule. Representation of host-guest complex, observed in **2c** along with the pertinent hydrogen bonds is shown in Figure 11.

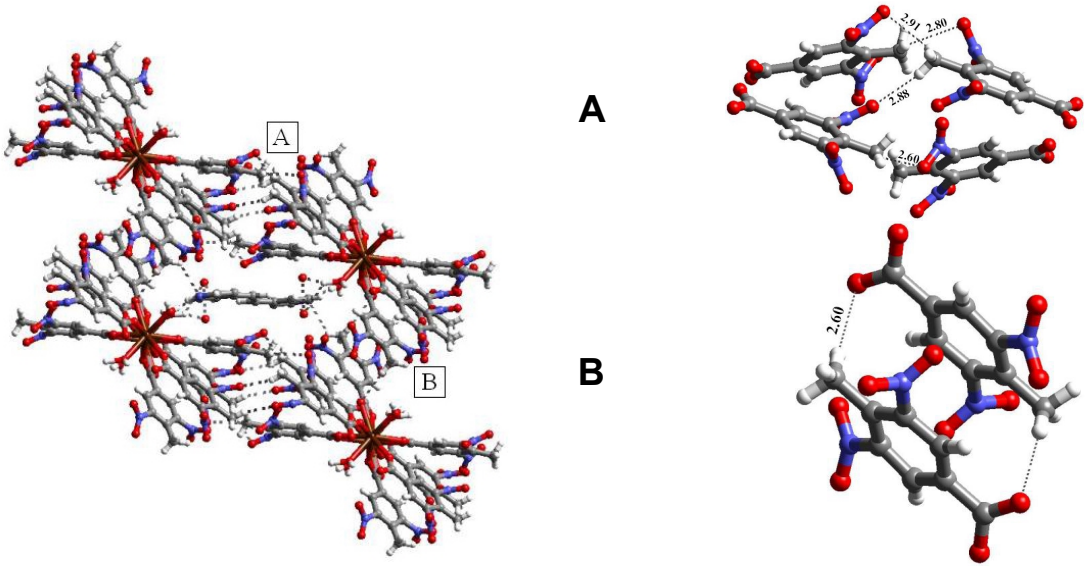

Figure 11: The porous assembly formed in the complex **2c**, with detailed demonstration of the hydrogen bonds involved in the assembly formation.

The coordination environment at the Pr(III) metal centre is similar to that of the earlier complexes (**2a** and **2b**) and exhibit tricapped trigonal prismatic polyhedral geometry. Each metal centre is coordinated to six molecules of **2** and two water molecules. The bimetallic units formed by the bridging and the tridentate coordination mode of the carboxylates extend in one-dimension to form coordination polymer. The polymers thus formed, undergo self-assembly to yield a porous structure, with

channels being occupied by a ***bpyee*** molecule and four water molecules. Thus, in the host-guest complex formed in the presence of ***bpyee***, the guest molecules interact with the host framework, through the formation of O-H···N, O-H···O as well as C-H···O hydrogen bonds.

3.4.4 Complex $[Pr_2(C_8H_5N_2O_6)_6(H_2O)_4](C_{12}H_{12}N_2).\ 4H_2O$, 2d

Hydrothermal reaction between **2** and Pr(III) acetate along with ***bpyea*****,** yielded yellow needle-like crystals of the complex, **2d** with formula unit, $[Pr_2(C_8H_5N_2O_6)_6(H_2O)_4](C_{12}H_{12}N_2).4(H_2O)$, as confirmed by x-ray diffraction technique. However, **2d** could not be prepared from **2a**, in contrast to the observation made in **2c**. Thus, it reveals the selectivity in the guest exchange property exhibited by the complex, **2a**. The complex, **2d** also is found to be isostructural to that of **2a - 2c** except for the guest species occupying the void space, as shown in Figure 12. The ***bpyea*** molecules, occupying the channels, are held to the host framework through the formation of O-H···N hydrogen bond.

Thus, the studies reveal that the weaker interactions like C–H···O hydrogen bonds between the coordination units maintained the requisite robustness and provide enough flexibility to perform guest exchange reactions, Although the assemblies are flexible enough to tune the channel dimensions to accommodate different guest molecules, the host-guest interactions were also found to be size specific.

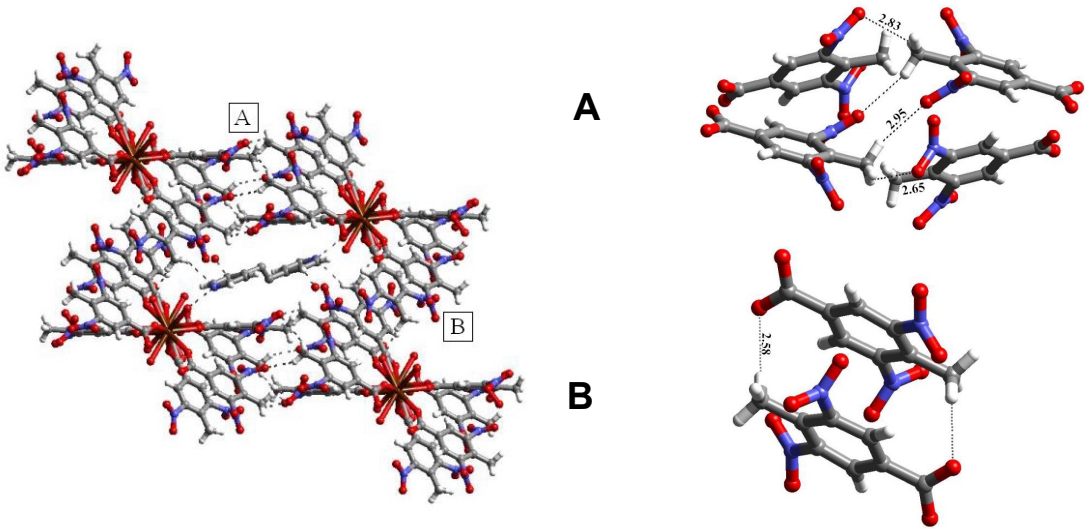

Figure 12: The coordination assembly formed in the case of complex **2d**, with ***bpyea*** and water molecules occupying the channels. The details of the hydrogen bonds stabilizing the channels are also shown

3.5 Complexes of Pr(III) and 4-amino-3,5-dinitro benzoic acid

To extend the study of preparation of open-frame networks mediated by other types of hydrogen bonds, a reaction of Pr(III)acetate was studied in conjunction with 4-amino-3,5-dinitrobenzoic acid, **3**, which gave an assembly with water molecules in the void space, while ***bpy*** molecules occupied the channels, when the reaction was carried out in the presence of the N-donor ligand.

3.5.1 Complex $[Pr_2(C_7H_4N_3O_6)_6(H_2O)_4].4H_2O$, 3a

A hydrothermal reaction between **3** and Pr(III) acetate yielded yellow needle-like crystals of the complex, **3a** with the formula unit, $[Pr_2(C_7H_4N_3O_6)_6\,(H_2O)_4].4H_2O$, as confirmed by the x-ray structure analysis. The crystallographic information is given in Table 3.8. In a typical metal centre, Pr(III) is coordinated to five molecules of **3** and

two water molecule, as shown in Figure 13a. Of the five molecules of **3**, only one binds to Pr(III) as a chelating ligand. In this complex, the Pr(III) exhibit an eight coordination environment, with a square antiprismatic polyhedral geometry, as shown in Figure 13b.

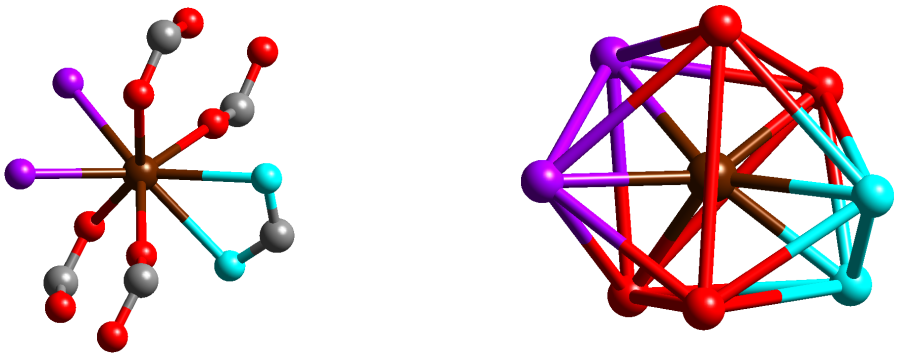

(a) **(b)**

Figure 13: (a) The coordination environment of Pr(III) in the complex, **3a**. (b) The square antiprismatic polyhedral coordination geometry exhibited by Pr(III). *((blue) the chelating carboxylate and (purple) the coordinated water molecules)*.

Further, the bridging carboxylates bind the neighboring metal units to form a one-dimensional coordination polymer, as shown in Figure 14a. Further, these one-dimensional polymers undergo self-assembly to yield a close-packed structure, as shown in Figure 14b.

In this complex, the free water molecules in the crystal lattice play a major role in the stabilization of the coordination assembly, by the formation of N-H···O hydrogen bonds with an average H···O distance of 2.5 Å and O-H···O hydrogen bonds with O···O distance 2.86 Å. A perspective view of the hydrogen bonds existing in the coordination assembly is shown in Figure 14c and 14d.

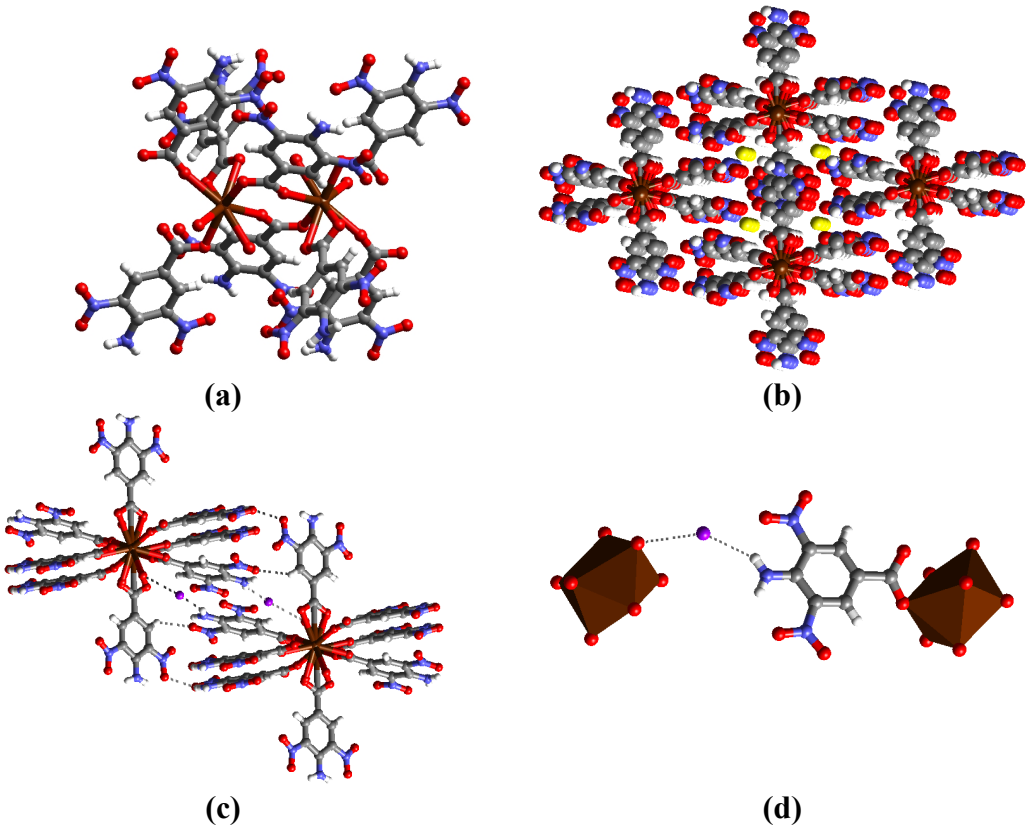

Figure 14: (a) Coordination polymer formed in the complex **3a**. (b) Close-packed arrangement of the coordination polymer. (c) and (d) The view of the hydrogen bonds formed between the coordination polymers and free water molecules.

3.5.2 Complex $[Pr_2(C_7H_4N_3O_6)_6(H_2O)_4].(C_{10}H_8N_2)$, 3b

4-Amino-3,5-dinitrobenzoic acid, **3**, with Pr(III) and ***bpy*** in a hydrothermal reaction gave crystals of the complex, $[Pr_2(C_7H_4N_3O_6)_6(H_2O)_4]$ $(C_{10}H_8N_2)$, **3b**, which were characterized by single crystal x-ray diffraction technique.

The structural analysis revealed that the ***bpy***, exist as a free ligand as in the case of complex, **2b**. In this complex, Pr(III) with eight coordination, exhibit a square antiprismatic polyhedral geometry. Each Pr(III) is surrounded by five molecules of **3** and two coordinated water molecules (see Figure 15a). The carboxylates in this

complex form both bridging as well as chelating modes of bonding. The bridging mode of the coordination holds the adjacent metal units together, leading to the formation of one-dimensional coordination polymer, as shown in Figure 15b.

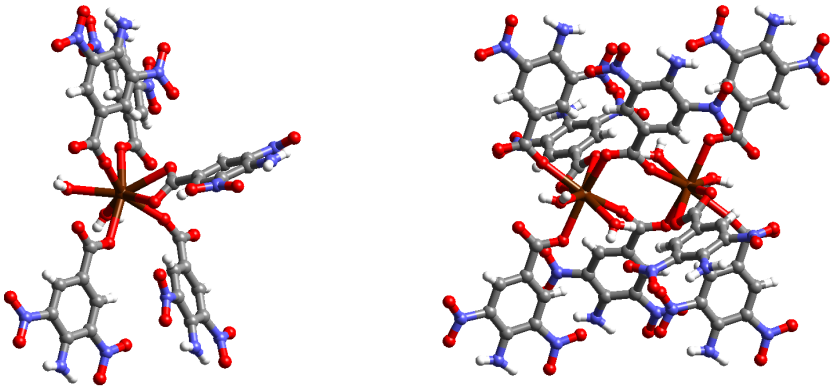

(a) **(b)**

Figure 15: (a) The coordination environment of Pr(III) in the complex **3b**. (b) The bimetallic units formed by the bridging carboxylates.

The coordination polymers, thus, formed, undergo self-assembly to form a metal-organic open framework with rectangular cavities. In this complex, the host framework stabilized by N-H···O as well as C-H···O hydrogen bonds. The annotation of the hydrogen bonds and the rectangular channels are shown in Figure 16a. The details of the hydrogen bonds are tabulated in the Table-3.10. The cavities thus formed are occupied by ***bpy*** molecules, which are held to the host framework through O-H···N as well as C-H···O hydrogen bonds as shown in Figure 16b.

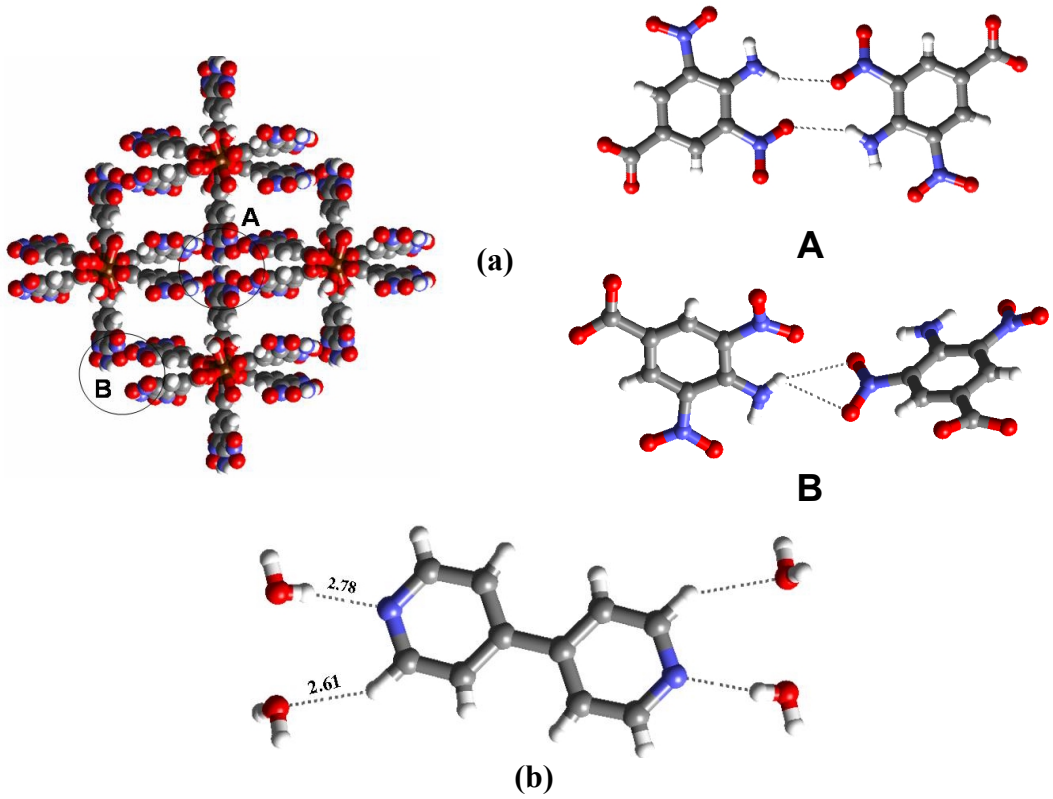

Figure 16: (a) The hydrogen bond patterns existing between the coordination units in in the complex **3b**. 'A' denotes the interactions in the vertical direction, while 'B' shows the sidewise interactions. (b) The detailed view of the hydrogen bonded interactions existing between the ***bpy*** unit and the host network.

3.6 Conclusions

The study demonstrates the utilization of both coordinate bonds as well as hydrogen bonds in a symbiotic way to form coordination assemblies that are stable and robust. Further, the robustness of the host networks formed by the organic ligands and Pr(III) is comparable to those of similar structures formed by purely coordinate bonds. The host networks, thus formed by the self-assembly of one-dimensional polymers were found to be stable enough to perform guest-exchange reactions

efficiently. Further, the guest exchange reactions were found to be selective to the guest molecules involved in the reaction. Due to the flexible nature of the hydrogen bonds involved in the stabilization of the porous network, the channels are able to be tuned with the incoming guest species with variable dimensions.

Tables

Table 3.1 Crystallographic information of complexes **1a** and **1b**.

Complex	1a	1b
Formula	$[Pr(C_7H_3N_2O_6)_3(H_2O)_2](H_2O)$	$[Pr(C_7H_3N_2O_6)_2(C_{10}H_8N_2)_2(C_2H_3O_2)(H_2O)]$
Formula Wt.	822.25	794.37
Crystal system	Triclinic	Triclinic
Space group	$P\bar{1}$	$P\bar{1}$
***a* (Å)**	9.282(3)	9.477(9)
***b* (Å)**	11.445(4)	12.340(9)
***c* (Å)**	13.803(5)	14.413(2)
***α* (deg)**	106.430(5)	109.529(2)
***β* (deg)**	90.340(5)	106.260(2)
***γ* (deg)**	94.220(5)	98.66(2)
***V* (Å^3)**	1402.1(8)	1468(3)
Z	2	2
***D*$_{calc}$ (g cm^{-3})**	1.948	1.797
***T* (K)**	298(2)	298(2)
***μ* (mm^{-1})**	1.847	1.745
2θ range (deg)	46.78	47.08
Total Reflns.	10329	12412
Unique Reflns. R(int)	4085	4277
Reflns. used	3528	3106
No. of Parameters	442	433
GOF on *F*^{2}	0.995	1.003
Final R1, wR2	0.0344, 0.0757	0.0602, 0.1260

Table 3.2 Coordination environment of Pr(III) in complex **1a**. (in Å)

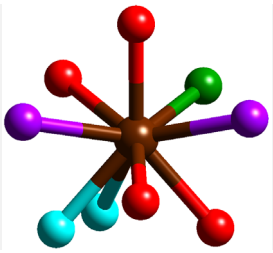

	Pr-O (carboxylate)		
Pr-O(water)	bridging	chelating	*μ*-oxo bridging
2.613(3) 2.540(3)	2.476(3) 2.383(3) 2.452(3) 2.401(3)	2.489(4) 2.962(3)	2.428(3)

Color Code

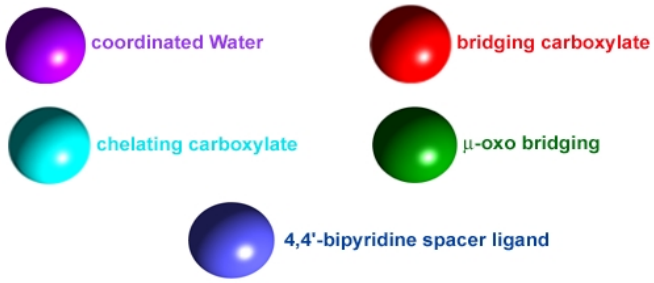

Table 3.3 Characteristics of hydrogen bonds (distances/Å and angles/deg).[#]

	1a	1b
C-H···O	2.860 3.773 168 2.725 3.611 159 2.763 3.635 156 2.832 3.547 135 2.721 3.651 179 2.822 3.580 140 2.785 3.476 132	2.640 3.562 172 2.463 3.330 155 2.747 3.581 150 2.996 3.565 121 2.956 3.824 151 3.061 3.651 121 3.056 3.801 138

[#] The three numbers in each column indicates H···A, D···A and angles respectively

Table 3.4 Coordination environment of Pr(III) in complex **1b**.[#]

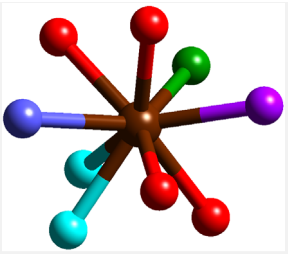

		Pr-O (carboxylate)		
Pr-$N_{(44bpy)}$	Pr-$O_{(water)}$	bridging	chelating	μ-oxo bridging
2.814(8)	2.562(7)	2.460(6) 2.477(8) 2.547(7) 2.411(7)	2.537(6) 2.635(7)	2.427(7)

[#] Bond distances are given in Å

Table 3.5 Crystallographic information of complexes **2a** to **2d**.

Complex	2a	2b	2c	2d
Formula	$[Pr(C_8H_5N_2O_6)_3(H_2O)_2]\ 3(H_2O)$	$[Pr(C_8H_5N_2O_6)_3(C_{10}H_8N_2)(H_2O)_2]$	$[Pr(C_8H_5N_2O_6)_3(C_{12}H_{10}N_2)_{0.5}(H_2O)_2]2(H_2O)$	$[Pr(C_8H_5N_2O_6)_3(C_{12}H_{12}N_2)_{0.5}(H_2O)_2]2(H_2O)$
Formula Wt.	896.33	1006.53	970.43	970.43
Crystal system	Triclinic	Triclinic	Triclinic	Triclinic
Space group	$P\bar{1}$	$P\bar{1}$	$P\bar{1}$	$P\bar{1}$
***a* (Å)**	9.483(3)	9.774(4)	9.510(12)	9.517(2)
***b* (Å)**	12.593(3)	12.721(6)	12.669(16)	12.747(2)
***c* (Å)**	15.517(4)	16.355(7)	16.43(2)	16.366(3)
α (deg)	76.89(4)	72.01(7)	72.28(2)	72.21(2)
β (deg)	78.10(4)	82.90(7)	78.06(3)	78.98(3)
γ (deg)	81.33(4)	83.15(7)	79.72(2)	79.84(2)
***V* (Å^3)**	1755.4(8)	1912.2(2)	1836(4)	1840.8(5)
Z	2	2	2	2
D_{calc} (g cm^{-3})	1.696	1.773	1.758	1.780
***T* (K)**	298(2)	298(2)	298(2)	298(2)
μ (mm^{-1})	1.487	1.372	1.428	1.428
2θ range (deg)	46.50	46.60	46.70	46.54
Total Reflns.	14587	16061	15345	11563
Unique Reflns.	5034	5502	5279	5293
R(int)				
Reflns. used	4903	5183	4253	5016
No. of Parameters	500	607	572	544
GOF on F^2	1.135	0.977	0.920	1.053
Final R1, wR2	0.0598, 0.1884	0.0255, 0.0661	0.0345, 0.0711	0.0283, 0.0768

Table 3.6 Coordination environment of Pr(III) in complexes **2a** to **2d**. (in Å)

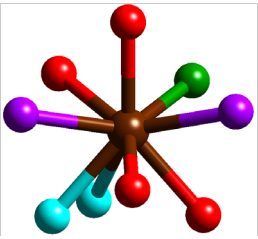

		Pr-O (carboxylate)		
Complex	**Pr-O(water)**	**bridging**	**chelating**	***μ*-oxo bridging**
2a	2.563(7) 2.610(6)	2.391(6)[a] 2.408(6)[a] 2.418(6)[b] 2.495(6)[b]	2.559(6) 2.772(6)	2.460(6)
2b	2.563(2) 2.563(2)	2.420(2)[a] 2.421(2)[a] 2.422(2)[b] 2.467(2)[b]	2.567(2) 2.828(2)	2.483(2)
2c	2.567(4) 2.628(4)	2.393(4)[a] 2.406(4)[a] 2.428(4)[b] 2.472(4)[b]	2.572(4) 2.708(4)	2.486(4)
2d	2.552(3) 2.617(3)	2.405(3)[a] 2.414(2)[a] 2.424(3)[b] 2.468(2)[b]	2.577(3) 2.730(2)	2.488(2)

Table 3.7 Characteristics of hydrogen bonds (distances/Å and angles/deg).

	2a	**2b**	**2c**	**2d**
C-H···O	2.432 3.383 170 2.521 3.459 166 2.631 3.497 150 2.864 3.658 144 2.906 3.503 121 2.927 3.663 134 2.946 3.818 152 2.964 3.567 122	2.287 3.084 139 2.486 3.310 149 2.534 3.217 128 2.586 3.492 165 2.597 3.282 129 2.638 3.540 157 2.672 3.575 157 2.860 3.707 148 2.923 3.726 142	2.553 3.443 147 2.600 3.558 176 2.601 3.373 138 2.660 3.264 121 2.798 3.704 158 2.829 3.554 136 2.844 3.703 154 2.857 3.760 169 2.882 3.700 144 2.905 3.752 152	2.487 3.244 136 2.584 3.540 174 2.635 3.485 154 2.652 3.380 133 2.819 3.666 152 2.827 3.732 158 2.827 3.622 141 2.845 3.581 137 2.861 3.743 153 2.880 3.779 163
C-H···N		2.893 3.704 143 2.946 3.738 140	2.716 3.508 140	2.811 3.603 140
O-H···N		2.770 2.801	2.749	2.745

Table 3.8 Crystallographic information of complexes **3a** and **3b**.

Complex	3a	3b
Formula	$[Pr(C_7H_4N_3O_6)_3(H_2O)_4]$	$[Pr(C_7H_4N_3O_6)(C_{10}H_8N_2)(H_2O)]$
Formula Wt.	883.31	1011.52
Crystal system	Monoclinic	Monoclinic
Space group	*C*2/*c*	*C*2/*c*
***a* (Å)**	24.463(6)	20.637(8)
***b* (Å)**	13.515(3)	18.815(7)
***c* (Å)**	9.372(2)	9.856(4)
α (deg)	90	90
β (deg)	97.824(6)	92.083(7)
γ (deg)	90	990
***V* (Å^3)**	3069.8(12)	3825(3)
Z	4	4
D_{calc} (g cm^{-3})	1.911	1.757
***T* (K)**	298(2)	298(2)
μ (mm^{-1})	1.699	1.374
2θ range (deg)	46.60	46.66
Total Reflns.	9423	8320
Unique Reflns. R(int)	2230	2767
Reflns. used	1975	2455
No. of Parameters	246	335
GOF on F^2	1.143	0.923
Final R1, wR2	0.0279, 0.0716	0.0317, 0.0622

Table 3.9 Coordination environment of Pr(III) in complexes **3a** and **3b**.[#]

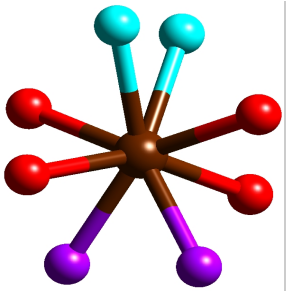

		Pr-O (carboxylate)	
Complex	**Pr-O(water)**	**bridging**	**chelating**
3a	2.525(4) 2.525(4)	2.441(4) 2.441(4) 2.460(4) 2.460(4)	2.560(4) 2.561(4)
3b	2.501(3) 2.501(3)	2.402(3) 2.402(3) 2.429(3) 2.429(3)	2.574(3) 2.474(3)

[#] Bond distances are given in Å

Table 3.10 Characteristics of hydrogen bonds (distances/Å and angles/deg).[#]

	3a	**3b**
O-H···N		1.811 2.779 168
N-H···O	2.494 3.259 149 2.407 2.956 122	2.783 3.469 126 2.768 3.469 127
N-H···N		2.859 3.562 12
C-H···O		2.285 3.316 158 2.612 3.489 138

[#] The three numbers in each column indicates H···A, D···A and angles respectively

3.7 References

(1) (a) Chen, B.; Liang, C.; Yang, J.; Contreras, D. S.; Clancy, Y. L.; Lobkovsky, E. B.; Yaghi, O. M.; Dai, S. *Angew. Chem. Int. Ed.* **2006**, *45*, 1390-1393. (b) Evans, O. R.; Lin, W. *Chem. Mater.* **2001**, *13*, 2705-2712. (c) Gómez-Lor, B.;

Gutiérrez-Puebla, E.; Iglesias, M.; Monge, M. A.; Ruiz-Valero, C.; Snejko, N. *Chem. Mater.* **2005**, *17*, 2568-2573. (d) Janiak, C. *Dalton Trans.* **2003**, 2781-2804.

(2) (a) Stallmach, F.; Gröger, S.; Künzel, V.; Kärger, J.; Yaghi, O. M.; Hesse, M.; Müller, U. *Angew. Chem. Int. Ed.* **2006**, *45*, 2123-2126. (b) Uemura, T.; Kitagawa, K.; Horike, S.; Kawamura, T.; Kitagawa, S.; Mizunob, M.; Endo, K. *Chem. Commun.* **2006**, 5968-5970. (c) Yaghi, O. M.; Li, H.; Davis, C.; Richardson, D.; Groy, T. L. *Acc. Chem. Res.* **1998**, *31*, 474-484. (d) Zhao, W.; Song, Y.; Okamura, T. A.; Fan, J.; Sun, W. Y.; Ueyama, N. *Inorg. Chem.* **2005** , *44*, 3330-3336.

(3) (a) Chen, B.; Ockwig, N. W.; Millward, A. R.; Contreras, D. S.; Yaghi, O. M. *Angew. Chem. Int. Ed.* **2005**, *44*, 4745-4749. (b) Chen, B.; Liang, C.; Yang, J.; Contreras, D. S.; Clancy, Y. L.; Lobkovsky, E. B.; Yaghi, O. M.; Dai, S. *Angew. Chem. Int. Ed.* **2006**, *45*, 1390-1393. (c) Evans, O. R.; Lin, W. *Acc. Chem. Res.* **2002**, *35*, 511-522. (d) Hermes, S.; Schrter, M.; Schmid, R.; Khodeir, L.; Muhler, M.; Tissler, A.; Fischer, R. W.; Fischer, R. A. *Angew. Chem. Int. Ed.* **2005**, *44*, 6237-6241.

(4) (a) Kesanli, B.; Cui, Y.; Smith, M. R.; Bittner, E. W.; Bockrath, B. C.; Lin, W. *Angew. Chem. Int. Ed.* **2005**, *44*, 72-75. (b) Panella, B.; Hirscher, M.; Pütter, H.; Müller, U. *Adv. Funct. Mater.* **2006**, *16*, 520-524. (c) Stallmach, F.; Gröger, S.; Künzel, V.; Kärger, J.; Yaghi, O. M.; Hesse, M.; Müller, U. *Angew. Chem. Int.*

Ed. **2006**, *45*, 2123-2126. (d)Tian, Y.; Cai, C.; Ji, Y.; You, X.; Peng, S.; Lee, G. *Angew. Chem. Int. Ed.* **2002**, *41*, 1384-1386.

(5) (a) Batten, S. R.; Murray, K. S. *Aust. J. Chem.* **2001**, *54*, 605-609. (b) Brammer, L. *Chem. Soc. Rev.* **2004**, *33*, 476-489. (c) Dalgarno, S. J.; Hardie, M. J.; Raston, C. L. *Cryst. Growth Des.* **2004**, *4*, 227-234. (d) Kitaura, R.; Seki, K.; Akiyama, G.; Kitagawa, S. *Angew. Chem. Int. Ed.* **2003**, *42*, 428-431. (e) Maji, T. K.; Uemura, K.; Chan, H.; Matsuda, R.; Kitagawa, S. *Angew. Chem. Int. Ed.* **2006**, *43*, 3269-3272. (f) Noro, S.; Kitagawa, S.; Kondo, M.; Seki, K. *Angew. Chem. Int. Ed.* **2000**, *39*, 2081-2084. (g) Uemura, T.; Kitagawa, K.; Horike, S.; Kawamura, T.; Kitagawa, S.; Mizunob, M.; Endo, K. *Chem. Commun.* **2006**, 5968-5970.

(6) (a) Chen, B.; Ockwig, N. W.; Fronczek, F. R.; Contreras, D. S.; Yaghi, O. M. *Inorg. Chem.* **2005**, *44*, 181-183. (b) Eddaoudi, M.; Moler, D. B.; Li, H.; Chen, B.; Reineke, T. M.; O'Keeffe, M.; Yaghi, O. M. *Acc. Chem. Res.* **2001**, *34*, 319-330. (c) Eddaoudi, M.; Kim, J.; Rosi, N. L.; Vodak, D.; Wachter, J.; O'Keeffe, M.; Yaghi, O. M. *Science* **2002**, *295*, 469-472.

(7) (a) Ockwig, N. W.; Friedrichs, O. D.; O'Keeffe, M.; Yaghi, O. M. *Acc. Chem. Res.* **2005**, *38*, 176-182. (b) Sudik, A. C.; Côté, A. P.; Wong-Foy, A. G.; O'Keeffe, M.; Yaghi, O. M. *Angew. Chem. Int. Ed.* **2006**, 2528-2433. (c) Hennigar, T. L.; MacQuarrie, D. C.; Losier, P.; Rogers, R. D.; Zaworotko, M. J. *Angew. Chem. Int. Ed.* **1997**, *36*, 972-973. (d) Wang, Z.; Kravtsov, V. C.;

Zaworotko, M. J. *Angew. Chem. Int. Ed.* **2005**, *44*, 2877-2880. (e) Zaworotko, M. J. *Angew. Chem. Int. Ed.* **2000**, *39*, 3052-3054.

(8) (a) Cotton, F. A.; Wilkinson, G.; Murillo, C. A.; Bochmann, M. *Advanced Inorganic Chemistry*; Wiley: Chichester, 1999. (b) Owen, S. M.; Brooker, A. T. *A Guide to Modern Inorganic Chemistry*, Longman Group; London, 1991.(c) Greenwood, N. N.; Earnshaw, A. *Chemistry of the Elements*, Pergamon Press: Oxford, 1993.

(9) (a) Piguet, C.; Bünzli, J. G. *Chem. Soc. Rev.* **1999**, *28*, 347-358. (b) Deluzet, A.; Maudez, W.; Daiguebonne, C.; Guillou, O. *Cryst. Growth Des.* **2003**, *3*, 475-479.

(10) (a) Gerrard, L. A.; Wood, P. T. *Chem. Commun.* **2000**, 2107-2108. (b) Li, Y.; Zou, X. *Angew. Chem. Int. Ed.* **2005**, *44*, 2012-2015. (c) Ouellette, W.; Yu, M. H.; O'Connor, C. J.; Hagrman, D.; Zubieta, J. *Angew. Chem. Int. Ed.* **2006**, *45*, 3497-3500. (d) Park, H.; Moureau, D. M.; Parise, J. B. *Chem. Mater.* **2006**, *18*, 525-531. (e) Zheng, Y.; Tong, M. L.; Chen, X. *New J. Chem.* **2004**, 1412-1415.

(11) Wang, Z.; Liu, J.; Chen, X.; Wan, J.; Qian, Y. *Chem. Eur. J.* **2006**, *11*, 160-163.

(12) Burchell, T. J.; Eisler, D. J.; Puddephatt, R. J. *Chem. Commun.* **2004**, 944-945.

(13) (a) Amoore, J. J. M.; Black, C. A.; Hanton, L. R.; Spicer, M. D. *Cryst. Growth Des.* **2005**, *5*, 1255-1261. (b) Dybtsev, D. N.; Chun, H.; Kim, K. *Angew. Chem. Int. Ed.* **2004**, *43*, 5033-5036. (c) Galet, A.; Oz, M. C.; nez, V.; Real, J. A. *Chem.*

Commun. **2004**, *10*, 2268-2269. (d) Hu, C.; Englert, U. *Angew. Chem. Int. Ed.* **2005**, *44*, 2281-2283. (e) Kitagawa, S.; Kitaura, R.; Noro, S. *Angew. Chem. Int. Ed.* **2004**, *43*, 2334-2375. (f) Maji, T. K.; Uemura, K.; Chan, H.; Matsuda, R.; Kitagawa, S. *Angew. Chem. Int. Ed.* **2006**, *43*, 3269-3272.

(14) Kitagawa, S.; Uemura, K. *Chem. Soc. Rev.* **2005**, *34*, 109-119 and the references within.

(15) (a) Bernstein, J.; Davis, R. E.; Shimoni, L.; Chang, N.-L. *Angew. Chem. Int. Ed.* **1995**, *34*, 1555-1573. (b) Etter, M. C.; MacDonald, J. C.; Bernstein, J. *Acta Crystallogr., Sect. B* **1990**, *B46*, 256-262. (c) Etter, M. C. *Acc. Chem. Res.* **1990**, *23*, 120-126. (d) Loehlin, J. H.; Franz, K. J.; Gist, L.; Moore, R. H. *Acta Crystallogr., Sect. B* **1998**, *B54*, 695-704. (e) Motherwell, W. D. S.; Shields, G. P.; Allen, F. H. *Acta Crystallogr., Sect. B* **2000**, *B56*, 857-871. (f) *The crystal as a supramolecular entity, Perspectives in supramolecular chemistry*; Wiley: Chichester, 1995. (g) Desiraju, G. R. *Crystal Engineering. The design of organic solids*; Elsevier: Amsterdam, 1989. (h) Desiraju,G. R. *Angew. Chem. Int. Ed.* **1995**, *34*, 2311-2327.

(16) (a) Sheldrick, G. M. SADABS, Area Detector Correction. 2002. Madison, WI, Siemens Industrial Automation, Inc. (b) Sheldrick, G. M. SAINT Area Detector Integration Software. 1998. Madison, WI, Siemens Industrial Automation, Inc. (c) Sheldrick, G. M. SHELX97 programs for crystal Strucutre Analysis. 1998.

Institüt für Anorganische Chemie der Universität. (d) Sheldrick, G. M. XPREP. (V5.1). 1997. Madison, WI, Bruker Analytical X-Ray Systems.

(17) Speck, A. L. PLATON. Acta Crystallogr., Sect.A A46, C34. 1990.

Chapter-4

Molecular Recognition Studies of 3,5-Dihydroxy and 4-Bromo-3,5-dihydroxybenzoic acids

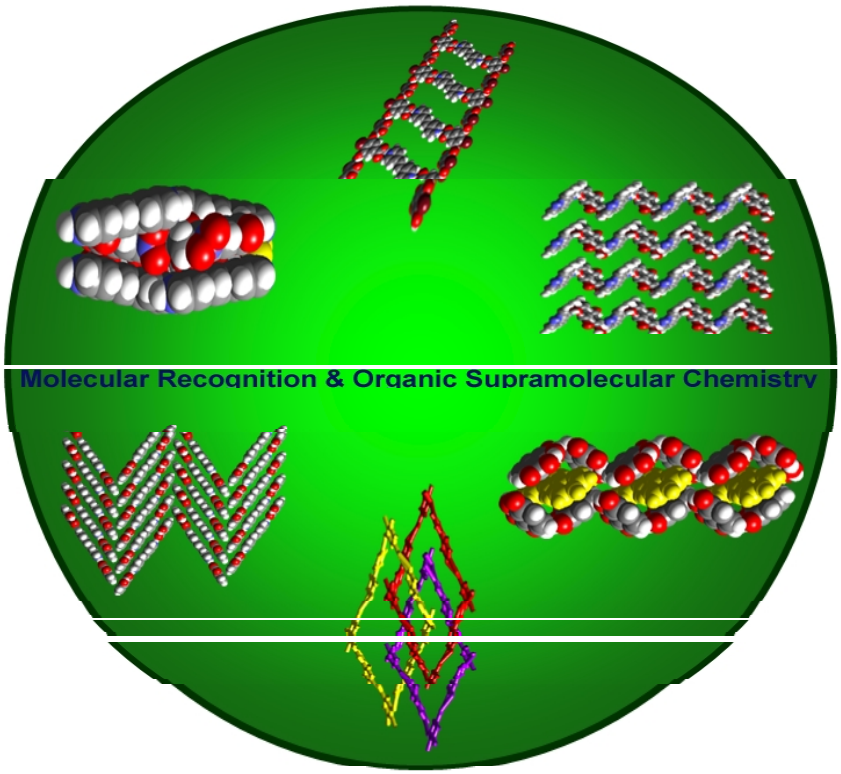

Imagination is more important than knowledge.

Knowledge is limited. Imagination encircles the world.

-Albert Einstein-

4.1 Introduction

The recognition between molecules, *molecular recognition*, is one of the most fundamental processes in biology and chemistry.[1] According to Lehn, molecular recognition is "…. *the selective binding of a substrate by a molecular receptor to form a supermolecule*".[2] The current understanding of molecular recognition had evolved from the host-guest chemistry of ions and the interactions between two or more molecules.[3] It is well recognized that, the selective binding of a substrate by a molecular receptor to form a supermolecule involves the *molecular recognition,* which rests on the size and shape compatibility of the interacting partners – *receptor* and *substrate*.[4]

Scheme 1

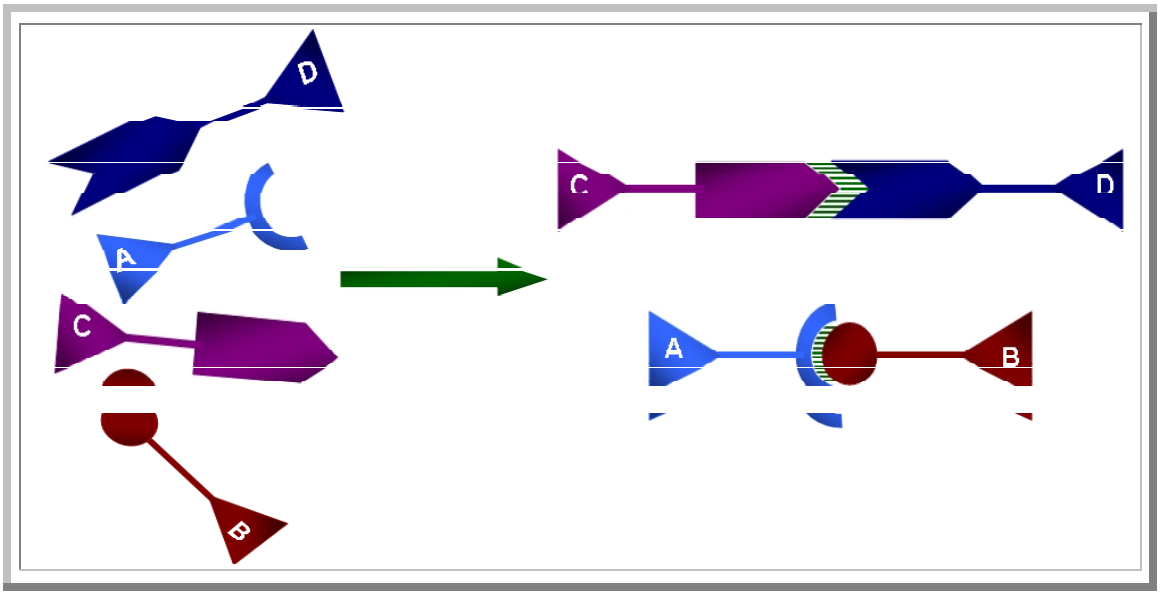

For the better understanding of the molecular recognition and the complimentarity between the receptor and substrate, Emil Fischer introduced the "lock and key" concept, over 100 years ago.[5] In this concept, as shown in Scheme 1, the

lock being the molecular receptor such as a protein or enzyme and the key being the substrate such as a drug that is recognized to give a defined receptor-substrate complex. In this regard, with an emphasis on the design of molecular receptors that can undergo spontaneous self-organization to generate well-defined supramolecular architectures by self-assembly processes, that can be utilized in different frontier technologies like catalysis, transport processes, etc., were extensively studied.[6] Towards this, several receptor molecules, possessing steric and electronic features complementary to those of the substrate to be bound and a balance between rigidity and flexibility suitable for various functions, were synthesized and studied. Such organization of molecular structural and dynamical features has been at the origin of the development of various host molecules like cryptands, cavitands, crown ethers and other ligands.[7]

The recognition and self-assembly processes are in general driven by non-covalent forces such as hydrogen bonding, electrostatics, van der Waals forces, π-π interactions, conformational energy, etc.[8] In this regard, the approaches of Lehn, Cram, Pederson, etc. are well documented in the literature.[9,10] Further, these noncovalent interactions between host and guest molecules lie at the heart not only of synthetic supramolecular complexes but also are the basis of promising new approaches in pharmacy, medicine, chemical analysis, chromatography, as well as catalysis and material science.[11]

Although, the molecular recognition studies gained popularity with the observation and recognition studies of cavitands, cryptands, etc. in solutions, a lot of further progress has been made in identifying and quantifying the hydrogen bond forming tendencies and recognition patterns in the solid state.[12] The crystallization process appears to involve the phenomenon of molecular recognition, or rather molecular self recognition, at an amazingly high degree of reliability. Indeed, crystallization is the process in practice, as a method of purification of mixtures, in particular, organic compounds. In the due course, co-crystallization has emerged as an important tool for the preparation of new materials by understanding various possibilities of interactions that can exist between the molecular components involved in the process.[13] Co-crystals involving the pre-determined hydrogen bond patterns are usually synthesized by slow evaporation of solution that contains stoichiometric amounts of the components (co-crystal formers); however, sublimation, growth from the melt, slurries, and grinding two solid co-crystal formers in a ball-mill are also suitable methodologies.[14]

Scheme 2

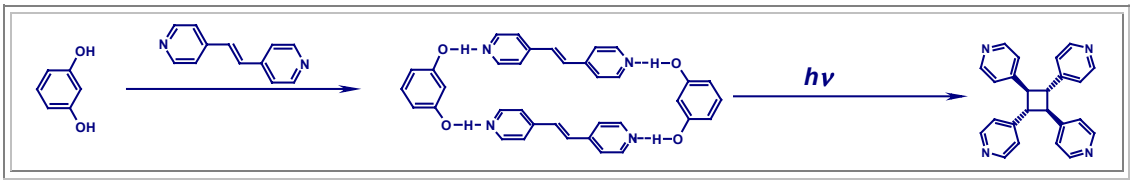

Further, making use of the understanding of the recognition between the complimentary molecules taking part in the co-crystallization process and the intermolecular interactions involved, attempts were made to synthesize targeted

assemblies, to perform unusual chemical transformations that otherwise appear to be either difficult or complex in nature.[15] In this regard, the elegant studies by MacGillivray and co-workers in the synthesis of ladderanes by co-crystallization and subsequent photochemical reaction by irradiation of the adducts of resorcinol and unsaturated N-donor molecules such as *trans*-1,2-bis(4-pyridyl)ethene, ***bpyee***, prepared by inducing recognition between the constituents through O-H···N hydrogen bonds, are superb examples that highlight the use of molecular recognition phenomenon for the generation of complex chemical systems.[16] The topological arrangement of the resulting cyclic assemblies is schematically represented in the Scheme-2. Further, it was noted that the recognition pattern between the –OH groups in the 1,3-positions and aromatic N-donor compounds are not perturbed by the presence of different functional groups, such as ethers, as was shown recently in a case study on a homologous series of phluroglucinols.[17]

However, the influence of functional group such as -COOH, -$CONH_2$, -NH_2, etc. (which are known to form various types of interactions with the pyridyl ligands) on the hydrogen bond patterns and the topological arrangement shown in Scheme 2, is not well explored. To begin with, the studies were carried out to understand the competition of –COOH and –OH for N-donor compounds, thinking that it would provide valuable information for the development of hitherto unknown assemblies. Taking into consideration of the utilization of O-H···N and O-H···N/C-H···O pair wise hydrogen bonds in supramolecular synthesis and molecular recognition, competitive recognition studies, employing molecular entities having both –OH and –COOH

groups by co-crystallization with different hetero-aromatic compounds, have been carried out. Towards this, derivatives of dihydroxybenzoic acids, as illustrated below (Scheme 3) were used in the co-crystallization reactions with *trans*-1,2-bis(4-pyridyl)ethene, ***bpyee***, 1,2-bis(4-pyridyl)ethane, ***bpyea***, and 4,4'-bipyridine, ***bpy***.

Scheme 3

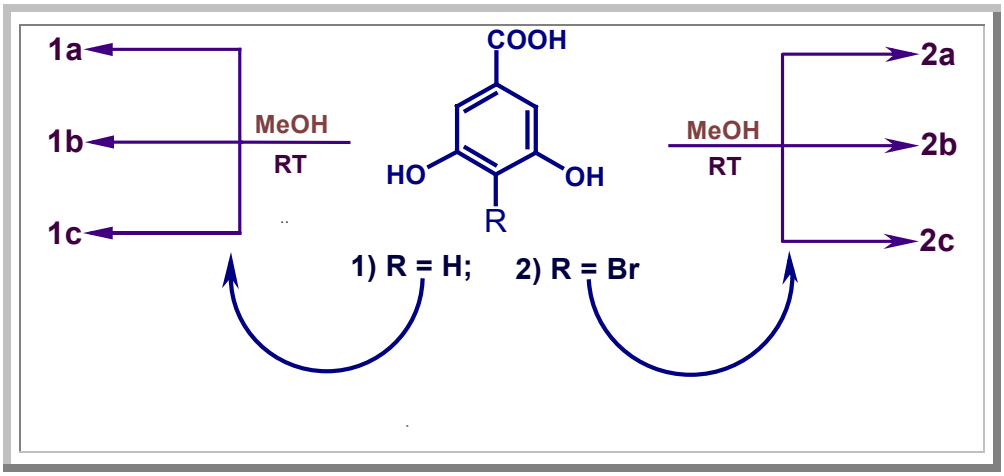

4.1.1 Experimental Section

All the chemicals reagents and solvents were obtained from commercial suppliers and used without further purification. We used spectroscopic-grade solvents in all cocrystallization studies. All co-crystals **1a** –**1c** and **2a** –**2c** were prepared by dissolving the respective reactants in a ratio of 1:1 in methanol and allowing the solvent to evaporate under ambient conditions. In all cases single crystals suitable for X-ray diffraction analysis were obtained over one week time.

A General procedure for the synthesis of complexes 1a-1c

In a typical cocrystallization experiment 3,5-dihydroxybenzoic acid (0.100 mmol) and the N-donor ligand (***bpyee***, ***bpyea*** or ***bpy***) (0.100 mmol), as the case may

be, were dissolved in methanol (10 mL) in a 25 mL conical flask by warming on a water bath. The resultant solution was allowed to evaporate under ambient conditions and colorless single crystals were obtained over a period of one week time. The crystals were separated from the mother liquor by filtration, washed with ice-cold methanol, and dried under vacuum.

A General procedure for the synthesis of complexes 2a-2c

In a typical cocrystallization experiment, a methanol solution (5 mL) of 4-bromo-3,5-dihydroxybenzoic acid (0.100 mmol) was added drop wise to a warm solution of the N-donor ligand (***bpyee***, ***bpyea*** or ***bpy***) (0.100 mmol), as the case may be, in methanol (5 mL) in a 25 mL conical flask. The resultant solution was allowed to evaporate under ambient conditions and colorless single crystals were obtained over a period of one week time. The crystals thus obtained were separated from the mother liquor by filtration, washed with ice-cold methanol, and dried under vacuum.

4.1.2 X-ray crystallography

Single crystals were analyzed under a Leica microscope equipped with a CCD camera and good-quality crystals were chosen for structure determination by x-ray diffraction with a Polaroid detector. The crystals were mounted on a goniometer by gluing to a glass fiber with cyanoacrylate adhesive and crystal data were collected on a CCD diffractometer with APEX detector. The intensity data were processed using SAINT software of the Bruker suite of programs. The structures were solved and refined using the SHELXTL package and no anomalies were observed at any stage of

structure solutions.[18] All calculations of intermolecular interactions were done with PLATON.

4.2 Supramolecular assemblies of 3,5-dihydroxybenzoic acid

The single-crystal x-ray diffraction studies of the organic complexes, revealed that the reactants recognize each other by making use of –OH and/or –COOH groups of the acid molecule and the hetero-atoms of the pyridyl ligands. Each adduct is unique in the aspects of structural arrangements with respect to the conformation and the nature of the hydrogen bonds formed by –OH and –COOH groups. However, collectively, they exhibit many common features, especially in the formation of ladder-like architectures. Thus, the description of the unique features of each adduct are followed by a comparison to deduce common features which maybe useful for evaluation and formulation of new assemblies with novel architectures and properties.

4.2.1 Molecular complex $2(C_7H_6O_4):3(C_{12}H_{10}N_2)$, 1a

The cocrystallization reaction of 3,5-dihydroxybenzoic acid, **1** and *trans*-1,2-bis(4-pyridyl)ethene, ***bpyee*** from a methanol solution gave colorless block-like single crystals of the complex, **1a**. The structure determination using single crystal x-ray diffraction technique revealed that **1** and ***bpyee*** are present in 2:3 ratio in the molecular complex and the asymmetric unit of the same is shown in Figure 1a. The crystallographic details of the complex are tabulated in Table 4.1. In this complex, the two –OH groups of **1** are arranged in a *syn–syn* orientation with respect to the H-atom

in the *para*-position. Further, one of the ***bpyee*** molecules is disordered around the olefinic bridge in a 53:47 distribution. For an easy representation, the acid molecule is denoted as **A**, while the ordered and disordered ***bpyee*** molecules are denoted as **B** and **C** respectively.

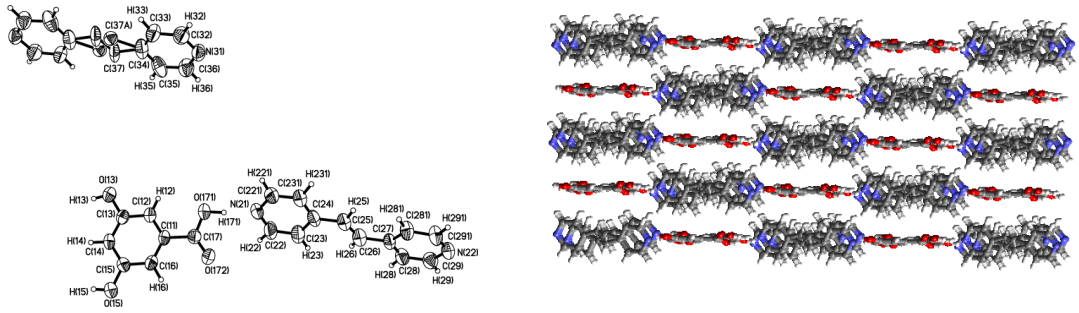

(a) **(b)**

Figure 1: (a) The asymmetric unit of complex **1a**. (b) The layered structure formed by the self-assembly of the molecules.

These molecules interact with each other and undergo self-assembly to yield a sheet structure in 3D arrangement, stacked along the *a*-axis, as shown in Figure 1b. Within a typical sheet, the recognition between **1** and ***bpyee*** is established through the formation of the O-H···N hydrogen bonds. The basic recognition pattern, as shown in Figure 2a, is established between the acid and the N-donor ligand, such that, each molecule of **1** is connected to one ordered and one disordered ***bpyee*** molecule, making use of the –OH groups, establishing the O-H···N hydrogen bonds, with an H···N distance of 1.77 and 1.97Å. The two ***bpyee*** molecules, in turn, interact with a pair of molecules of **1**, by the formation of O-H···N hydrogen bonds (H···N 1.97 and 1.62Å) involving –OH and –COOH groups of the acid moiety. The two acid molecules,

however, held to each other by centrosymmetric C-H···O hydrogen bonds (H···O 2.68Å). The details of the hydrogen bonds are listed in Table 4.2.

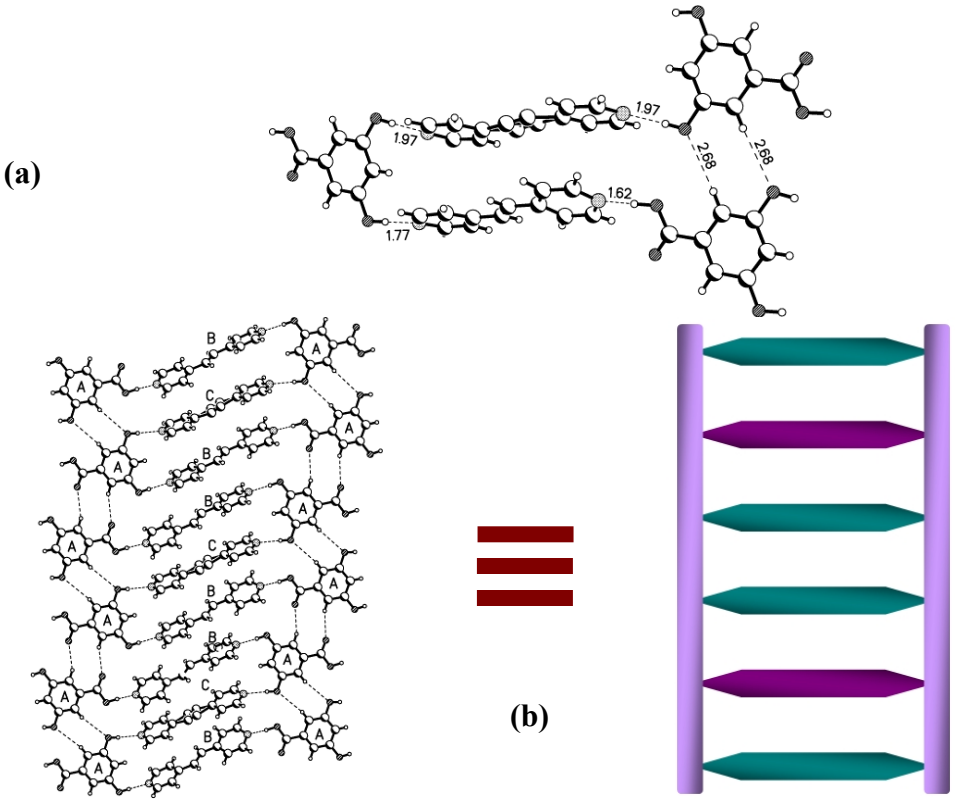

Figure 2: (a) Recognition pattern between **1** and ***bpyee*** to give a five-membered cyclic moiety. (b) Ladder-like structure observed in complex **1a** along with a schematic representation. *(The different colors of the rungs represent ordered and disordered bpyee)*.

Thus, the recognition between two ***bpyee*** units and three **1** units leads to the formation of a five-membered supramolecular entity. As a result, it appears that the –COOH group is able to perturb the recognition pattern, shown in Scheme 2, suggesting that a possible hierarchy in the intermolecular interactions.

The supramolecular ensembles, thus, formed constitute a ladder-like architecture in two-dimensional arrangement, as shown in Figure 2b. In the ladder-like structure, the ***bpyee*** molecules function as the rungs inserted between the rods of the acid molecules. From the structural analysis, it was revealed that the distance between the rungs is 4.2Å, which is still at a reactive distance for the solid-state photodimerisation reactions. Thus, it was found that, even though the –COOH group is able to perturb the fundamental recognition pattern established between the resorcinol and ***bpyee*** units, the gross structure was still maintained, thus, the properties of the structures remain intact for the utilization in further reactions, such as [2+2] cycloaddition reactions.

4.2.2 Molecular complex of $(C_7H_6O_4)$:$(C_{12}H_{12}N_2)$, 1b

Complex **1b**, prepared under similar conditions as that of the complex **1a**, was found to be a 1:1 complex of **1** and ***bpyea***, as revealed by the crystal structure analysis. The asymmetric unit contains two symmetry-independent molecules of each of the components in the complex and is shown in Figure 3a.

While two symmetry-independent molecules of **1** were denoted as **A** and **B**, those of ***bpyea*** were represented as **C** and **D**. Furthermore, the molecular geometries of **A** and **B** are more or less the same, but, **C** and **D** have some differences, which are mainly due to the variable conformational arrangement of methylene bridge, as shown in Figure 3b. The dihedral angle calculations revealed that the two phenyl moieties in ***bpyea*** are twisted by 5.2^{o} in **C** and 7.3^{o} in **D**.

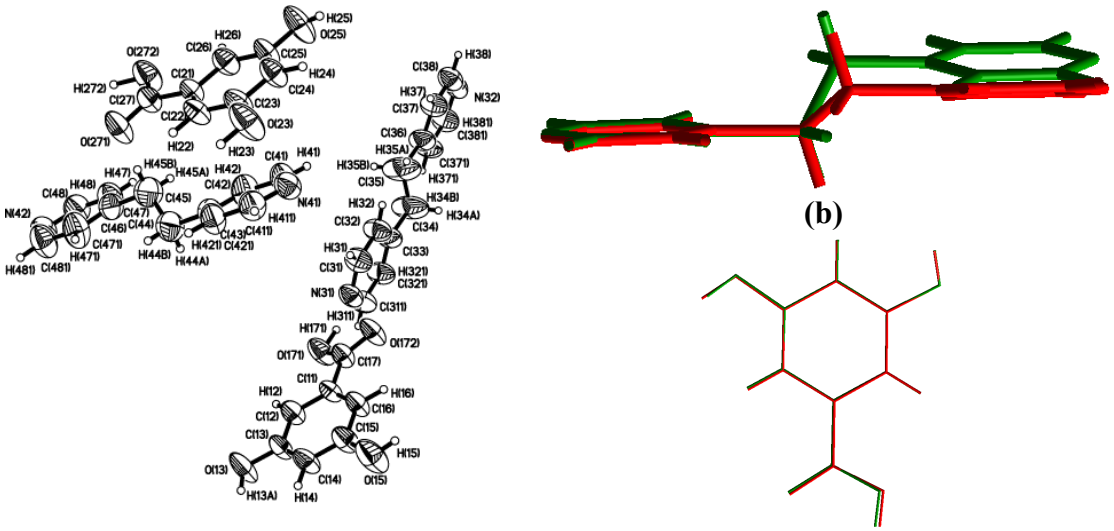

Figure 3: (a) The asymmetric unit of complex **1b.** The overlap diagram of the symmetry independent molecules of (b) ***bpyea*** and (c) **1**.

The molecules in complex **1b**, form a planar sheet-like structure stacked along the *c*-axis. The detailed analysis of the intermolecular interactions in a typical layer revealed that the hydrogen bonds are established by making use of hetero-atom of the pyridyl ring and the –OH and the –COOH group of the acid molecules.

Unlike in the complex **1a**, the recognition between **1** and ***bpyea*** is established such that each molecule of ***bpyea*** in the complex **1b** is held by two symmetry-independent molecules of **1** by the formation of O-H···N hydrogen bonds, with H···N distances in the range 1.72 to 1.90Å, involving both –OH and –COOH groups, as shown in Figure 4a and 4b. Such ensembles are held together, forming crinkled tapes through the formation of O-H···O hydrogen bonds, with H···O distance of 1.81 and 1.85Å, making use of the –OH and –COOH groups. These interactions are further

supported by the formation of C-H···O hydrogen bonds, with H···O distances of the range, 2.67–2.79Å.

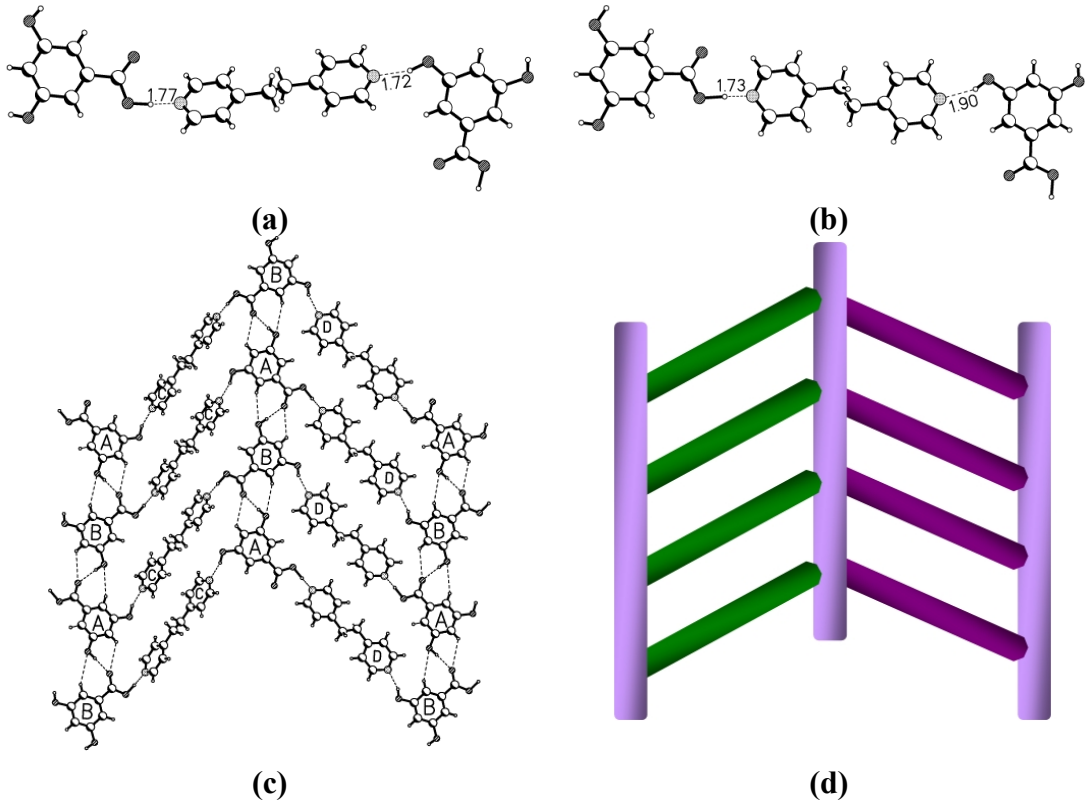

Figure 4: (a) and (b) Different recognition patterns formed by the two symmetry-independent molecules of ***bpyea***. (c) and (d) Two-dimensional ladder-like arrangement in the crystal lattice and its schematic representation. *(The different colors of rungs in the ladder represent different symmetry-independent molecules).*

In two-dimensional arrangement, the tapes thus formed, constitute a ladder-like structure with the rods made up of two symmetry-independent molecules of **1** and the molecules of ***bpyea*** of particular symmetry (**C** or **D**) are inserted as the rungs. This leads to the formation of two different types of ladders, arranged in a crinkled manner, as schematically represented in Figure 4d.

Thus, although the basic recognition pattern in **1b** is entirely different to that established between the resorcinol and ***bpyee*** or that observed in **1a**, retention of the global packing motif, by the formation of the cyclic building blocks and ladder-like structures, suggests the significance and the stability of such supramolecular architectures in the solid state structures.

4.2.3 Molecular complex of $2(C_7H_6O_4):3(C_{10}H_8N_2)$, 1c

A reaction of **1** and ***bpy*** in a 1:1 ratio from methanol at room temperature yielded single crystals of **1c**. However, a Cambridge Structural Database, CSD search revealed that the crystal structure of **1c** in a 2:3 molecular ratio is known in the literature.[19]

Furthermore, the unit-cell dimensions obtained by the x-ray analysis of the crystals of the complex **1c** (a = 9.666, b = 14.359, c = 14.769Å, α = 63.21, β = 83.22, γ = 80.14^o) were similar to those of the reported structure (a = 9.683(1), b = 14.378(3), c = 14.797(3)Å, α = 63.17(6), β = 83.25(11), γ = 80.17(10) ^{o}). However, the focus of the earlier study was to compare the ability of the –COOH group to yield O-H···N hydrogen bonds with N-donor compounds in a series of carboxylic acids. Hence, the competitive nature of different functional groups was not addressed. Since the reported structure is quite accurate with a good R-factor, we retrieved the crystallographic data form the CSD, to carry out further structural analysis to have a comparison with **1a** and **1b**.[20]

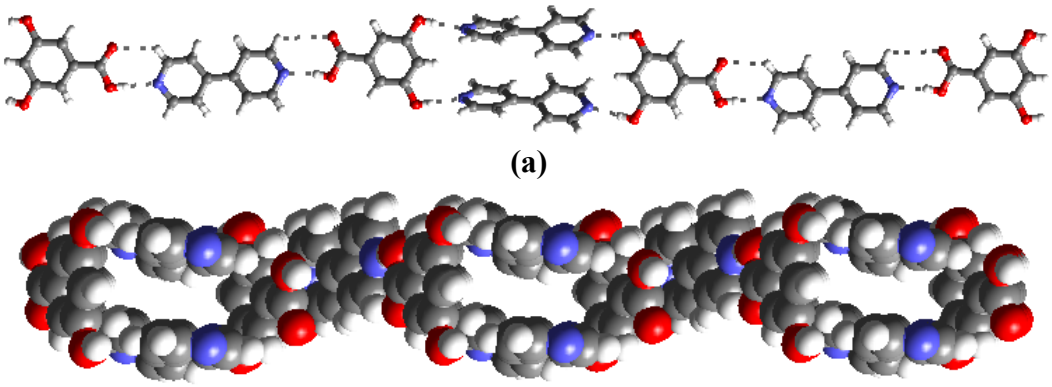

Figure 5: (a) Basic recognition pattern and formation of molecular tape in **1c**. (b) Arrangement of adjacent tapes in a bracelet-like network.

The basic recognition pattern observed in the complex, **1c** is shown in Figure 5a. The acid and ***bpy*** interact with each other, through O-H···N hydrogen bonds (H···N, 1.89–1.98Å), making use of the –OH groups of **1**, yielding a network of cyclic tetramers comprising two molecules each of **1** and ***bpy***. The adjacent tetrameric units, thus, formed were held together by an additional molecule of ***bpy*** by forming O-H···N/C-H···O pair-wise hydrogen bonds formed between the -COOH group and the hetero-atom. As a result an infinite open bracelet-like structure is formed, which is shown in Figure 5b. Thus, the two functional groups –OH and –COOH, interact with ***bpy*** as if they were on two different molecules.

Furthermore, the adjacent bracelets are held together differently in two different directions. The two orientations are shown in Figure 6. While, they are held together by a combination of C-H···O hydrogen bonds and C-H···π interactions along the *a*-axis, a combination of O-H···N (H···O 1.89Å) and C-H···O (H···O, 2.52Å) hydrogen bonds binds neighboring units in a quartet manner along the *b*-axis.

However, it is quite surprising that in the three-dimensional arrangement, ladder-like structure was not observed unlike in **1a** and **1b**.

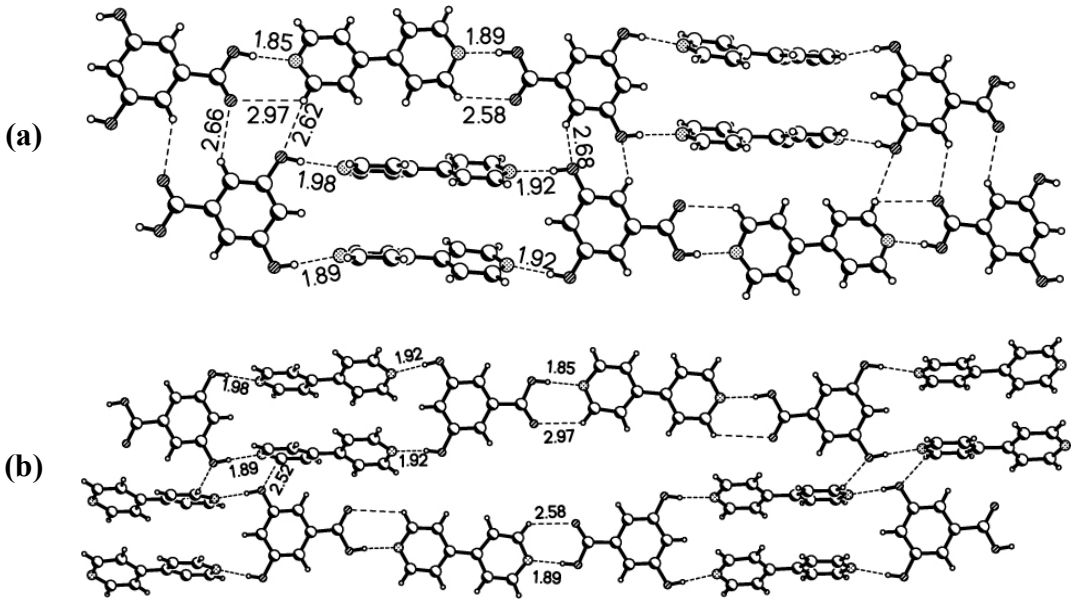

Figure 6: (a) Close-packed model of the bracelet (along *a*-axis). (b) Arrangement of the tapes in the perpendicular direction forming an unusual tetrameric hydrogen-bonding network.

Encouraged by the subtle variations observed in **1a**-**1c** and the formation of exotic ladder-like structures, the study was extended to evaluate molecular complexes of other derivatives of dihydroxybenzoic acid. Thus 4-bromo-3,5-dihydroxybenzoic acid has been chosen, as the halo-derivatives are known to influence the recognition between the –OH groups and the hetero-atoms of the pyridyl ligands, as demonstrated by MacGillivray and co-workers in their analysis of the recognition patterns of resorcinol and its chloro-derivatives towards the ***bpyea*** ligand.[21]

4.3 Organic assemblies of 4-bromo-3,5-dihydroxy benzoic acid

Co-crystallization reaction of 4-bromo-3,5-dihydroxbenzoic acid, **2**, with ***bpyee***, ***bpyea*** and ***bpy*** gave molecular adducts **2a**-**2c** respectively, which were analyzed using single crystal x-ray diffraction technique. While **2** and ***bpyee*** led to the deprotonation of the –COOH group and the formation of ladders arranged in zig-zag fashion, ***bpyea*** yielded organic adducts made of ladders arranged in an edge-sharing mode. However, ***bpy***, and **2** yielded a three-fold interpenetrated network. The detailed assessment of the structural details of the complexes **2a** - **2c** is discussed in the following sections.

4.3.1 Molecular complex of $2(C_7H_4O_4Br):(C_{12}H_{12}N_2)$, 2a

Cocrystallization of 4-bromo-3,5-dihydroxybenzoic acid, **2** and *trans*-1,2-bis(4-pyridyl)ethene, ***bpyee*** from methanol yielded colorless single crystals of the complex **2a**, with a formula unit $2(C_7H_4O_4Br):(C_{12}H_{12}N_2)$, as confirmed by the x-ray diffraction technique. The crystallographic details of the complex are tabulated in Table 4.3. The asymmetric unit of the complex is shown in Figure 7a.

The recognition between **2** and ***bpyee*** is established through the carboxylate group and the protonated N-atom of ***bpyee*** by formation of N^+–$H^{\cdots}O^-$ ($H^{\cdots}O^-$ 1.67Å) and C–$H^{\cdots}$O ($H^{\cdots}$O 2.40Å) pair-wise hydrogen bonds. The recognition pattern is shown in Figure 7b. The resultant three molecule supramolecular ensembles are further held together by the interactions formed between carboxylate and –OH groups of acid molecules of adjacent ensembles, arranged in perpendicular direction, by

establishing O–H···O$^-$ hydrogen bonds with an average H···O$^-$ distance of 1.81Å, as shown in Figure 7d.

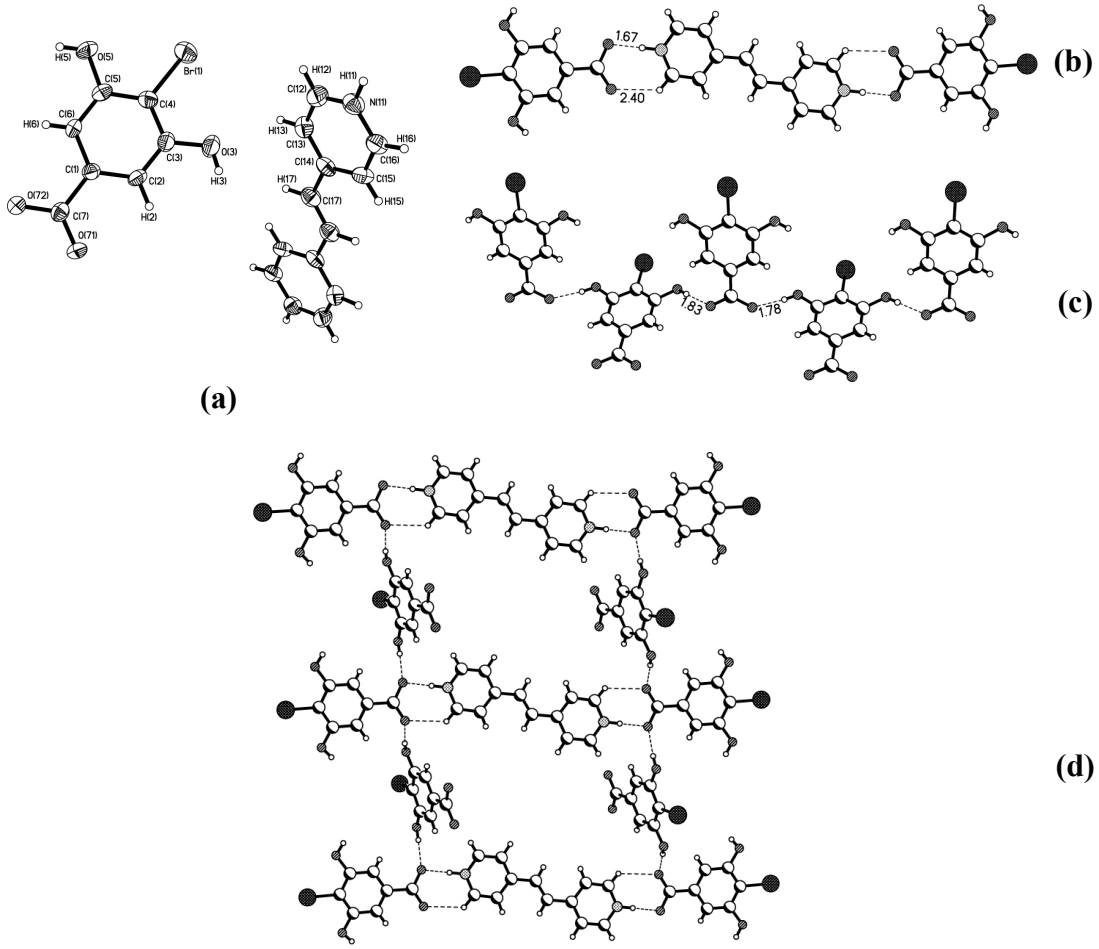

Figure 7: (a) The asymmetric unit of **2a**. (b) The basic recognition pattern formed exclusively by interaction between –COO$^-$ of the **2** and protonated pyridyl rings of ***bpyee***. (c) Arrangement of molecules of **2** showing *cisoid* orientation of –Br atoms. (d) The ladder assembly formed in complex **2a**.

In the complex **2a** also, a ladder structure prevails, but not exactly as the one observed in **1a** and **1b**. While the acid molecules that constituted rods of the ladders

lie in the same plane in the case of complexes **1a** and **1b**, they are twisted by almost 90^{o} in the complex **2a**. Further, the adjacent ladders exhibit a translational symmetry such that they slide over one another and close the void space formed in between the rungs of the ladders. The pictorial representation of the translational symmetry is shown in Figure 8a.

(a) 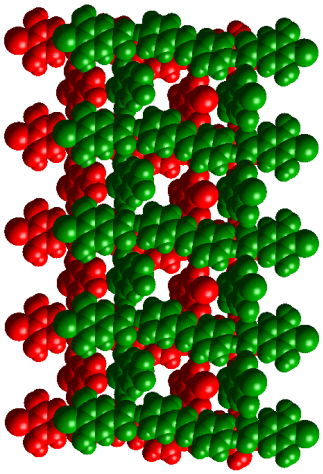 **(b)** 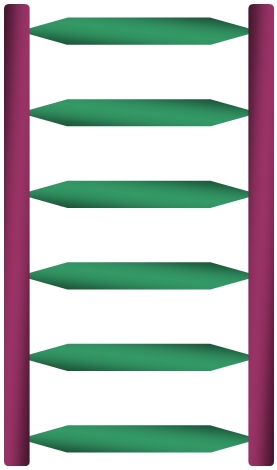

Figure 8: (a) The adjacent ladders arranged in a translational symmetry. (b) The schematic representation of the ladder-like assembly formed in the complex **2a**.

4.3.2 Molecular complex of 2($C_7H_5O_4Br$):2($C_{12}H_{12}N_2$), 2b

From a methanol solution, **2** and ***bpyea*** yielded single crystals of complex **2b**, in which the constituents are in 1;1 ratio, with two molecules of each reactant in the asymmetric unit. An ORTEP plot of the complex **2b** is shown in Figure 9a. While one of the molecules of ***bpyea*** is fully ordered, the other one is disordered around the ethylene bridge, in 68:32 ratio. Further, the conformational flexibility exhibited by the ***bpyea*** molecules in the complex is shown in Figure 9b and 9c.

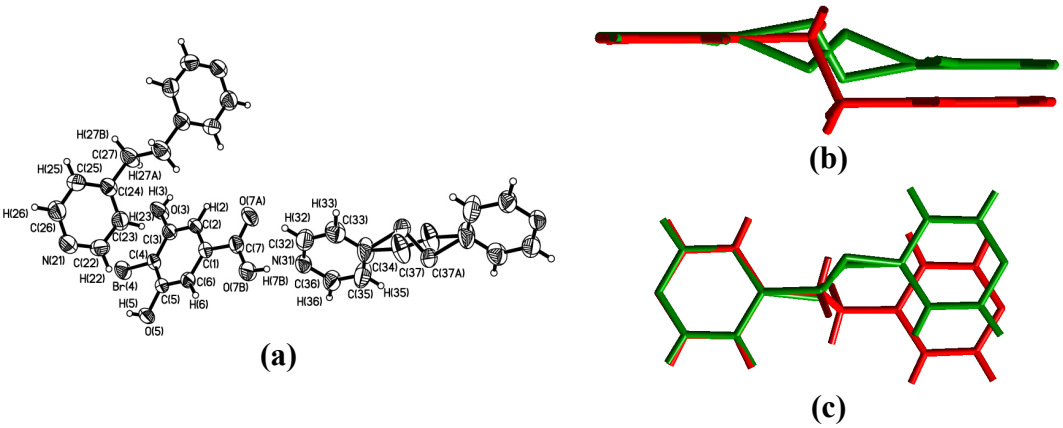

Figure 9: (a) The asymmetric unit of the complex **2b**. (b) and (c) View of the variation in the conformations of the ***bpyea*** in the complex viewed along *c*-axis and *a*-axis respectively

In the three-dimensional arrangement, these molecules pack to form sheets stacked along the *b*-axis. The interactions among the molecules in the sheets are quite interesting and show many common features with the packing observed in the complex **1b**. Further, the two molecules of ***bpyea*** interact with **2** in different modes. In one case, a disordered molecule of ***bpyea*** forms O-H···N hydrogen bonds (H···N 1.70 Å) by interacting exclusively with the –COOH groups on two acid molecules (see Figure 10a).

The second molecule of ***bpyea***, with an ordered ethylene bridge, interacts with **2** exclusively utilizing the –OH groups and forms O-H···N hydrogen bonds, with H···N distance of 1.92Å, as shown in Figure 10b. The hydrogen bond details are given in Table 4.4. Thus, infinite chains with alternately ordered and disordered ***bpyea*** molecules, separated by the molecules of **2** are observed in the complex **2b**.

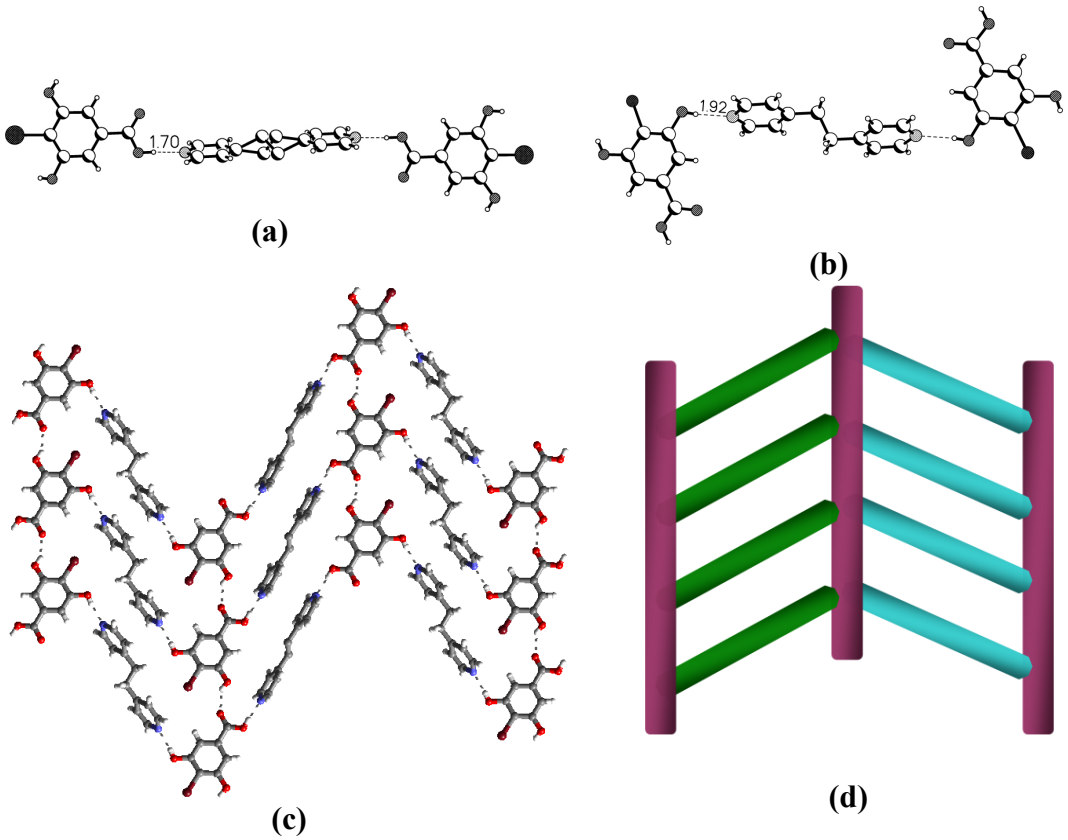

Figure 10: (a) and (b) Different recognition patterns shown by the two molecules of ***bpyea*** with **2** in the complex **2b**. (c) A ladder-like structure formed by the self-assembly ***bpyea*** with molecules of **2**. (d) Schematic representation of the ladder (viewed along *c*- axis)

These chains arrange in two-dimension to yield a sheet-like structure through O-H···O hydrogen bonds (H···O 2.03Å) between –OH and –COOH groups of **2** associated with the adjacent chains. As a result, a ladder-like structure is formed, exactly as observed in **1b**. While in the case of the complex **1b**, the alternating ladders have ***bpyea*** molecules of different orientation, the ordered and disordered ***bpyea*** molecules are observed, as rungs, in the adjacent ladders, in complex **2b**, as shown in Figure 10c and 10d. Thus, the influence of Br-substituent in the global packing seems

to be minimal. But it has a major impact on the recognition patterns of the acid molecules in the ladder structures.

4.3.3 Molecular complex of ($C_7H_5O_4Br$): ($C_{10}H_8N_2$), 2c

Cocrystallization reaction of acid **2** with ***bpy*** from a methanol solution gave a 1:1 complex, **2c**. The asymmetric unit of the complex is shown in Figure 11a. The crystal structure analysis reveals that, the packing arrangement in the crystal lattice is intriguing in many aspects.

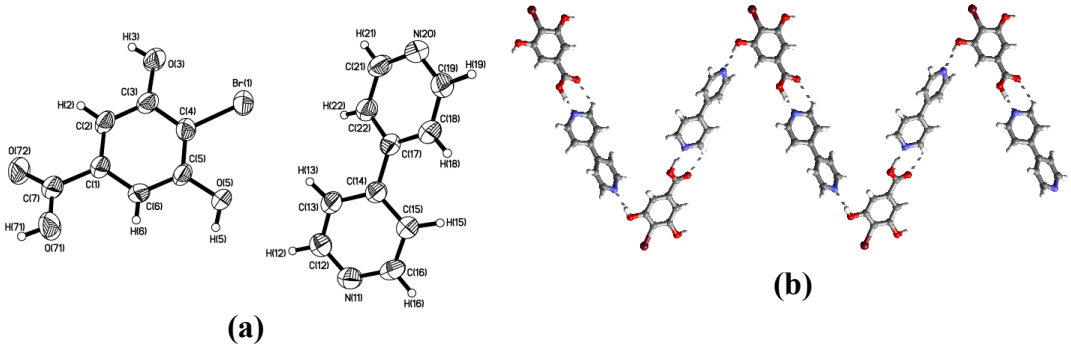

Figure 11: (a) The symmetric unit of the complex **2c.** (b) Recognition pattern between **2** and ***bpy*** through the formation of O-H···N and O-H···N/C-H···O pair wise hydrogen bonds, to form a crinkled tape.

The basic recognition between **2** and ***bpy*** involves both –COOH as well as –OH groups, interacting through O-H···N hydrogen bonds as in the case of complex **1c**. In the complex **2c**, each ***bpy*** interacts with two molecules of **2**, forming O-H···N hydrogen bonds (H···N 1.92Å) with –OH groups and pair-wise O-H···N (H···N 1.74 Å) and C-H···O (H···O, 2.71 Å) hydrogen bonds formed by –COOH groups. Further, a crinkled tape is observed in the complex **2c**, formed by the recognition between **2** and

bpy, as shown in Figure 11b, unlike closed network observed in complex **1c**. Thus, it is assumed that the bulky nature of the –Br atoms have played a major role in the formation of the crinkled tapes.

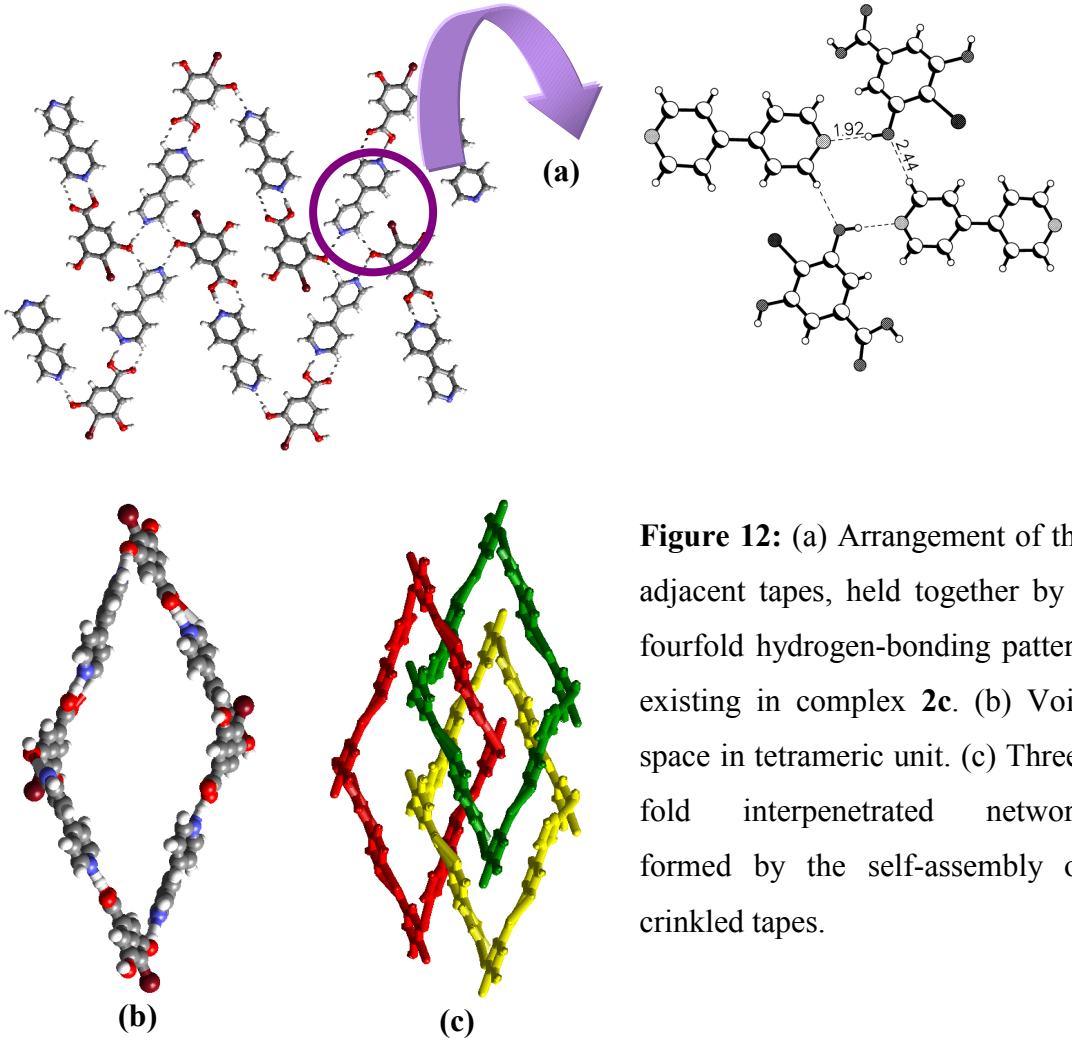

Figure 12: (a) Arrangement of the adjacent tapes, held together by a fourfold hydrogen-bonding pattern existing in complex **2c**. (b) Void space in tetrameric unit. (c) Three-fold interpenetrated network formed by the self-assembly of crinkled tapes.

In the two-dimensional arrangement, these chains meet at periodic junctions and are held together by the formation of a four-membered O-H···N and C-H···O hydrogen-bond coupling as shown in Figure 12a. In the resulted tetrameric unit, the H···N and H···O distances are found to be 1.92 and 2.44Å, respectively. Interestingly, a

similar network was observed in the crystal structure of complex **1c**. The interaction between two crinkled tapes leads to the formation of a huge void space, (12×29 Å^2), as shown in Figure 12b. Since such void structures are quite unstable, they are generally occupied by guest species if an appropriate molecule is available; otherwise, catenation or interpenetration results through self-assembly. In the complex **2c**, due to absence of an appropriate guest species, the void space is filled by a self-assembly process leading to the formation of an exotic threefold interpenetrated network. The resulted interpenetration is shown in Figure 12c, with three units shown in different colors for a better representation of the interpenetration.

Although the –Br atom is not involved directly in any appreciable nonbonding interactions or hydrogen bonds, its effect is fully reflected in the formation of an interpenetrated network structure.

Thus, it is apparent from the study of molecular complexes **1a-1c** and **2a-2c** that, ladder-like structures are predominately formed as observed in the complexes **1a**, **1b**, **2a**, and **2b**. In particular, it is noteworthy that ***bpy*** did not yield ladder-like structures with either **1** or **2**. This can be attributed to the smaller size of ***bpy*** compared to ***bpyee*** and ***bpyea***, which were involved in the ladder structures. Further, ***bpyea***, irrespective of the nature of the acid, gave the same type of three-dimensional architecture, whereas ***bpyee*** showed variations.

The observed transition from ladders to interpenetration could be related to the dimensions of the molecular components involved in the recognition studies and their ability to form closed ensembles. In this process, if the dimension of the void space is

within the van der Waals limits, a regular ladder-like structure results, otherwise an interpenetrated or host–guest network would be formed. A schematic representation of the relations among the global architectures, observed in this study, is shown in Scheme 4.

Scheme 4

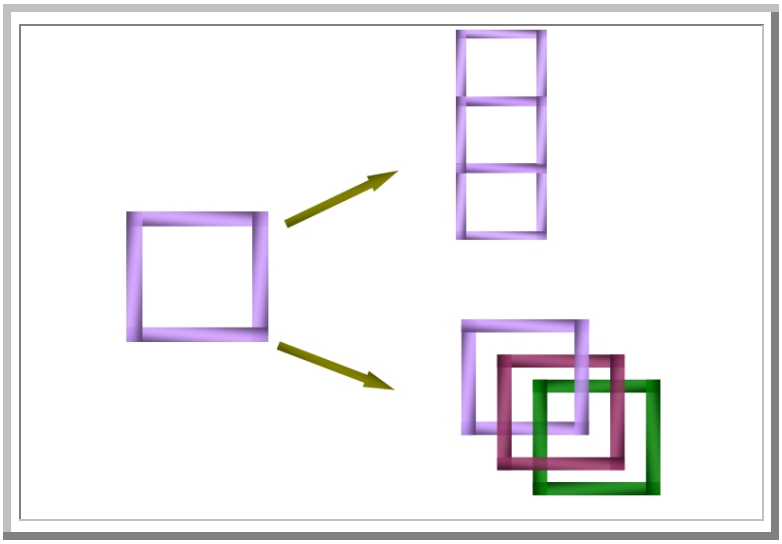

Further, a collective analysis of all the complexes reveal that the conformations of acids **1** and **2** in **1a**–**1c** and **2a**–**2c** are different due to the differences in the arrangement of –OH groups, and it appears that this is the prime factor in the formation of specific structural arrangements. The different conformations observed in the complexes are shown in Figure 13. While in the complexes **1a** and **1c** the -OH group adopts a *syn–syn* arrangement, they are *anti–anti* conformations in the case of the complexes **2a** and **2c**. In the complexes **1b** and **2b**, the arrangement is *syn–anti*. The above classification is with respect to the orientation of the H-atom on the –OH group towards the H/Br atom at the *para*-position on molecules, **1** and **2**.

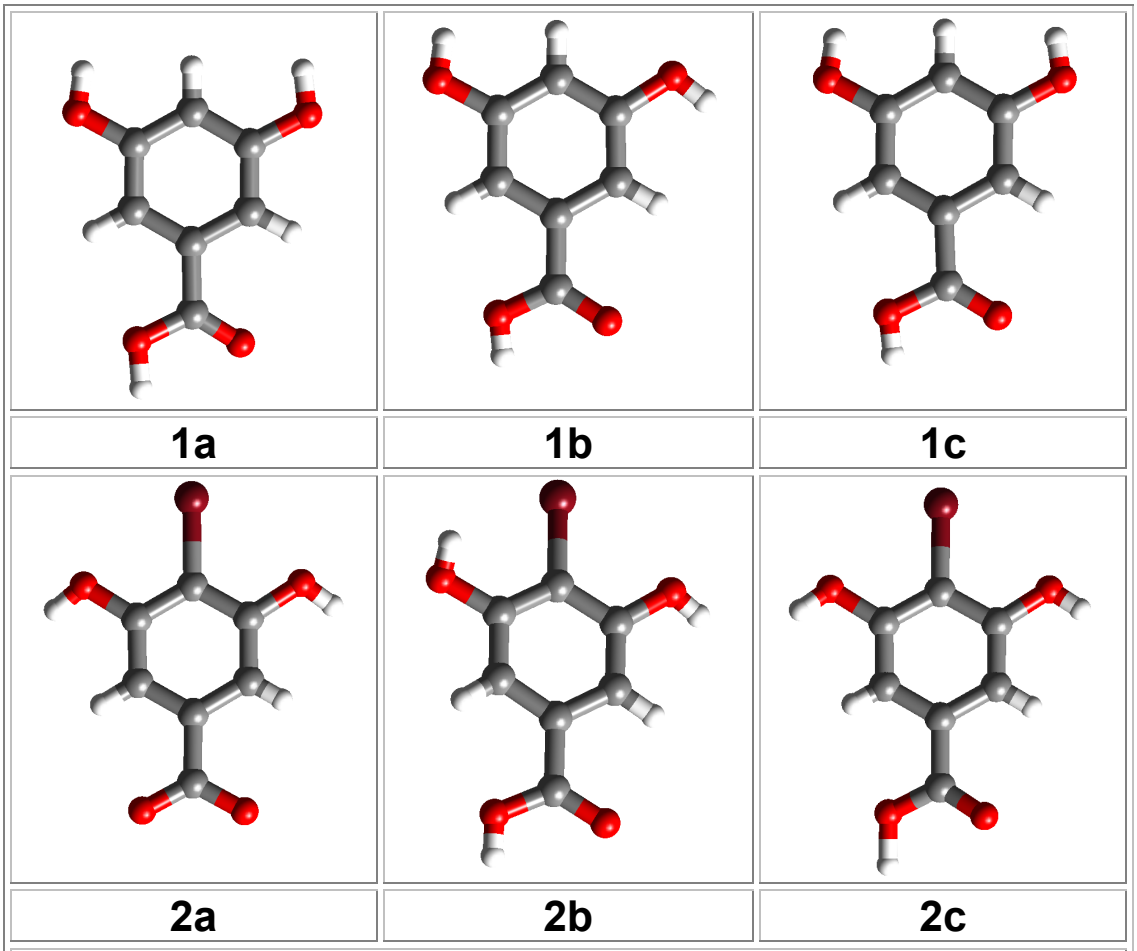

Figure 13: Representation of different conformations of **1** in complexes **1a**–**1c** and **2** in complexes **2a**–**2c**.

It is apparent that ***bpy*** and ***bpyee*** directed the *syn–syn* conformation in **1**, while they induced the *anti–anti* conformation in **2**. In contrast, ***bpyea*** always strongly favored the *syn–anti* conformation. This could be the reason for the formation of same ladder-like architecture in the complexes **1b** and **2b**, whereas the nature of the global structure varied in the other complexes due to the variations in the conformations of –OH groups. Furthermore, the *syn–anti* arrangement is intact in both **1b** and **2b**, irrespective of the presence of a Br-atom. Similarly, the *anti–anti* arrangements in **2a**

and **2c** could also be attributed to the bulky nature of the –Br atom. Although global packing and molecular interactions could not give conclusive information about the role of the –Br atom, the conformational analysis more or less demonstrates its size effect, based on the observed variations in the lattice arrangements between **1a**–**1c** and **2a**–**2c**.

4.4 Conclusions

In conclusion, it is evident that the affinities of –COOH and –OH groups towards N-donor compounds are fairly competitive, and this is in a way reflected in the formation of different recognition patterns. However, the global packing arrangement is not much perturbed, perhaps due to the operation of same principles in all the complexes, that is, effective space filling in accordance with crystallographic symmetry rules. Thus, the ladder-like structures and the interpenetrated networks appeared, depending on the size of the available molecular components and dimensions of resultant void space.

Tables

Table-4.1 Crystallographic information of molecular complexes **1a-1c.**

Complex	*1a*	*1b*	*1c*
Formula	$3(C_{12}H_{10}N_2)$, $2(C_7H_6O_4)$	$(C_{12}H_{12}N_2)$, $(C_7H_6O_4)$	$2(C_7H_6O_4)$, $3(C_{10}H_8N_2)$
Formula Wt.	852.88	338.35	776.79
Crystal system	Triclinic	Triclinic	Triclinic
Space group	$P\bar{1}$	$P\bar{1}$	$P\bar{1}$
***a* (Å)**	9.035(8)	7.234(2)	9.683(1)
***b* (Å)**	10.648(9)	13.914(3)	14.378(3)
***c* (Å)**	12.813(9)	17.141(4)	14.797(3)
***α* (deg)**	107.46(9)	78.54(4)	63.17(6)
***β* (deg)**	102.50(9)	82.50(4)	83.25(11)
***γ* (deg)**	109.12(9)	84.00(4)	80.17(10)
***V* (Å^3)**	1041.0(2)	1671.0(7)	1809.4(5)
Z	1	4	2
D_{calc} (g cm^{-3})	1.360	1.345	1.426
***T* (K)**	298(2)	298(2)	100(2)
***μ* (mm^{-1})**	0.094	0.095	0.100
2θ range (deg)	46.74	46.66	50.20
Total Reflns.	6482	14115	6384
Unique Reflns. R(int)	3000	4816	
Reflns. used	1924	2213	
No. of Parameters	374	455	530
GOF on F^2	1.038	0.819	0.932
Final R1, wR2	0.0527, 0.1069	0.0493, 0.0973	0.056, 0.134

Table-4.2 Characteristics of hydrogen bonds (distances/Å and angles/deg).[#]

	1a	1b	1c
O–H···O		1.812 2.631 177 1.846 2.666 178	
O–H···N	1.624 2.599 178 1.773 2.692 179 1.965 2.814 174	1.717 2.535 175 1.729 2.547 175 1.767 2.681 163 1.898 2.673 157	1.853 2.685 171 1.882 2.721 177 1.886 2.720 172 1.918 2.750 170 1.917 2.756 178 1.976 2.814 176
C–H···O	2.359 3.321 174 2.567 3.431 144 2.626 3.332 128 2.669 3.473 143 2.680 3.565 153 2.711 3.594 147 2.936 3.857 166	2.666 3.578 167 2.674 3.329 128 2.693 3.547 153 2.708 3.339 126 2.730 3.416 131 2.730 3.463 136 2.781 3.688 165 2.785 3.636 153 2.831 3.740 156 2.839 3.625 143 2.841 3.454 125 2.876 3.796 170 2.910 3.634 136	2.450 3.342 156 2.496 3.393 157 2.515 3.373 151 2.569 3.236 128 2.582 3.264 129 2.618 3.486 152 2.655 3.572 162 2.662 3.452 141 2.676 3.429 137 2.687 3.364 129 2.748 3.414 128 2.756 3.367 123 2.764 3.479 133 2.792 3.403 123 2.936 3.641 132 2.972 3.628 127 2.973 3.612 126 2.980 3.568 122
C–H···N	2.701 3.342 128 2.782 3.472 133	2.913 3.676 136 2.892 3.643 135	2.522 3.254 134 2.611 3.304 130 2.690 3.375 130 2.737 3.679 171 2.815 3.477 128 2.911 3.837 165 2.979 3.692 133

[#] The three numbers in each column indicate H···A, D···A and angles respectively

Table-4.3 Crystallographic information of molecular complexes **2a-2c.**

Complex	*2a*	2b	2c
Formula	$2(C_7H_4O_4Br)$: $(C_{12}H_{12}N_2)$	$2(C_7H_5O_4Br)$: $2(C_{12}H_{12}N_2)$	$(C_7H_5O_4Br)$: $(C_{10}H_8N_2)$
Formula Wt.	648.26	830.48	389.20
Crystal system	Monoclinic	Triclinic	Monoclinic
Space group	$P2_1/n$	$P\bar{1}$	$P2_1/n$
***a* (Å)**	6.693(2)	7.321(2)	10.247(4)
***b* (Å)**	16.425(4)	8.047(2)	9.270(3)
***c* (Å)**	11.197(3)	8.047(2)	17.130(6)
***α* (deg)**	90	98.34(5)	90
***β* (deg)**	91.55(5)	90.74(5)	99.39(5)
***γ* (deg)**	90	114.91(4)	90
***V* (Å^3)**	1230.5(6)	886.0(4)	1605.4(9)
Z	2	1	4
D_{calc} (g cm^{-3})	1.750	1.556	1.610
***T* (K)**	298(2)	298(2)	298(2)
***μ* (mm^{-1})**	3.350	2.347	2.585
2θ range (deg)	46.58	46.62	46.56
Total Reflns.	5235	7360	9552
Unique Reflns. R(int)	1785	2554	2306
Reflns. used	1399	2072	1939
No. of Parameters	212	305	270
GOF on F^2	0.930	0.910	1.001
Final R1, wR2	0.0267, 0.0623	0.0363, 0.0914	0.0274, 0.0731

Table-4.4 Characteristics of hydrogen bonds (distances/Å and angles/deg).[#]

	2a	2b	2c
O–H···O	1.778 2.595 169 1.830 2.655 173	2.034 2.708 150	1.888 2.668 169
O–H···N		1.703 2.539 173 1.919 2.633 174	1.744 2.557 171 1.917 2.741 172
N^+–H···O^-	1.667 2.608 179 2.529 3.121 121		
C–H···O	2.400 3.077 129 2.482 3.281 149 2.835 3.440 124 2.874 3.636 141	2.680 3.523 167 2.791 3.755 172 2.916 3.741 147 3.018 3.871 164	2.443 3.429 175 2.709 3.305 124 2.827 3.389 121
C–H···N		2.882 3.473 123	2.910 3.455 128

[#] The three numbers in each column indicate H···A, D···A and angles respectively

4.5 References

(1) (a) Endo, T.; Tasai, H.; Miyazawa, K.; Endo, M.; Kato, K.; Uchida, A.; Ohashi, Y.; Sasada, Y. *J. Chem. Soc., Chem. Commun.* **1983**, 636-638. (b) Garst, J. F. *J. Chem. Soc., Chem. Commun.* **1990**, 211-213. (c) Glusker, J. P. *Top.Curr.Chem.* **1998**, *198*, 1-56.

(2) Lehn, J.-M. *Angew. Chem. Int. Ed.* **1990**, *29*, 1304-1319.

(3) (a) Cram, D. J. *Angew. Chem. Int. Ed.* **1988**, *27*, 1009-1020. (b) Ramamurthy, V.; Eaton, D. F. *Chem. Mater.* **1994**, *6*, 1128-1136. (c) Rebek, Jr. J. *Angew. Chem. Int. Ed.* **1990**, *29*, 245-255. (d) Sekiya, R.; Nishikiori, S. *Chem. Eur. J.* **2002**, *8*, 4803-4810. (e) Worm, K.; Schmidtchen, F. P. *Angew. Chem. Int. Ed.* **1995**, *34*, 65-66.

(4) (a) Lehn, J.-M. *Supramolecular chemistry: concepts and perspectives*; VCH: Weinheim, 1995. (b) Lehn, J.-M. *Angew. Chem. Int. Ed.* **1988**, *27*, 89-112. (c) Cram, D. J. *Angew. Chem. Int. Ed.* **1988**, *27*, 1009-1020. (d) Rebek, Jr. J. *Acc. Chem. Res.* **1990**, *23*, 399-404.

(5) Fischer, E. *Ber. Dtsch. Chem. Ger.* **1894**, 2985-2997.

(6) (a) Lehn, J.-M.; Mascal, M.; DeCian, A.; Fischer, J. *J. Chem. Soc., Chem. Commun.* **1990**, 479-481. (b) Mecozzi, S.; Rebek, Jr. J. *Chem. Eur. J.* **1998**, *4*, 1016-1022. (c) Swiegers, G. F.; Malefetse, T. J. *Chem. Rev.* **2000**, *100*, 3483-3537. (d) Whitesides, G. M.; Simanek, E. E.; Mathias, J. P.; Seto, C. T.; Chin, D. N.; Mammen, M.; Gordon, D. M. *Acc. Chem. Res.* **1995**, *28*, 37-44. (e) Williams, A. R.; Northrop, B. H.; Houk, K. N.; Stoddart, J. F.; Williams, D. J. *Chem. Eur. J.* **2004**, *10*, 5406-5421.

(7) (a) Kobayashi, K.; Ishii, K.; Yamanaka, M. *Chem. Eur. J.* **2005**, *11*, 4725-4734. (b) Ma, S.; Rudkevich, D. M.; Rebek, Jr. J. *Angew. Chem. Int. Ed.* **1999**, *38*,

2600-2602. (c) Pinalli, R.; Suman, M.; Dalcanale, E. *Eur. J. Org. Chem.* **2004**, 451-462.

(8) (a) Carlucci, L.; Gavezzotti, A. *Chem. Eur. J.* **2005**, *11*, 271-279. (b) Dunitz, J. D.; Gavezzotti, A. *Acc. Chem. Res.* **1999**, *32*, 677-684. (c) Dunitz, J. D.; Gavezzotti, A. *Angew. Chem. Int. Ed.* **2005**, *44*, 1766-1787.

(9) (a) Barboiu, M.; Vaughan, G.; Kyritsakas, N.; Lehn, J. M. *Chem. Eur. J.* **2003**, *9*, 763-769. (b) Lehn, J. M. *Neurosci. Res. Program Bull.* **1976**, *14*, 133-137. (c) Lehn, J. M. *Science* **1993**, *260*, 1762-1763. (d) Lehn, J. M. *Science* **2002**, *295*, 2400-2403. (e) Petitjean, A.; Cuccia, L. A.; Lehn, J. M.; Nierengarten, H.; Schmutz, M. *Angew. Chem. Int. Ed. Engl.* **2002**, *41*, 1195-1198. (f) Skene, W. G.; Couzigne, E.; Lehn, J. M. *Chem. Eur. J.* **2003**, *9*, 5560-5566.

(10) (a) Pederson, C. J. *J. Am. Chem. Soc.* **1967**, *89*, 7017-7036. (b) Pederson, C. J. *J. Am. Chem. Soc.* **1967**, *89*, 2495-2496. (c) Rebek, Jr. J. *Angew. Chem. Int. Ed.* **2005**, *44*, 2068-2078.

(11) (a) Borovkov, V. V.; Inoue, Y. *Top. Curr. Chem.* **2006**, *265*, 89-146. (b) Maeda, K.; Yashima, E. *Top. Curr. Chem.* **2006**, *265*, 47-88. (c) Mecozzi, S.; Rebek, Jr. J. *Chem. Eur. J.* **1998**, *4*, 1016-1022. (d) Worm, K.; Schmidtchen, F. P. *Angew. Chem. Int. Ed.* **1995**, *34*, 65-66.

(12) (a) Brammer, L.; Bruton, E. A.; Sherwood, P. *Cryst. Growth Des.* **2001**, *1*, 277-290. (b) Holman, K. T.; Pivovar, A. M.; Ward, M. D. *Science* **2001**, *294*,

1907-1911. (c)Jansen, M.; Schön, J. C. *Angew. Chem. Int. Ed.* **2006**, *45*, 3406-3412. (d) Aoyama, Y. *Top. Curr. Chem.* **1998**, *198*, 131-161. (e) Hosseini, M. W. *Acc. Chem. Res.* **2005**, *38*, 313-323. (f) Pauling, L. *The Nature of the Chemical Bond*; Cornell Univ. Press: New York, 1960. (g) Swift, J. A.; Reynolds, A. M.; Ward, M. D. *Chem. Mater.* **1998**, *10*, 4159-4168.

(13) (a) Boese, R.; Kirchner, M. T.; Billups, E.; Norman, L. R. *Angew. Chem. Int. Ed.* **2003**, *42*, 1961-1963. (b) Etter, M. C.; Frankenbach, G. M. *Chem. Mater.* **1989**, *1*, 10-12. (c) Friscic, T.; MacGillivray, L. R. *J. Organomet. Chem.* **2003**, *666*, 43-48. (d) Trask, A. V.; Motherwell, W. D. S.; Jones, W. *Cryst. Growth Des.* **2005**, *5*, 1013-1021.

(14) (a) Ahn, S.; PrakashaReddy, J.; Kariuki, B. M.; Chatterjee, S.; Ranganathan, A.; Pedireddi, V. R.; Rao, C. N. R.; Harris, K. D. M. *Chem. Eur. J.* **2005**, *11*, 2433-2439. (b) Bond, A. D. *Chem. Commun.* **2003**, 250-251. (c) Braga, D.; Maini, L.; de Sanctis, G.; Rubini, K.; Grepioni, F.; Chierotti, M. R.; Gobetto, R. *Chem. Eur. J.* **2003**, *9*, 5538-5548. (d) Fan, E.; Vicent, C.; Geib, S. J.; Hamilton, A. D. *Chem. Mater.* **1994**, *6*, 1113-1117. (e) Koshima, H.; Miyauchi, M. *Cryst. Growth Des.* **2001**, *1*, 355-357. (f) Morissette, S. L.; Almarsson, O.; Peterson, M. L.; Remenar, J. F.; Read, M. J.; Lemmo, A. V.; Ellis, S.; Cima, M. J.; Gardner, C. R. *Adv. Drug. Del. Rev.* **2004**, *56*, 275-300. (g) Trask, A. V.; Jones, W. *Top. Curr. Chem.* **2006**, *254*, 41-70. (h) Zerkowski, J. A.; MacDonald, J. C.; Whitesides, G. M. *Chem. Mater.* **1997**, *9*, 1933-1941.

(15) (a) Amirsakis, D. G.; Garcia-Garibay, M. A.; Rowan, S. J.; Stoddart, J. F.; White, A. J. P.; Williams, D. J. *Angew. Chem. Int. Ed.* **2001**, *40*, 4256-4261. (b) Braga, D.; Grepioni, F. *Angew. Chem. Int. Ed.* **2004**, *43*, 4002-4011. (c) Braga, D.; D'Addario, D.; Giaffreda, S. L.; Maini, L.; Polito, M.; Grepioni, F. *Top. Curr. Chem.* **2006**, *254*, 71-94. (d) Byrn, S. R.; Xu, W.; Newman, A. W. *Adv. Drug. Del. Rev.* **2001**, *48*, 115-136. (e) Garibay, M. A. G. *Acc.Chem.Res.* **2003**, *36*, 491-498. (f) Hu, C.; Englert, U. *Angew. Chem. Int. Ed.* **2005**, *44*, 2281-2283. (g) Kaupp, G. *CrystEngComm* **2003**, *5*, 117-133. (h) Yang, Z.; Garcia-Garibay, M. A. *Org. Lett.* **2000**, *2*, 1963-1965.

(16) (a) Gao, X.; Frišcic, T.; MacGillivray, L. R. *Angew. Chem. Int. Ed.* **2004**, *43*, 232-236. (b) MacGillivray, L. R.; Reid, J. L.; Ripmeester, J. A. *J. Am. Chem. Soc.* **2000**, *122*, 7817-7818.

(17) Frišcic, T.; Drab, D. M.; MacGillivray, L. R. *Org. Lett.* **2004**, *6*, 4647-4650.

(18) (a) Sheldrick, G. M. SADABS, Area Detector Correction. 2002. Madison, WI, Siemens Industrial Automation, Inc. (b) Sheldrick, G. M. SAINT Area Detector Integration Software. 1998. Madison, WI, Siemens Industrial Automation,Inc. (c) Sheldrick, G. M. SHELX97 programs for crystal Strucutre Analysis. (97-2). 1998. Institüt für Anorganische Chemie der Universität. (d) Sheldrick, G. M. XPREP. (V5.1). 1997. Madison, WI, Bruker Analytical X-Ray Systems.

(19) Allen, F. H.; Kennard, O. *Chem. Des. Automat. News* **1993**, *8*, 31-37.

(20) Wheatley, P. S.; Lough, A. L.; Ferguson, G.; Glidewell, C. *Acta Crystallogr., Sect. C* **1999**, *55*, 1489-1492.

(21) Papaefstathiou, G. S.; MacGillivray, L. R. *Org. Lett.* **2001**, *3*, 3835-3838.

Publications

1. A Competitive Molecular Recognition Study: Syntheses and Analysis of Supramolecular Assemblies of 3,5-Dihydroxybenzoic Acid and Its Bromo Derivative with Some N-Donor Compounds
   S. Varughese and V. R. Pedireddi,
   Chemistry, A European Journal, **2006***, 12,* 1597-1609.

2. A novel supramolecular assembly of 3,5-dinitro-4-methylbenzoic acid and *trans*-1,2-bis(4-pyridyl)ethene.
   S. Varughese and V. R. Pedireddi,
   Tetrahedron Letters **2005**, *46*, 2411-2415.

3. Hydrogen Bond Mediated Open-frame Networks in Coordination Polymers: Supramolecular Assemblies of Pr(III) and 3,5-Dinitro-4-methylbenzoic Acid with Aza-donor Compounds.
   S. Varughese and V. R. Pedireddi,
   Chemical Communications **2005**, 1824-1826.

4. Solvent Dependent Coordination Polymers: Cobalt Complexes of 3,5-Dinitrobenzoic Acid and 3,5-Dinitro-4-methyl benzoic Acid with 4,4'-Bipyridine.
   V. R. Pedireddi and S. Varughese
   Inorganic Chemistry **2004**, *43*, 450-457.

Courseworks and Seminars Attended

International

1. **International School of Crystallography; 35th Course**
   Diversity Amidst Similarity: A Multidisciplinary Approach To Polymorphs, Solvates and Phase Relationships
   Erice, Italy, 09-20 June 2004.

2. **Indo-US Workshop on Collaborations and Networking in Materials**
   National Chemical Laboratory, Pune, 19-21 December 2004

National

1. **XXXV National Seminar on Crystallography**
   National Physical Laboratory, Delhi, February 22-24 2006.

2. **First National Conference on Nano Science and Technology**
   National Chemical Laboratory, Pune, 07-08 March 2005.

3. **The Annual Meeting of the M.R.S.I., MRSI-2005**
   National Chemical Laboratory, Pune, 08-11 February 2005.

4. **Current Trends in Inorganic Chemistry (CTIC)**
   Cochin University, Cochin, 12-15 March 2004.

5. **Sixth National Symposium in Chemistry**
   IIT Kanpur, 06-08 February 2004.

6. **XXXIII National Symposium in Crystallography**
   National Chemical Laboratory, Pune, 08-10 January 2004.